

**framatome**

---

**Fluence Methodologies for SLR**

ANP-10348NP  
Revision 0

Topical Report

July 2020

© 2020 Framatome Inc.

**Copyright © 2020**

**Framatome Inc.  
All Rights Reserved**

### Nature of Changes

Item	Section(s) or Page(s)	Description and Justification
1	All	Initial Issue

## Contents

		<u>Page</u>
1.0	SUMMARY .....	1-1
2.0	REGULATORY REQUIREMENTS .....	2-1
2.1	10 CFR 50, Appendix H .....	2-1
2.2	Regulatory Guide 1.99, Revision 2 <sup>8</sup> .....	2-2
2.3	60 Year License Renewal .....	2-3
2.4	Regulatory Guide 1.190 <sup>9</sup> .....	2-4
2.5	80 Year Subsequent License Renewal .....	2-5
2.6	Irradiation & Fracture Mechanics Safety Analysis .....	2-8
3.0	MEASUREMENTS .....	3-1
3.1	Davis Besse Experiment's Configuration .....	3-4
3.2	Davis Besse Experiment .....	3-5
3.3	Measurement Methodology .....	3-7
3.3.1	Fissionable Radiometric Dosimeters .....	3-8
3.3.2	Non-Fissionable Radiometric Dosimeters .....	3-9
3.3.3	Niobium Dosimeters .....	3-10
3.3.4	Stainless Steel Chains .....	3-12
3.3.5	Helium Accumulation Fluence Monitors (HAFMs) .....	3-13
3.4	Standard and Reference Field Validation <sup>19</sup> .....	3-14
3.5	Uncertainty Methodology .....	3-16
3.5.1	Relative Random Uncertainties .....	3-17
3.5.2	Uncertainty Above & Below the Fuel-Beltline .....	3-19
3.5.3	[ ] Uncertainty Methodology .....	3-20
3.5.4	[ ] .....	3-21
3.5.5	[ ] .....	3-23
4.0	SVAM METHODOLOGY .....	4-1
4.1	Background .....	4-2
4.2	Validation of Concerns & Solutions .....	4-3
4.3	SVAM Methodology .....	4-5
4.3.1	MCNP Geometric Modeling .....	4-8
4.3.2	Cross-Sections & Materials .....	4-10
4.3.3	Source Modeling .....	4-10
4.3.4	ADVANTG .....	4-11
4.3.5	SOLIDWORKS – VICTORIA .....	4-12

4.4	ART Effective Fluence .....	4-12
4.5	Best Estimate Fluence .....	4-17
5.0	BENCHMARKS .....	5-1
5.1	[ ] .....	5-3
5.2	SVAM Beltline Benchmark .....	5-5
5.3	SVAM Nozzle Region Benchmark .....	5-7
6.0	SENSITIVITY .....	6-1
6.1	Statistical Modeling .....	6-2
6.2	Sensitivity Modeling .....	6-3
6.3	Cross Section Covariance Data .....	6-5
6.4	Geometric Configurations .....	6-6
6.5	Isotopic Composition of Materials .....	6-7
6.6	Neutron Sources .....	6-9
<del>6.7</del>	<del>Calculational Methods and Procedures .....</del>	<del>6-10</del>
6.8	Statistical Application of Uncertainties .....	6-11
7.0	FUTURE MONITORING .....	7-1
7.1	60-Year Vessel Monitoring .....	7-4
	7.1.1 Monitoring Analytics .....	7-4
	7.1.2 Dosimetry Measurements .....	7-5
	7.1.3 Cycle Monitoring .....	7-6
7.2	SLR Vessel Monitoring .....	7-8
	7.2.1 Monitoring Safety Limits .....	7-9
	7.2.2 Deviations .....	7-10
	7.2.3 Verifying Results .....	7-11
7.3	Dosimetry .....	7-11
8.0	SUMMARY AND CONCLUSIONS .....	8-1
9.0	REFERENCES .....	9-1

**List of Tables**

Table 3-1	Cavity Dosimetry Loading Plan.....	3-26
Table 3-2	Coordinate Location of Dosimetry .....	3-33
Table 3-3	Photopeak Analyzed for Each Reaction .....	3-34
Table 3-4	Measurement Deviations.....	3-35
Table 3-5	Measurement Uncertainties.....	3-37
Table 5-1	[ ].....	5-16
Table 5-2	Framatome Databases .....	5-17
Table 5-3	Benchmark Database Summary.....	5-43
Table 6-1	ENDF/B U-235 Uncertainties <sup>7</sup> MT= 1 total .....	6-14

**List of Figures**

Figure 1-1 Calculations and Measurements\* ..... 1-4

Figure 2-1 Reactor Vessel Beltline and Nozzle Regions ..... 2-11

Figure 2-2 Nozzle Region Details ..... 2-12

Figure 3-1 General Arrangement of Cavity Dosimetry Benchmark Experiment..... 3-24

Figure 3-2 Cavity Dosimetry Experiment Plan View ..... 3-25

Figure 4-1 Reactor Vessel Nozzles and Supports ..... 4-20

Figure 4-2 *dpa* Reactions..... 4-21

Figure 5-1 X-Y Quadrant Benchmark ..... 5-12

Figure 5-2 W-X Quadrant Benchmark ..... 5-13

Figure 5-3 Z-W Quadrant Benchmark..... 5-14

Figure 5-4 [ ..... ]..... 5-15

## Nomenclature

<b>Acronym</b>	<b>Definition</b>
ABB	Above and Below the Fuel-Beltline
ANS	American Nuclear Society
ANSI	American National Standards Institute
ART	Adjusted Reference Temperature
ASME	American Society of Mechanical Engineers
ASTM	American Society for Testing and Materials
BWR	Boiling Water Reactor
CADIS	Consistent Adjoint Driven Importance Sampling
<i>dpa</i>	displacements per atom
EOL	End of Licensed-Life
FW-CADIS	Forward-Weighted CADIS
GALL	Generic Aging Lessons Learned
HAFMs	Helium Accumulation Fluence Monitors
LOI	Locations of Interest
MABB	Measured Data in regions above and below the fuel-beltline
MB	Measured Data in the Fuel-Beltline
NIST	National Institute of Standards and Technology
NRC	United States Nuclear Regulatory Commission
PCA	Pool Critical Assembly
P-T	Pressure-Temperature
PWR	Pressurized Water Reactor
PTS	Pressurized Thermal Shock
RT	Reference Temperature
RT <sub>PTS</sub>	Reference Temperature for Pressurized Thermal Shock
SLR	Subsequent License Renewal
SSTRs	Solid State Track Recorders
U.S.	United States
USE	Upper Shelf Energy
$\Delta RT_{\text{NDT}}$	Change in Reference Temperature for Nil Ductility Transition



## ABSTRACT

Framatome is the largest provider of services supporting the construction and operation of nuclear reactors in the world. In the United States (U.S.) the original operating license for PWRs and BWRs was for 40 years. As the end of licensed-life approached, electric utilities requested a renewed license extending operation to 60 years. As the end of licensed-life for 60 years is approaching, electric utilities are requesting a subsequent license renewal to operate for 80 years. With the 60 and 80 year extension, the U.S. Nuclear Regulatory Commission examined the key safety issues.

One of the safety issues for both 60 and 80 years is the degradation of the reactor vessel's structural toughness. The vessel's steel can be damaged by irradiation. Thus, a key issue for license renewal is the ability to accurately and precisely determine the irradiation. Previously Framatome developed an advanced technology to address the irradiation deep within the vessel's steel for extending operation to 60 years.

This topical report furthers the advances in the technology for analyzing fluence-radiation to the reactor vessels. Framatome has advanced the methodology for determining irradiation degradation in all reactor vessel components. The nozzle region is of particular interest for 80 years of operation. As explained in the report, the benchmark database verifies that Framatome's advanced methodology is sufficiently accurate and precise to have a 95 / 95 level of confidence in the safety analyses for all PWRs and BWRs.

## 1.0 SUMMARY

The Framatome fluence methodologies for SLR (Subsequent License Renewal) are based on two topical reports. The first one, BAW-2241P-A, Revision 2, "Fluence and Uncertainty Methodologies",<sup>1</sup> has been reviewed and approved by the United States Nuclear Regulatory Commission (NRC). It is approved for analysis of all commercial Pressurized Water Reactors (PWRs) and Boiling Water Reactors (BWRs). There are of course "Limitations and Conditions" specified for the range of applications in the "Final Safety Evaluation" by the NRC.

The NRC has indicated in Reference 2 that SLR requires an expanded analysis of reactor regions that will possibly experience increased irradiation degradation. This second topical report, "Fluence Methodologies for SLR", ANP-10348P, presents a significantly more complex system of analyses and computer-code calculations than the first one. The reason for developing a more complex system than the "Fluence and Uncertainty Methodologies"<sup>1</sup> used for the fuel-beltline region is that Reference 2 addresses much more complex geometric locations than previously analyzed; these are the nozzle regions, etc.

The complex system of computer codes used to analyze reactor regions beyond the beltline includes SOLIDWORKS<sup>3</sup>, VICTORIA<sup>4</sup> (a plugin for ANSYS<sup>5</sup>), ADVANTG<sup>6</sup> and MCNP.<sup>7</sup> This new system is known as SVAM. The fuel-beltline computer-code system in Reference 1 is known as (MERLIN) DORT – Synthesis. [

]

As explained in this topical report, the benchmark and calculational uncertainty analyses of the methodologies for SLR are an extension of the analyses performed for the "Fluence and Uncertainty Methodologies" topical report.<sup>1</sup> The additional benchmark and uncertainty analyses have demonstrated that the [

]

The beltline benchmark results for SVAM compared to DORT – Synthesis were exactly as expected. As shown by the dosimetry data in Figure 1-1, [

] the root mean square relative standard deviation in the measured data is estimated as 7.0%. Since the measured data is the standard for judging the accuracy and precision in the calculations, the calculated results cannot be more accurate, nor have a lower standard deviation than the measured data. [

]

[

] The benchmark comparison clearly indicated that [ ] SVAM is accurate (bias removal being actuated) and the relative standard deviation in SVAM's

results is [

] Thus, with respect to SLR analyses [

]

The beltline in Figure 1-1 goes from the top of the fuel, [

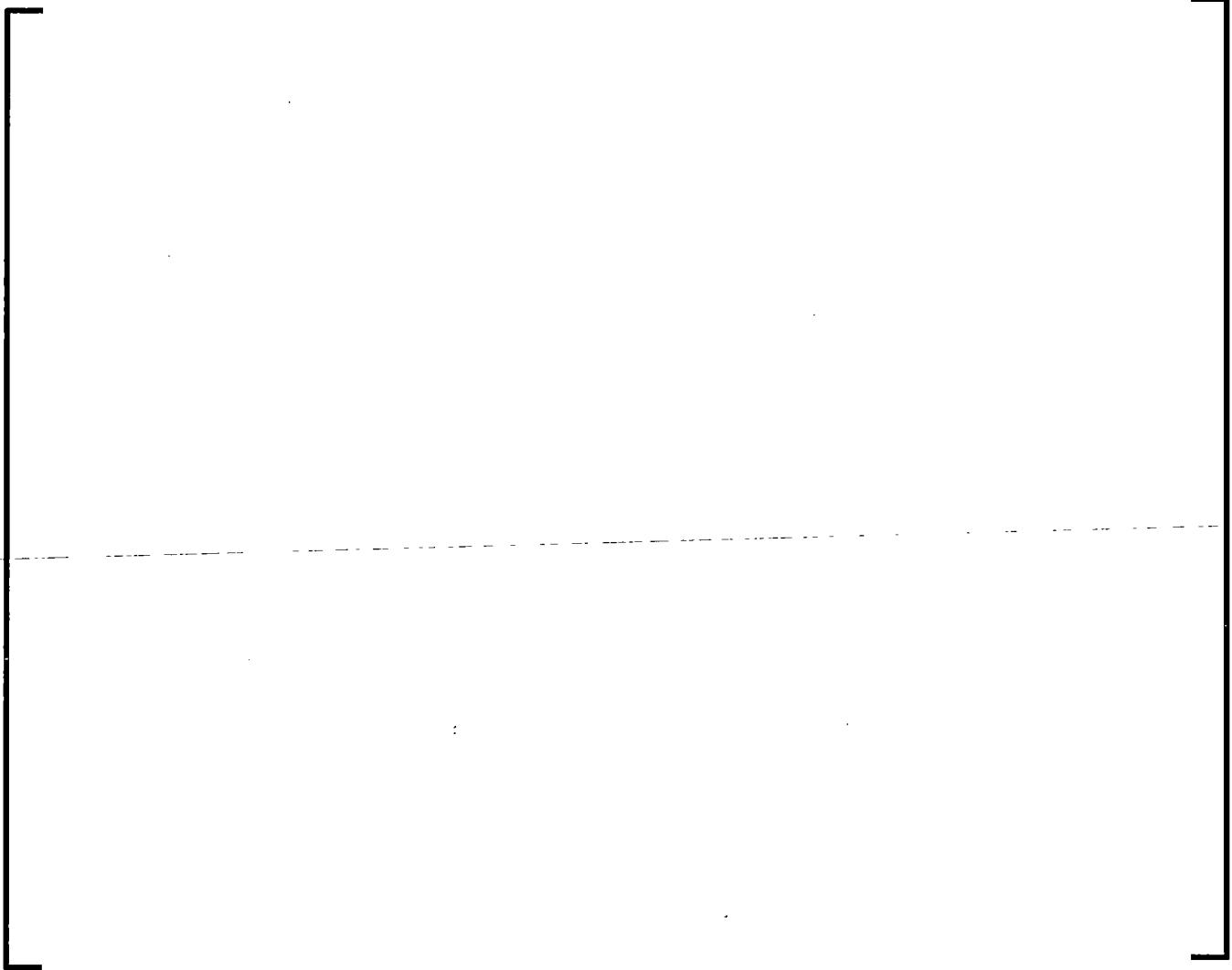
] The nozzle region, with the vessel support beams, extends to the top of the core flood nozzle. [

] The results in the following sections demonstrate that SVAM is accurate in the nozzle region with a well-defined random uncertainty.

Thus, [

] SVAM is valid in the nozzle regions.

**Figure 1-1**  
**Calculations and Measurements\***



---

\*[

]

## 2.0 REGULATORY REQUIREMENTS

Regulatory requirements for SLR are concerned with the uncertainties in irradiation degradation, along with other licensing issues. Beginning in the 1960s, evaluations of irradiation uncertainties have followed a progression of updates to maintain the appropriate safety margins for reactor operation. In 1961, the American Society for Testing and Materials established a standard for reactor vessel surveillance programs (ASTM E 185-61, "Standard Practice for Conducting Surveillance Tests for Light-Water Cooled Nuclear Power Reactor Vessels"). Framatome (Babcock & Wilcox in 1961) developed a surveillance program to monitor changes in the mechanical properties of vessel material test specimens in accordance with the ASTM standard.

### 2.1 10 CFR 50, Appendix H

ASTM E 185-61 provided a satisfactory material test program. However, the accuracy and reliability of irradiation damage predictions was based on empirical techniques; the results were unreliable. In 1973, the NRC implemented 10 CFR 50, Appendix H, "Reactor Vessel Material Surveillance Program Requirements". The updated program improved the quality of irradiation damage predictions by relying on the theoretical concepts of fracture mechanics.

When Charpy specimens from surveillance programs in operating reactors began to be available, the correlation of the data to the theory resulted in large uncertainties in the predictions of embrittlement ( $\Delta RT_{NDT}$ ). A significant part of the problem was the large variation in irradiation values. In 1977, the NRC initiated the "Light Water Reactor Pressure Vessel Surveillance Dosimetry Improvement Program". Part of the Program was the PCA (Pool Critical Assembly) Experiment and Blind Test. The NRC requested that Westinghouse, CE, B&W and others analyze the PCA Experiment and provide them their calculated results. The analysts at the various organizations did not know the measured results from the Blind Test. Thus, the differences between the calculated and measured results would provide a good indication of the industry's uncertainties.

Based on Westinghouse, CE, B & W and others' Charpy material specimen measurements and associated fluence values, the NRC concluded that the industry's mean fluence uncertainty was 21.0 %. Framatome (Babcock & Wilcox in 1977) had developed the most technologically advanced methods for performing dosimetry measurements and fluence analyses; their uncertainty was 12.0 %.<sup>1</sup> The accuracy and consistency of the Framatome methods were independently confirmed by R.L. Simons, E.P. Lippincott, et alia, from the Westinghouse Hanford Company.<sup>11</sup> NUREG/CR-1861 discusses the PCA results.

## **2.2 Regulatory Guide 1.99, Revision 2<sup>8</sup>**

Assuming a relative standard deviation of 20.0 %, material scientists adjusted the fluence values to determine "chemistry factors" and uncertainties for an embrittlement model. The model was based on correlating the shift ( $\Delta$ ) in the reference temperature ( $RT$ ) for the nil-ductility transition ( $NDT$ ) in the material's properties ( $\Delta RT_{NDT}$ ) to the greater than 1.0 MeV fluence. While some changes in fluence values were greater than 20.0 %, others were less. The root mean change was not greater than 20.0 %.

Subsequently, the modeling of the data formed the basis for Regulatory Guide 1.99, Revision 2. The industry's radiation analysts adopted a standard whereby the fluence irradiation would be "unfolded" using dosimetry measurements and analytical procedures. Based on the uncertainty of the dosimetry measurements, the overall uncertainty in the fluence was less than 20.0 %.

The analytical procedures used to unfold the fluence were also used to assess the irradiation damage "lead factor". Lead factors related (a) the test specimen material irradiation – embrittlement to (b) the irradiation – embrittlement of the actual vessel material. With reactor licensing limited to 40 years, 32 effective full power years with an 80 % capacity factor, the lead factors demonstrated that there was more than adequate margin to ensure that irradiation embrittlement of the reactor vessel would never be a safety issue.

### 2.3 60 Year License Renewal

When the industry began discussing renewing the licenses of PWRs and BWRs, the NRC began to review the licensing and safety issues. Irradiation experts at the NRC and those supporting the NRC had questions concerning the fluence uncertainties. The industry was not only going to a 60 year license, but the capacity factors were also increasing to values higher than 90 %. Irradiation of vessel materials could be increased by more than a factor of 1.7 compared to a 40 year license.

A concern expressed by the NRC's irradiation – embrittlement experts was the consistency between the fluence uncertainty and the embrittlement margin. The Regulatory Guide 1.99, Revision 2 model for assessing embrittlement is based on a “least squares” correlation. That is, the “chemistry factors” and the fluence are best-estimate values; completely unbiased. The only uncertainty is from random deviations related to a “normal” probability distribution. As a consequence, the confidence in the embrittlement degradation predictions is based on 2 standard deviations ( $\sigma$ ) for the Guide's margin term. This provides a greater than 95 % confidence that 95 % of the predictions (95 / 95) will bound the embrittlement degradation.

The problem for the NRC's irradiation – embrittlement experts was that most of the unfolded specimen fluence results were biased. That is, they were not truly best-estimate mean values. Biased results, that were too high, were initially thought to be conservative. However, as the experts assessed the specimen measurements and the vessel irradiation lead factors, it became clear that biases could be a problem.

If the causes of the biases are unknown, then a possible 10 % positive bias at the capsule, but an unknown 20 % positive bias at the vessel would actually be non-conservative. The effect of biases becomes clearer when considering the standard deviation ( $\sigma$ ) in the measurements ( $x$ ).

$$\sigma_x = \sqrt{\frac{\sum_{i=1}^N (x_i - \bar{x})^2}{N - 1}} \quad (2-1)$$



The number of measurements ( $i$ ) in Equation 2-1 begins with "1", and ends with a total of  $N$  values. Equation 2-2 expresses the evaluation of biases with respect to the expected mean value ( $\bar{x}$ ) of the measurements and the "one" True Value.

$$\text{Bias} = \sum_{i=1}^N \frac{x_i - (\text{True Value})_i}{N} = \bar{x} - \text{True Value} \quad (2-2)$$

As indicated by Equation 2-2, if there are no biases (Bias = 0.0), then the mean value ( $\bar{x}$ ) of the measured results would accurately represent the "True Value". Moreover, the Equation 2-1 standard deviation would be significant. There could be at least a 95 % confidence that the embrittlement damage was bounded by the  $2\sigma$  margin term. However, if there were biases in  $\bar{x}$  due to unknown causes, then using Equation 2-1 to assess the standard deviation would be meaningless. With unknown biases it would be impossible to say that the deviation around  $\bar{x}$  could be represented by a normal distribution of deviations. There would be no confidence in bounding the embrittlement degradation with a tolerance factor of "2" times the standard deviation ( $\sigma$ ).

In addition to biases in the "unfolded" results being a concern for license renewal, the fundamentals of the fluence methodology were an NRC concern because of the reliance on measurements. There are no measurements at the "one-quarter" (T/4) vessel thickness (T) where the fracture toughness safety analysis is evaluated. Therefore, it would not be possible to actually have confidence in the safety of the fracture toughness results based on the Regulatory Guide 1.99, Revision 2 margin term.

#### 2.4 **Regulatory Guide 1.190**<sup>9</sup>

In 1988, the NRC met informally with members of the industry to discuss their concerns. The concerns were expressed in a "white paper" for the industry to consider. The "white paper" eventually became Regulatory Guide 1.190,<sup>9</sup> "Calculational and Dosimetry Methods for Determining Pressure Vessel Neutron Fluence". It recommended that updated fluence methodologies be developed to calculate best-estimate values. Moreover, the calculations would need to be independent of the measurements. [

]

[

]

Framatome updated its fluence methodology and presented it in a topical report to the NRC in May of 1997.<sup>1</sup> The topical report adhered to the guidance in an early draft of Regulatory Guide 1.190 (Draft Regulatory Guide DG-1025). It was approved for licensing in February of 1999.<sup>1</sup> [

]

## 2.5 80 Year Subsequent License Renewal

As reactors began to operate in the 60 year license renewal period, the industry began to discuss a subsequent renewal period. Again, the NRC's irradiation experts reviewed the licensing and safety issues. The experts again recommended that the industry's radiation methods, models and procedures be updated.<sup>2</sup>

While Regulatory Guide 1.190<sup>9</sup> provides an excellent basis for determining the fluence for irradiation degradation, it is based on the fuel region beltline. This is explained in Section 1.3.3 of the Regulatory Guide<sup>9</sup>, "Fluence Determination", on pages 12 and 13. Specifically (page 13):

"To account for the neutron spectrum dependence of  $RT_{NDT}$  when the  $E > 1$  MeV fluence is extrapolated from the inside of the pressure vessel to the T/4- and 3T/4-vessel locations {T is the thickness}, a spectral lead factor (which accounts for the change in neutron spectrum between downcomer and vessel internal locations) must be applied to the fluence for the calculation of  $\Delta RT_{NDT}$ . This spectral lead factor has been included

in the Equation 3 attenuation formula of Revision 2 of Regulatory Guide 1.99,<sup>(8)</sup> and therefore is not required when this formula is used.”

The Regulatory Guide 1.190 discussion of (a) the “spectral lead factor” being equivalent to (b) “Regulatory Guide 1.99, Revision 2, Equation 3”, is only valid within the fuel-beltline region. Within the beltline, there is no need to consider spectral lead factors; Equation 3 is valid.<sup>8</sup> The NRC’s irradiation experts, however, are questioning the industry about vessel regions beyond the fuel-beltline being impacted by SLR.

Figure 2-1 illustrates the concern of the NRC’s irradiation experts. The fuel-beltline region is adjacent to the active fuel (noted by the blue dashed lines with the legend description – Approximate location of the active fuel). This region is geometrically simple compared to the nozzle region above it. The primary system’s fluid nozzles are geometrically complex. The complexity is not only difficult to model, but it also leads to complex neutron spectrum effects. The effects cannot be modeled with the spectral lead factors that are provided in Regulatory Guide 1.99, Revision 2, Equation 3.<sup>8</sup>

In the regions above and below the fuel-beltline, spectral lead factors (based on displacements per atom {*dpa*} ) are clearly needed. Thus, the Regulatory Requirements for an 80 year SLR need to be expanded beyond those for 60 year license renewal. The 80 year SLR needs to focus on regions that are above and below the fuel-beltline. An updated 80 year SLR radiation (fluence) Regulatory Guide would be useful.

The NRC has agreed that the industry, including themselves, should write a revised ANS / ANSI Standard that is based on Regulatory Guide 1.190, but is updated to reflect the uncertainties and methods appropriate for SLR. Just as Framatome previously updated its methodologies to comply with Regulatory Guide 1.190 before the final Guide was complete, Framatome agrees with the NRC’s assessment of updates for SLR. Thus, the SLR licensing and safety issues that the NRC has shared with the industry<sup>2</sup> are the bases for the Regulatory Requirements in this topical report. The complex system of analyses and computer-codes (SVAM) presented in this topical report provides an updated methodology that meets updated regulatory requirements.

The updated system of computer codes (SVAM) [

] The SVAM development occurred over a

period of years, from initial trial tests [

] SVAM [ ]

satisfies the fluence – radiation degradation part of the SLR Regulatory Requirements.

The key to SLR Regulatory Requirements [

]

The updated [

]

The updated [

]

As previously discussed in the "Fluence and Uncertainty Methodologies"<sup>1</sup> topical report, the updated [ ]

[ ] the SVAM methodology is accurate, with critical-spectrum results, and has well-defined relative standard deviations beyond the beltline, in nozzle regions. The accuracy extends throughout the internal components. The uncertainties in this topical report satisfy the Regulatory Requirements that concern the NRC with respect to SLR.

## 2.6 *Irradiation & Fracture Mechanics Safety Analysis*

While neutron irradiation of the reactor vessel and the vessel internal structures is the mechanism causing degradation of the steel's toughness, neutron irradiation *per se* is not a safety parameter. In 1973, when 10 CFR 50, Appendix G, "Fracture Toughness Requirements" was implemented along with 10 CFR 50, Appendix H, "Reactor Vessel Material Surveillance Program Requirements", the NRC noted that fracture mechanics analyses are the basis for the vessel's safety limits. Thus, the Regulatory Requirements in this section (2.0) are directly related to Fracture Mechanics Safety Analysis.

Neutron irradiation degrades the crystalline structure of the reactor vessel's steel resulting in embrittlement. Regulatory Guide 1.99, Revision 2<sup>8</sup> provides guidance for calculating the shift ( $\Delta$ ) in the reference temperature ( $RT$ ) for the nil-ductility transition ( $NDT$ ) in the steel material's properties due to irradiation. When the  $\Delta RT_{NDT}$  shift is

added to the initial reference temperature, along with a 95 / 95 statistical margin term, the result is an adjusted reference temperature (ART). ART values are used in the fracture toughness safety analyses of reactor vessels.

The fracture mechanics ART values are directly related to (a) the material properties (copper and nickel concentrations) of the vessel steel, and (b) the correlation of the  $\Delta RT_{NDT}$  shift to irradiation. The "shift to irradiation" correlation comes from capsule test specimens. The cause of the shift is – neutron reactions with the atoms in the steel's crystalline structure. The reactions cause the atoms to be displaced leaving vacancies and interstitials. While the "displacements per atom" ( $dpa$ ) are the cause of the shift, the correlation of the shift to  $dpa$  had a larger uncertainty than correlating the shift to the greater than 1.0 MeV neutron fluence. As a consequence, the Material analysts who developed the Regulatory Guide 1.99, Revision 2 methods used the greater than 1.0 MeV neutron fluence as the radiation parameter for determining  $\Delta RT_{NDT}$ .

The fracture mechanics safety analysis includes the  $\Delta RT_{NDT}$  random uncertainty in the Regulatory Guide 1.99, Revision 2 margin term. This term was developed by Guthrie in Reference 10. The margin is consistent with the least squares correlation between the greater than 1.0 MeV neutron fluence and the material's reference temperature ( $RT$ ) shift ( $\Delta$ ) in the nil-ductility transition ( $NDT$ ). The standard deviation ( $\sigma$ ) for welds was 28°F (degrees Fahrenheit), and was 17°F for base metal. The standard deviations are applied statistically with a 95 / 95 tolerance factor ( $\pm 2$ ) giving a margin of " $2 \times \sigma$ ".

The basis for the correlation was a 20.0 % root mean change in the fluence values that had been calculated by the industry.<sup>11</sup> Thus, the relation between neutron irradiation uncertainties and fracture mechanics safety analysis (ART values) uncertainties is a 20.0 % standard deviation in the neutron fluence with energies above 1.0 MeV.

Material and Radiation Transport scientists supporting the NRC determined that the  $dpa$  conditions at the capsule were essentially the same as the  $dpa$  conditions at the vessel inside – wetted surface. Thus, fluence analysts calculate the greater than 1.0 MeV fluence at the vessel's inside wetted surface for application to the fracture mechanics

safety analyses. The fracture mechanics analysts however perform their safety analyses at one-quarter increments of the vessel's minimum thickness ( $x$ ). To transport the  $dpa$  irradiation to the inside of the vessel, a  $dpa$  attenuation coefficient was calculated by fluence analysts. Using Equation 3 ( $\exp^{-0.24 x}$ ) from Regulatory Guide 1.99, Revision 2, material analysts determine an "effective" fluence at the vessel's interior locations ( $x$ ) for fracture mechanics safety analyses.

Fracture mechanics analysts are beginning to evaluate irradiation degradation in the vessel's nozzle region. High stress intensity factors in the nozzles with small ARTs have been more limiting than large ARTs in the vessel beltline with smaller stress intensity factors. Figure 2-1 shows the vessel beltline and the nozzle regions. Figure 2-2 shows the nozzle region details. This region has significantly different  $dpa$  values than the capsules and the inside vessel wetted surface. Consequently, " $dpa$  effective" fluence values are needed for fracture mechanics safety analyses.

The reason that an "effective  $dpa$ " fluence has been used in the vessel interior is that the capsule specimen  $dpa$  is not the same as the  $dpa$  within the vessel. This is also the case for the nozzle region. The fracture mechanics ART values need to take into account nozzle region  $dpa$  spectrum effects. The ART margin term used for the nozzle region fracture mechanics safety analyses continues to be based on the Regulatory Guide 1.99, Revision 2 database. The uncertainty criterion for the " $dpa$  effective fluence" thereby needs to meet a relative standard deviation of 20.0%.

**Figure 2-1**  
**Reactor Vessel Beltline and Nozzle Regions**

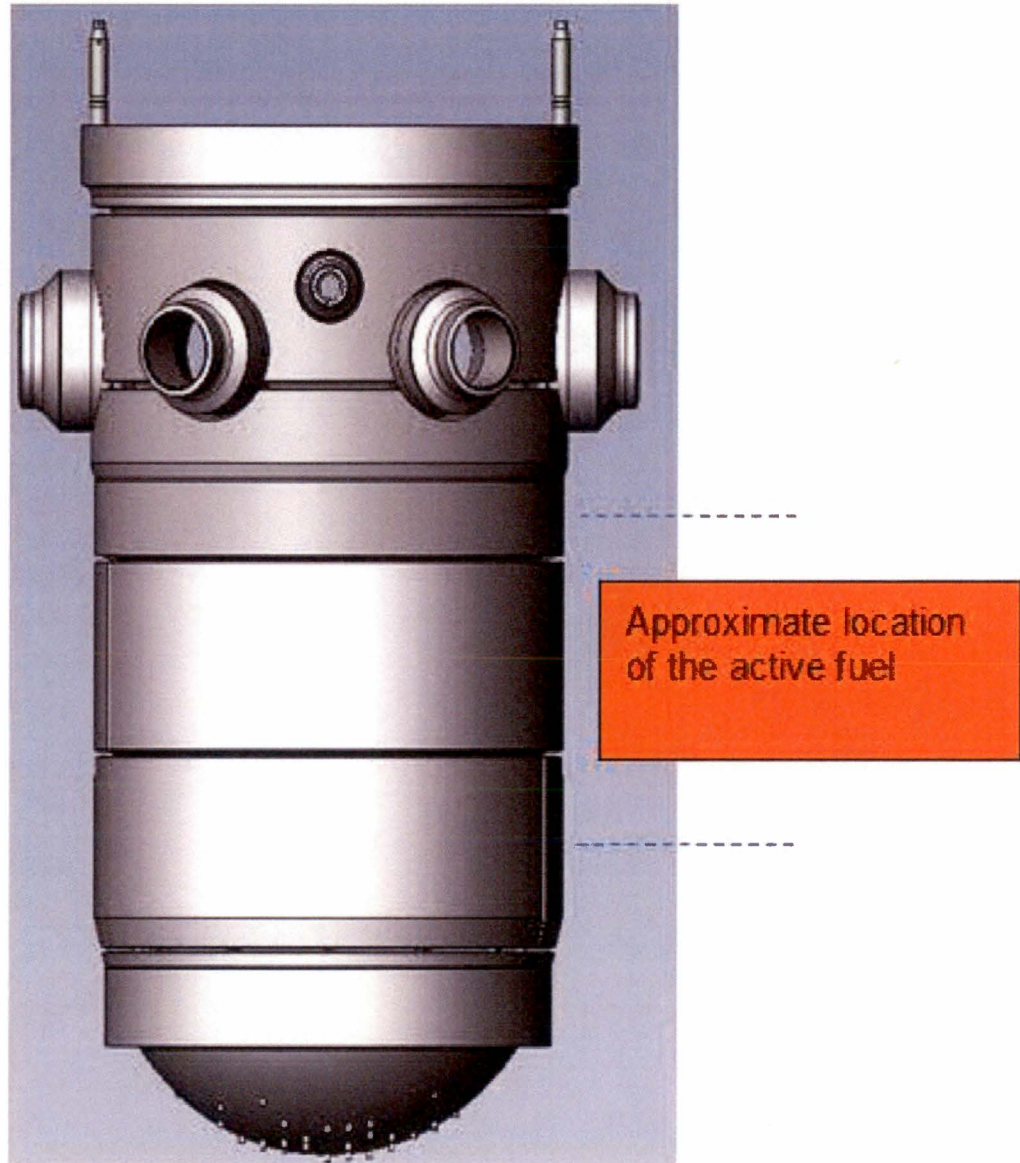
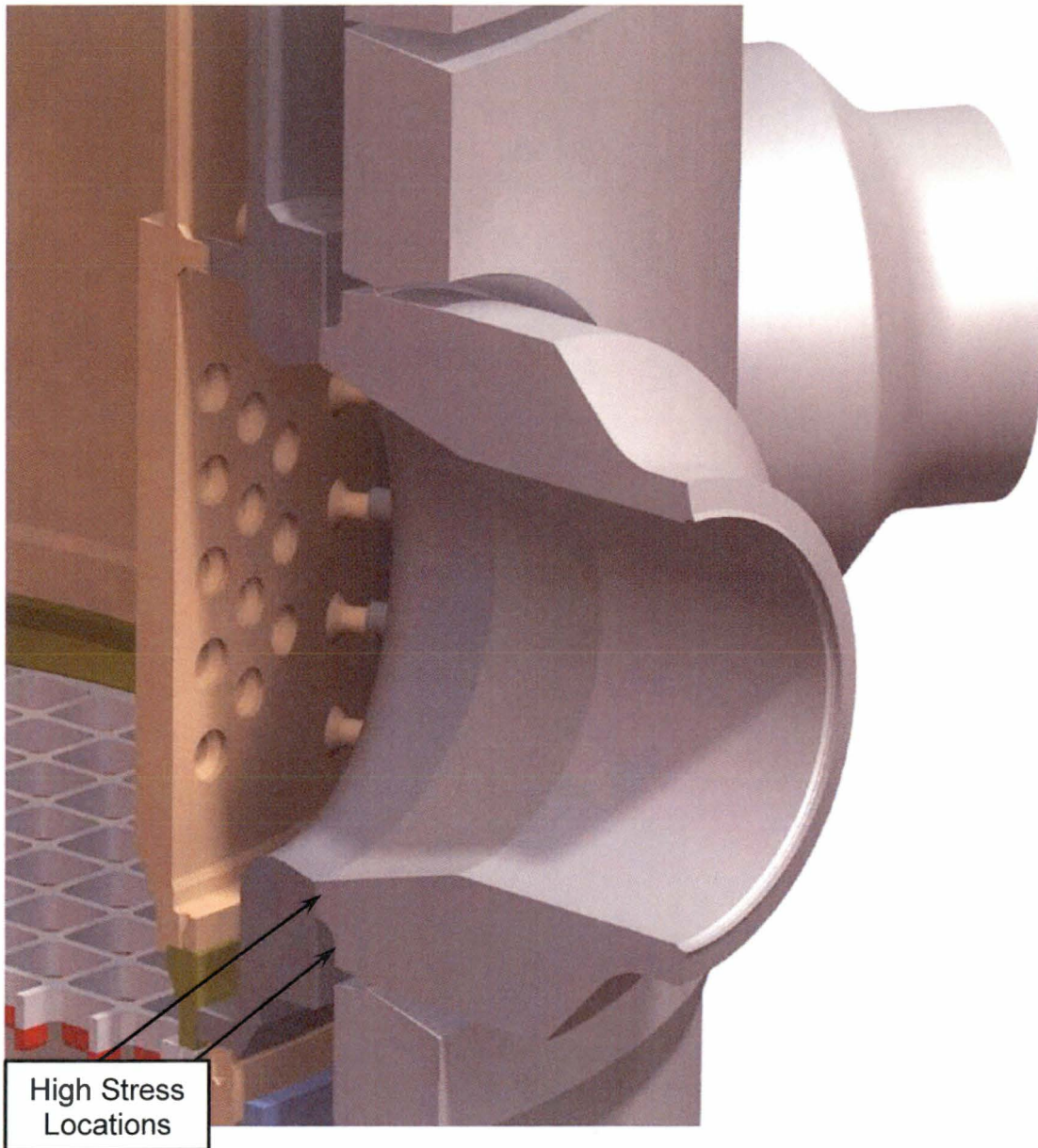




**Figure 2-2**  
**Nozzle Region Details**



### 3.0 MEASUREMENTS

The update of the Measurement database is one of the most important advancements related to the development of the SVAM methodology (Section 4). Even more important than the data is the uncertainty associated with the data. [

]

The Measurement database for SVAM includes [

] dosimetry data above and

below the fuel-beltline.

In addition, the measured data has been expanded to cover a wider range of neutron energies. Thermal reactions in  ${}^6\text{Li}$ -HAFMs (helium accumulation fluence monitors) and

[

] The updated data

covers the entire energy range for *dpa* reactions. This range is from fractions of an eV ( $1.0 \times 10^{-5}$  eV) to 20.0 MeV (see Figure 4-2). (The thermal reactions are an extension of Regulatory Position 2.1.1 which addresses "Spectrum Coverage".<sup>9)</sup>

The Framatome measurement database [

]

One of the more important data sets in Reference 1 is that from the Davis Besse Experiment. This Experiment was performed during the same time period that the NRC (U.S. Nuclear Regulatory Commission) was developing the drafts to Regulatory Guide 1.190.<sup>9</sup> The Experiment provided the means of using cavity dosimetry as part of the 10 CFR 50, Appendix H, vessel monitoring requirements. It also provided the means of re-confirming the uncertainty in the measurement methodology based on the National Institute of Standards and Technology's "Standard and Reference Field Validation".<sup>19</sup>

The cavity data [

] The measurement database presented in

Reference 1 [

] This topical

report's updated measurement database includes [

] dosimetry in the fuel-beltline and dosimetry above and below the fuel-beltline.

An important part of the Research and Development supporting this topical report was the application of Mathematical Statistics to the Measurement database. As stated above, [

] Fracture Mechanics safety analyses are

based on a greater than 95 % confidence that 95 % (95 / 95) of the analytical predictions will bound the actual toughness of the structural material. The 95 / 95 confidence level is further supported by a tolerance factor of  $\pm 2.00$ . For there to be 95 / 95 confidence

with a tolerance factor of  $\pm 2.00$  [ ]

The Reference 1 dosimetry measurement database [ ]

[ ] would not automatically support the Fracture Mechanics safety analyses. One or two data sets would require a much larger tolerance factor (for example,  $\pm 4.00$ ) to be consistent with the Regulatory Guide 1.99, Revision 2<sup>8</sup> adjusted reference temperature (ART) 95 / 95 margin term.

This is the same statistical issue that occurred when Framatome developed the "Fluence and Uncertainty Methodologies"<sup>1</sup> topical report [ ]

[ ] The key to the data supporting Fracture Mechanics safety analyses was the Uncertainty Methodologies part of the topical report.<sup>1</sup>

Mathematical Statistics modeling demonstrated that [ ]

[ ] Fracture Mechanics safety analyses could apply the ART margin term with a tolerance factor of [ ]

The Mathematical Statistics modeling presented below has also demonstrated that

[

] The details of the statistical modeling are presented in Section 3.5, "Uncertainty Methodology".

The following Subsections, 3.1, 3.2 and 3.3 use the Davis Besse Experiment as an example for the discussion of the measurement modeling, experimental techniques, and procedures. The Experiment's dosimetry was loaded during the outage prior to the operation of Cycle 6. It was removed following Cycle 6 and sent to various laboratories for measurement. The Experiment had a large amount of data including [

]

### **3.1 *Davis Besse Experiment's Configuration***

Figure 3-1 shows the general arrangement of the cavity dosimetry holders. The cavity dosimetry consisted of sixteen specially fabricated aluminum dosimetry holders, each containing five sets of dosimeters. The holder design secured the dosimetry in a fixed direction – either facing towards the core or away from it. Some dosimeters were loaded into gadolinium cans to shield them from the thermal flux, while others were placed in aluminum cans (thereby being unshielded).

Five 41 foot-long beaded stainless steel chains were also placed in the cavity region quadrants at the azimuthal positions of interest. The chain assemblies were mounted beneath the Nuclear Instrumentation boxes in open source tube penetrations. The chains were anchored on the containment floor to limit lateral movement during plant operation. A planar view shown in Figure 3-2 displays the relative positions of the

temporary cavity dosimetry assemblies, the permanent cavity dosimetry holder, the stainless steel chains, and the in-vessel standard surveillance capsules.

### 3.2 *Davis Besse Experiment*

The Davis Besse Experiment was an extensive test [

] The

Experiment included the 554 radiometric activation and fission dosimeters, including 243 activation foils or wires, 46 fission foils, and 265 stainless steel chain segments. In addition, the Experiment had many developmental dosimeters. These included: 71 Solid State Track Recorders (SSTRs), 40 Helium Accumulation Fluence Monitors (HAFMs), 22 Ultra-high Purity Niobium Dosimeters, 9 Lithium-Fluoride Detector Chips, and 3 Paired Uranium Detectors.

The in-vessel dosimetry consisted of two standard unirradiated surveillance capsules installed in the surveillance capsule holder tube at the peak flux location. These capsules contained eight standard B & W radiometric dosimeter sets.

The standard radiometric dosimeter set is designed to cover the upper range of the energy spectrum. This set includes an assortment of foil and wire dosimeters. The target isotopes in these dosimeters are activated (or fissioned) and the daughter products are measured.

In addition to the standard capsule and cavity dosimetry, the SVAM methodology was benchmarked against [

]

[

]

Unlike the standard radiometric detectors, the SSTRs do not rely on the counting of activation products, which have limited half-lives. The SSTRs create a permanent record of their irradiation history and do not require prompt counting. They also do not become significantly activated when irradiated, making shipping and handling easier and less expensive. In order to qualify the SSTR detectors for future use, they were installed in identical locations as the standard radiometric detectors. A total of eighty-five SSTR neutron dosimeters were installed at Davis Besse during Cycle 6. After irradiation, several of the dosimeters were discarded due to insufficient mass calibrations or physical damage. In the end, a total of thirty-one dosimeters remained with usable measurements. Due to the high failure rate, the SSTR dosimeters were not included in this topical.

HAFMs are passive neutron dosimeters that use the accumulation of helium gas as the measurable quantity that is related to neutron fluence. The helium is generated through  $(n, \alpha)$  reactions in the target material and remains, unchanged, in the detector material for several years after formation. The amount of helium is measured by high-sensitivity gas mass spectrometry. The Davis Besse experiment included lithium HAFMs. These detectors cover the "thermal" energy range.

Twenty-two high purity Niobium dosimeters were exposed in the cavity at Davis Besse during Cycle 6. Twenty of these were near midplane, one was at the upper active fuel elevation and one was at the nozzle elevation. The Niobium measurement uncertainty was consistent at all axial locations.

In addition to various types of neutron dosimeters, lithium-7 fluoride (LiF) optical absorbance gamma dosimeters were placed at eight cavity locations. The purpose of these dosimeters was to indirectly measure the gamma field in the vicinity of the neutron dosimeters.

After being removed from the reactor, the LiF chips were shipped to the National Institute of Standards and Technology (NIST) for measurement of the optical absorbance, annealing, and re-calibration in a known gamma ray field. The neutron flux spectrum at each LiF chip location was calculated using a semiempirical methodology that reconciles measured neutron dosimeter data to calculated neutron spectra. Appropriate energy-dependent normalization factors were developed and applied to the calculated flux. The neutron flux spectra were then used to determine the total neutron dose absorbed in each LiF chip. Finally, the calculated neutron dose was subtracted from the measured (total) dose, yielding the integrated gamma-ray dose. Calculated-to-measured (C/M) gamma dose ratios were then established for each LiF chip. Since this topical focuses on neutron fluence uncertainty, the gamma LiF detectors were not included. However, they may be revisited in future if accurate gamma fluxes are required.

### **3.3 *Measurement Methodology***

There were three categories of neutron dosimeters irradiated in the experiment:

1. Radiometric Dosimeters:
  - a. Fissionable (Subsection 3.3.1),
  - b. Non-fissionable activation (Subsection 3.3.2),
  - c. Niobium (Subsection 3.3.3), and
  - d. Stainless steel chains (Subsection 3.3.4),
2. Solid State Track Recorders (not included, see Section 3.1), and
3. Helium Accumulation Fluence Monitors (Subsection 3.3.5).

Each subsection provides a discussion of the measurement techniques and the corrections required to determine specific activity from counting data. The



measurement results are provided in Section 5 (Table 5-2). A more thorough discussion of the measurement methodology is provided in Section 5.0 of Reference 1.

### 3.3.1 Fissionable Radiometric Dosimeters

The fissionable dosimeters ( $^{235}\text{U}$ ,  $^{238}\text{U}$ , and  $^{237}\text{Np}$ ) in the form of wires and foils were counted directly using a gamma spectrometer. Dosimeter diameter or thickness was measured and the sample was weighed. The target for the final count was 10,000 counts in the photo-peak of interest while keeping the counter dead time below 15.0 %.

The  $^{137}\text{Cs}$  662 keV gamma was counted and analyzed for all of the fissionable radiometric dosimeters. In addition, the  $^{233}\text{Pa}$  312 keV gamma was counted for some  $^{237}\text{Np}$  dosimeters, the  $^{235}\text{U}$  186 keV gamma for the  $^{235}\text{U}$  dosimeter, and the  $^{234\text{m}}\text{Pa}$  1001 keV gamma for some  $^{238}\text{U}$  dosimeters. The detectors were calibrated using a NIST-traceable mixed gamma "point source" standard. The source was actually a thin mass a few millimeters in diameter. The placement of the dosimeters was such that the side of the dosimeter closest to the detector was in the same plane as the standard source. A correction was required in most cases for the fact that the effective distance from the dosimeter to the detector differed slightly from the standard to detector distance.

A different measurement technique was used for the fissionable oxide powders. The uranium oxide and neptunium oxide dosimeters were dissolved and diluted in a scintillation vial. The activity for each was determined by counting the  $^{137}\text{Cs}$  662 keV gamma. A NIST-traceable mixed gamma standard was counted in an identical geometry; therefore, no corrections for geometry or attenuation were required for the dissolved dosimeters. The mass of uranium was determined by inductively coupled plasma atomic emission spectroscopy and the mass of neptunium was determined from the measured  $^{233}\text{Pa}$  content using the 312 keV gamma.

The data is reported in micro-Curies per gram of target ( $\mu\text{Ci/gm}$ ) where the target is the first named isotope in the designation of each reaction. The fraction of the dosimeter mass that corresponds to the mass of each fissionable isotope was required. It was

determined from information on the fraction of the aluminum alloy mass that was  $^{238}\text{U}$  or  $^{237}\text{Np}$ , the fraction of the oxide mass that was  $^{238}\text{U}$ ,  $^{235}\text{U}$  or  $^{237}\text{Np}$ , and the fraction of the mass of encapsulated dosimeters that was vanadium.

The data for all of the fissionable radiometric dosimeters were corrected for the difference between the effective distance from dosimeter to detector and the standard to detector distance. The dosimeters are partitioned into four slabs parallel to the face of the detector. A correction factor is determined for each slab assuming that the response varies as the reciprocal of the distance to the detector squared. The geometry factor for the dosimeter is then obtained from a weighted average of the slab factors using the cross-sectional area of each slab as the weight. The dosimeter results are also corrected for self-absorption of the 662 keV gamma used to measure the  $^{137}\text{Cs}$  activity and decay corrected to January 26, 1990.

### 3.3.2 Non-Fissionable Radiometric Dosimeters

The measurement technique is basically the same as described in Section 3.3.1 for fissionable wires and foils. Dosimeter diameter or thickness was measured and the sample was weighed. The target for the final count was 10,000 counts in the photopeak of interest while keeping the counter dead time below 15.0 %.

The photopeaks used to determine the activity for each dosimeter are listed in Table 3-3. The detector was calibrated with a NIST-traceable mixed gamma "point source". The data is reported in micro-Curies per gram of target isotope. The fraction of the dosimeter mass corresponding to the target isotope mass is therefore required. This was obtained from the weight fraction of the element in the alloys and/or the weight fraction of the target in the element. The impurities in the dosimeters were sufficiently low such that they did not affect the target weight.

The data for all of the non-fissionable radiometric dosimeters were corrected for the difference between the effective distance from dosimeter to detector and the standard to detector distance. The dosimeter results are also corrected for self-absorption and decay corrected to January 26, 1990.

### 3.3.3 Niobium Dosimeters

The measurement technique for the reaction  $^{93}\text{Nb} (n,n') ^{93m}\text{Nb}$  is significantly different from the other radiometric monitors used in the benchmark experiment. The activation product  $^{93m}\text{Nb}$  decays with a 16.13 year half-life by internal conversion. The  $^{93m}\text{Nb}$  energy level is 30 keV above the ground state; however, the decay does not take place with a transition to the ground state giving off a 30 keV gamma. Instead, all of the energy is transmitted to an orbital electron. The electron leaves the atom with an energy equal to 30 keV minus the binding energy of the electron. An electron in a higher energy level then drops into the level of the ejected electron giving off an X-ray, another electron replaces that electron, etc. On the average, 9.26 % of the decays result in the production of one of the two X-rays which form the 16.6 keV doublet. The  $^{93m}\text{Nb}$  activity is determined using this doublet. Self-absorption in the dosimeter and absorption in other materials is much more of a factor in this measurement than is the case with normal gamma counting.

The apparent activity of  $^{93m}\text{Nb}$  is first determined for each dosimeter by counting the dosimeters and a NIST prepared reference "point source" standard with an X-ray detector. The dosimeters and standard are positioned such that no materials are located between the dosimeters or standard and the X-ray detector. The geometry is such that the location of the side of the dosimeter, foil or wire, that is opposite the detector coincides with the location of the thin "point source" standard. A Monte Carlo program called NIOBIUM is executed for each dosimeter and the standard. The geometry of the dosimeter, foil or wire, and X-ray detector is modeled in the code as is the attenuation coefficient of the 16.6 keV X-rays in the dosimeter. X-rays with this energy are started randomly throughout the dosimeter with a random direction. A determination is made as to whether each X-ray escapes the dosimeter and intersects with the detector. A sufficient number of histories are included such that approximately 10,000 hits are recorded. The same code is executed with the point source geometry. In this case, the X-rays are generated in a very thin region with a low attenuation coefficient.

The apparent  $^{93m}\text{Nb}$  activity in Becquerel (Bq) is then obtained from:

$$\text{Act } (^{93m}\text{Nb}) = S \times \text{CR} \times \text{DR} \quad (3-1)$$

where:

- S = Standard source activity (Bq).
- CR = Ratio of dosimeter counts per second to the standard counts per second on the X-ray detector.
- DR = Ratio of results from the NIOBIUM calculation standard to the result of the NIOBIUM calculation for the dosimeter.

The NIOBIUM code calculates the fraction of the starting 16.6 keV X-rays which reach the detector from the dosimeter and standard. Combining the ratio of the NIOBIUM calculations with the ratio of counts per second cancels out effects such as attenuation through the window of the detector and the fraction of the X-rays which hit the detector that are actually observed. Therefore, it is not necessary to know values for such effects that are common to both the dosimeter and standard measurements.

The  $^{93m}\text{Nb}$  activity determined above was referred to as the apparent  $^{93m}\text{Nb}$  activity. This is because in addition to the true  $^{93m}\text{Nb}$  activity it may also include fluorescence caused by  $^{182}\text{Ta}$  and  $^{94}\text{Nb}$  decays. The  $^{182}\text{Ta}$  is produced by activation of  $^{181}\text{Ta}$  impurity in the niobium and  $^{94}\text{Nb}$  is produced by activation of  $^{93}\text{Nb}$  during the irradiation. Both decays give rise to betas and gammas. Interactions of this radiation with orbital electrons can lead to production of the same 16.6 keV X-rays as are observed from the  $^{93m}\text{Nb}$  decays. This is termed fluorescence. Two Monte Carlo codes are used to correct for the fluorescence. One called BPTRACE is executed for each beta and gamma or for an averaged effective beta and an averaged effective gamma. The code first determines whether the betas or gammas are stopped in the dosimeter, and, if so where. It then generates 16.6 keV X-rays at these points with an externally determined yield and determines whether the X-rays escape from the dosimeter and hit the detector.

Another Monte Carlo program called IP is used to generate one of the required inputs to the BPTRACE code when it is used for betas. The part of the apparent  $^{93m}\text{Nb}$  activity due to fluorescence is determined from measured  $^{182}\text{Ta}$  and  $^{94}\text{Nb}$  activities with a germanium detector and the BPTRACE Monte Carlo calculations. After correcting for fluorescence, the  $^{93m}\text{Nb}$  activity is converted to micro-Curies per gram of target  $^{93}\text{Nb}$  and is decay corrected to January 26, 1990.

### 3.3.4 Stainless Steel Chains

Five stainless steel chains located as shown in Figures 3-1 and 3-2 were irradiated during Cycle 6. The chains consisted of [

]

The chains extended from near the seal plate to the concrete floor. Samples were cut from the chains and analyzed for the  $^{54}\text{Fe}(n,p)^{54}\text{Mn}$  reactions to provide axial fluence rate data.

The measurement technique for the chain segments was similar to that for the other radiometric dosimeters. However, because of the significant difference in geometry, the corrections were determined in a different way. After cleaning, the chains were cut as required and each measurement segment was weighed and mounted on a PetriSlide™ using double-sided tape, spiraling the chain segments around the center of the slide. Measurement segments were cut [

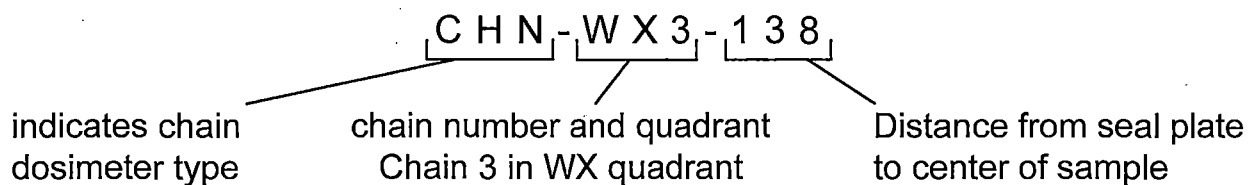
]

The 834 keV photo-peak from  $^{54}\text{Mn}$  was used for the measurement. The detector was calibrated with a NIST traceable mixed gamma "point source" and the data was processed with a computer-based multichannel analyzer.

The fraction of the mass of the chain segments corresponding to  $^{54}\text{Fe}$  is required to express the activity in micro-curies per gram of target isotope. Unirradiated samples of the chains were dissolved in acid and analyzed by inductively coupled plasma atomic emission spectrometry. The Fe weight fraction was determined. Applying the isotopic weight fractions, the fraction of the chain mass that is  $^{54}\text{Fe}$  was determined.

The data for all of the stainless steel chains were corrected for the difference between the effective distance from dosimeter to detector and the standard to detector distance and decay corrected to January 26, 1990. The chain results are also corrected for the absorption within the chain systems of the 834 keV gammas in the  $^{54}\text{Mn}$  case. The standard wire geometric formula gives a good approximation for the geometry factor. The Monte Carlo method was used to confirm that this is an appropriate value for chain segment at the same shelf distance.

The following chain locations are shown in Figure 3-2: Chain 3 is in the WX quadrant, Chain 4 is in the XY quadrant, Chain 1 is in the YZ quadrant, and Chain 2 is in the ZW quadrant. The chain segment identifiers explained below are based on the chain location, chain number, and sample distance below the seal plate.



### 3.3.5 Helium Accumulation Fluence Monitors (HAFMs)

HAFMs are neutron dosimeters that use the accumulation of helium gas as the measurable quantity that is related to neutron fluence. The helium is generated through  $(n, \alpha)$  reactions in the target material and remains, unchanged, in the detector material for several years after formation. The amount of helium is measured by high-sensitivity gas mass spectrometry.

Following identification by package number, each Al-Li wire package was carefully unwrapped and the individual samples removed. Each sample was then examined under a low power optical microscope to verify sample integrity. In addition, the samples were weighed to compare their post-irradiation mass with that obtained during sample fabrication. In each case, no significant mass change was observed.

After identification and inspection, the individual Al-Li wire HAFMs in each package were prepared for helium analysis. This preparation involved first etching the sample to remove ~0.05 mm off the surface, followed by weighing to determine the etched sample mass. The purpose of the etching step was to remove surface material which could have been affected by  $\alpha$  – recoil either into or out of the samples during irradiation.

The helium content of each specimen was determined by isotope-dilution mass spectrometry following vaporization of each in a resistance-heated tungsten-wire crucible in one of the mass spectrometer system's high-temperature vacuum furnaces. The absolute amount of  $^4\text{He}$  released was measured relative to a known quantity of added  $^3\text{He}$  "spike".

The  $^3\text{He}$  spikes were obtained by expanding and partitioning a known quantity of gas through a succession of calibrated volumes. The mass spectrometer was calibrated for mass sensitivity during each series of runs by analyzing known mixtures of  $^3\text{He}$  and  $^4\text{He}$ . The results of the measurements are in terms of helium concentrations in atomic parts per million or atomic parts per billion. Helium concentrations are relative to the total number of  $^6\text{Li}$  atoms in each specimen.

### 3.4 *Standard and Reference Field Validation*<sup>19</sup>

The large amount of measurements that were performed for the Davis Besse Experiment provided an opportunity for the National Institute of Standards and Technology (NIST) to cross-calibrate the measured results (M). For Framatome, this cross-calibration provided a means of (a) re-assessing biases ( $B_M$ ) that could possibly be in the measurement methods and procedures, and (b) re-validating the magnitude of the root mean square standard deviation ( $\sigma_M$ ).

The measurement uncertainties were validated by standard NIST reference field evaluations. NIST found that the laboratory uncertainties had no biases and appropriately bracketed the differences between their reference results and the laboratory's results. The bracketing provided verification of Framatome's estimated standard deviation.

The re-validation included (1) the measurement of NIST reference field dosimetry coupled with uncertainty analyses, (2) the confirmation of uncertainties in the equipment, methods, and procedures used by the laboratory, (3) a comprehensive quality assurance verification of the uncertainties, and (4) an independent verification of the measurement uncertainties by consultants R. Gold of the MC<sup>2</sup> corporation and W. N. McElroy of the CTS corporation. This re-validation provided Framatome with [

] the calculated results from SVAM.

The re-validation of the accuracy and precision in the laboratory's measurements not only provided [

]



The conclusions from the "Standard and Reference Field Validation" are that:

- 1) no statistically significant biases ( $B$ ) can be identified in the laboratory's measurements ( $M$ ), nor were there ever any identifiable biases,  $B_M = 0.0$ ,
- 2) the relative standard deviation [ ]
- 3) [ ]

### 3.5 *Uncertainty Methodology*

As discussed above in Section 3.4, the National Institute of Standards and Technology (NIST) found that Framatome's Measurement database has no biases,  $B_M = 0.0$ . The measurement uncertainty methodology was thereby defined in terms of combined standard deviations. The standard deviations are from (a) the NIST traceable calibration standards, (b) the experimental equipment, and (c) the procedures used to predict the measured activities. [ ]

[ ] These parameters are listed in Table 3-4 along with the typical value.

This section (3.5) is divided into subsections to provide clarity with respect to the overall Measurement Uncertainty Methodology. The laboratory's random uncertainties are of course the basis for all measurement uncertainties. Table 3-4 provides a good basic understanding of the measurement methodology's uncertainties. For the regions above and below the fuel-beltline, more discussion is provided in Subsection 3.5.2.

Whether dealing with measured data in the fuel-beltline (MB) or the regions above and below the fuel-beltline (MABB), there are no measurement biases,  $B_{MB} = 0.0$  and  $B_{MABB} = 0.0$ . Moreover, whether the measurements are in the fuel-beltline or above and below the fuel-beltline, the laboratory's random uncertainties are estimated with exactly the same methodology as outlined in Table 3-4. As seen in Table 3-5 however, there is a difference in the estimates of the fuel-beltline relative standard deviation ( $\sigma_{MB} \%$ ) versus the deviations above and below the fuel-beltline ( $\sigma_{MABB} \%$ ).

Looking at the values of the Measurement Deviations in Table 3-4, (a) some of the parameter's deviations are dependent on the mean value of the radiation reactions, while (b) some of the deviations are constant. [

]

### 3.5.1 Relative Random Uncertainties

Equation 2-1 is the usual formula for determining the root mean square standard deviation in a set of data. The standard deviation is a positive constant. It is a random variable and thereby not dependent on any other variable. It is only dependent on the methodology used to determine the values of the measured (or calculated) parameter. The units of the standard deviation are the same as those of the parameter being measured (or calculated).

Frequently, it is necessary to convert a standard deviation into a relative standard deviation when combining deviations. Equation 3-2 is the transformation of the usual standard deviation formula (Equation 2-1) to a relative standard deviation.

$$\sigma_{x/\bar{x}} = \left( \frac{\sum_{i=1}^N \left( \frac{x_i}{\bar{x}} - 1 \right)^2}{N-1} \right)^{1/2} \quad (3-2)$$

The reason for making the transformation from a standard deviation with specific units to a relative percentage is to be able to combine the deviation in one random variable with the deviation in another. For example, the uncertainty of interest for irradiation degradation is the fluence related *dpa* (displacements per atom). Several of the measured parameters in Table 3-4 have standard deviations in units that are much different from neutrons per centimeter-squared, activation reactions per unit of weight, or displacement reactions per atom. Therefore, when combining the Table 3-4 standard deviations, all the random deviations are transformed to relative standard deviations.

The ART (Adjusted Reference Temperature) values used for Fracture Mechanics safety analyses are in units of temperature according to the Regulatory Guide 1.99, Revision 2 equations. Likewise, the margin term uncertainties are in units of temperature. The *dpa* effective fluence uncertainty part of ART however is a relative standard deviation. To ensure the validity of the safety analyses, there must be consistency between the temperature uncertainty and the fluence uncertainty. Regulatory Guide 1.190<sup>9</sup> explains that the consistency is statistically acceptable as long as the fluence standard deviation is no greater than 20 %.

When constant standard deviations, with specific dimensions (for example, temperature or micro-Curies), are transformed to dimensionless relative values, there is an implicit dependency on the parameter's mean value (for example, temperature or micro-Curies). Considering the methods of Mathematical Statistics, the relative standard deviation could not be constant. If it were, the Equation 2-1 constant standard

deviations would not be independent random variables, but would have some dependency. Thus, when a constant relative random variable is applied to the fuel-beltline region, the implication is that [

]

### 3.5.2 Uncertainty Above & Below the Fuel-Beltline

Based on the discussion above (Section 3.5.1) concerning Relative Random Uncertainties, if the fuel-beltline relative standard deviation was a constant 7.00 %, then above and below the fuel-beltline the relative standard deviation would be huge.

Equation 3-3 is based on the methods of mathematical statistics. [

]

$$\left[ \right] \quad (3-3)$$

As seen in the Equation 3-3 left-hand expression, the fuel-beltline's relative standard deviation is 7.00 %. [

] the methods of mathematical statistics require that the standard deviation [ ] be a constant.

In the regions above and below the fuel-beltline the magnitude of the radiation reactions drops dramatically. It is quite common for radiation reaction values ( $\psi$ ) above and below the fuel-beltline to be 100 times smaller than the beltline's mean value. Using the example of Equation 3-3, [

]

[ (3-4) ]

Table 3-5 shows that the laboratory's relative root mean deviations in the measurements above and below the fuel-beltline are [

]

[ ] well-defined root mean deviations above and below the fuel-beltline [

] The discussions in the

following sections explain the [

]

**3.5.3 [ ] Uncertainty Methodology**

When the mean ART value is used in Fracture Mechanics safety analyses, there is 95 / 95 confidence that the value is acceptable. The probability that positive deviations influence the results is balanced by the probability that negative deviations influence the results. The statistical probability is such that the mean ART value is unchanged by random uncertainties. That is, the statistical application of uncertainties is symmetric with additive and subtractive operations ( $\pm \sigma$ ). The net effect is "0.00".

[ ] the random fluence uncertainty estimated for the Regulatory Guide 1.99, Revision 2 database is 20 %. The positive application to the mean value is  $(1 + .20)$ .<sup>9</sup> The

statistical problem is that [ ] This  
is not consistent with mathematical statistics' methods; [ ]  
]

The mathematical statistical application [

] is "0.00".

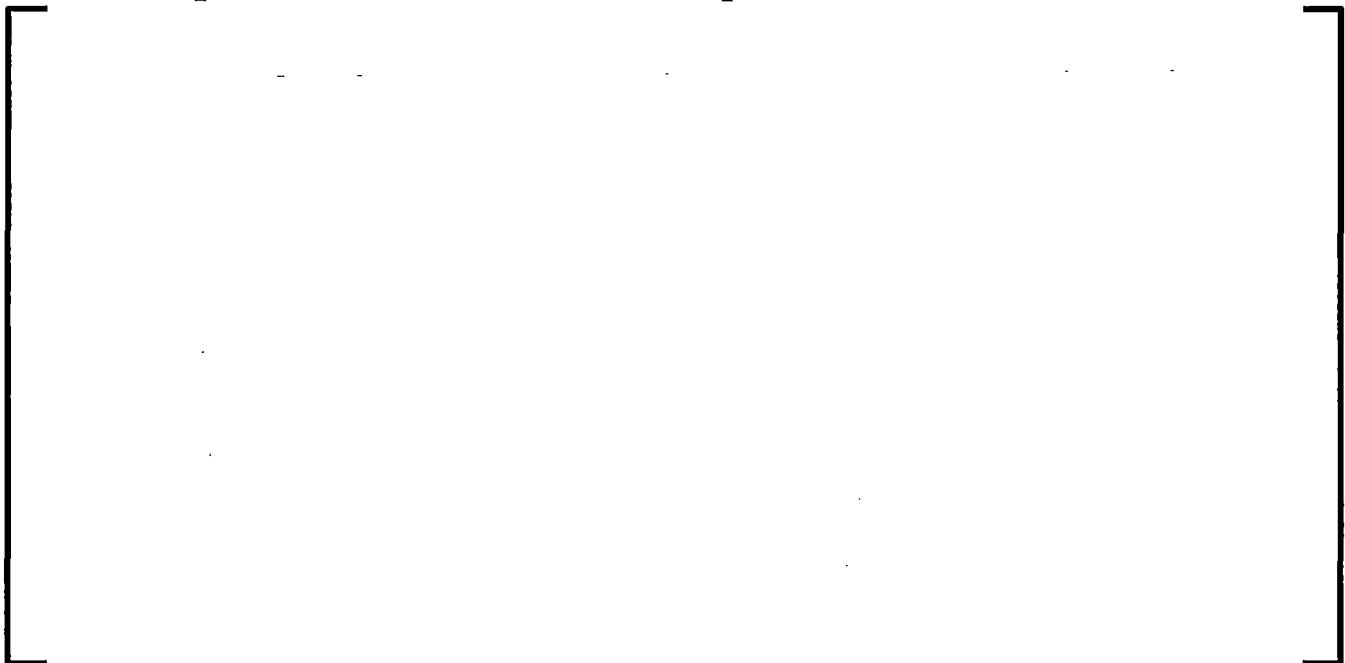
It is the application of [

] random uncertainties above and below the fuel-  
beltline (ABB). The following Section (3.5.4) explains [

]

3.5.4 [

]





The measurement database has the standard deviations and radiation reactions for the fuel-beltline and for the regions above and below the fuel-beltline. It is thereby straightforward [

]



The general application of Equation 3-8 is based on [

] the root mean

deviations in the fuel-beltline [

]

3.5.5 [ ]

[

] The measurements not

only included the value of the laboratory's radiation reactions but also included the value for the relative root mean deviation. [

] With respect to the

measurement database uncertainties, [

]

There are several important points with respect to the information in Table 3-5 that are listed below the table. The most important is that [

]



**Figure 3-1**

**General Arrangement of Cavity Dosimetry Benchmark Experiment**



**Figure 3-2**  
**Cavity Dosimetry Experiment Plan View**



**Table 3-1  
Cavity Dosimetry Loading Plan**

<b>Holder and Location</b>	<b>Unshielded Positions 1, 2 (Aluminum Cases)</b>	<b>Shielded Positions 3, 4, 5 (Gadolinium Cases)</b>
<p>A [                    ]</p>	<p>1 – B &amp; W RMs Fe Co</p> <p>2 – B &amp; W RMs Fe Co</p>	<p>3 – LiF</p> <p>4 – B &amp; W RMs Fe Co HAFM 3 Be Li</p> <p>5 – B &amp; W RMs Fe Ni 3 Cu Co</p>
<p>B [                    ]</p>	<p>1 – HEDL RM</p> <p>2 – B &amp; W RMs Fe Co</p> <p>B &amp; W SSTR (2B)</p>	<p>3 – LiF</p> <p>4 – HEDL RM HEDL SSTR (23H)</p> <p>5 – B &amp; W SSTR (2C2) B &amp; W RMs Fe Ni 2 Cu Co</p>
<p>C [                    ]</p>	<p>1 – B &amp; W RMs Fe Co</p> <p>2 – B &amp; W RMs Fe Co</p>	<p>3 – SS Chain #1</p> <p>4 – B &amp; W RMs Fe Ni 2 Cu Co Nb (ToyoSoda) HAFM 3 Be – 1 Li</p>



Holder and Location	Unshielded Positions 1, 2 (Aluminum Cases)	Shielded Positions 3, 4, 5 (Gadolinium Cases)
<p>G [                    ]</p>	<p>1 – HEDL RM PUD</p> <p>2 – B&amp;W RMs Fe Co Co-Al Wire Fe Wire PUD</p>	<p>3 – LiF</p> <p>4 – LiF</p> <p>5 – HEDL RM B &amp; W RMs Ni Wire Co-Al Wire Np-Al Wire U-Al Wire</p>
<p>H [                    ]</p>	<p>1 – B&amp;W RMs Fe Co</p> <p>2 – SS Chain #4</p>	<p>3 – LiF</p> <p>4 – B &amp; W RMs Fe Co Nb (ToyoSoda) HAFM 3 Be – 1 Li</p> <p>5 – SS Chain #5 U-238 Powder Np-237 Powder</p>
<p>J [                    ]</p>	<p>1 – B&amp;W RMs Fe Co Co-Al Wire Fe Wire</p> <p>2 – SS Chain #6</p>	<p>3 – B &amp; W RMs Fe Co Nb (ToyoSoda) Nb (MOL) HAFM 3 Be – 1 Li</p> <p>4 – B &amp; W RMs Fe Co</p> <p>5 – Co-Al Wire Ni Wire Np-Al Wire U-Al Wire</p>

Holder and Location	Unshielded Positions 1, 2 (Aluminum Cases)	Shielded Positions 3, 4, 5 (Gadolinium Cases)
K [ ]	1 – U of A RM  2 – B & W RMs Fe Co SS Chain #7	3 – U of A RM  4 – U of A RM  5 – B & W RMs Fe Co
L [ ]	1 – HEDL RM B & W RMs Co-Al Wire Fe Wire  2 – B & W RMs 2 Fe 2 Co Co-Al Wire Fe Wire	3 – HEDL RM B & W RMs Co-Al Wire Ni Wire Np-Al Wire U-Al Wire  4 – B & W RMs Fe Ni Cu Co Co-Al Wire Ni Wire Np Wire U-Al Wire  5 – B & W RMs Fe Co
N [ ]	1 – B & W SSTR (33B)  2 – B & W RMs Fe Co Co-Al Wire Fe Wire	3 – B & W RMs Fe Ni Cu Co  4 – Co-Al Wire Ni Wire Np Wire U-Al Wire B & W SSTR (33C)  5 – 2 Np-237 Powder

Holder and Location	Unshielded Positions 1, 2 (Aluminum Cases)	Shielded Positions 3, 4, 5 (Gadolinium Cases)
P [ ]	1 – 2 Co-Al Wire 2 Fe Wire  2 – B & W RMs Fe Co Co-Al Wire Fe Wire	3 – LiF  4 – 2 Co-Al Wire 2 Ni Wire 2 Np Wire 2 U-Al Wire  5 – U-Al Wire Np Wire Co-Al Wire Ni Wire
Q [ ]	1 – B & W RMs Fe Co  2 – B & W RMs Fe Co	3 – B & W RMs Fe Ni Cu Co Nb (ToyoSoda) HAFM 3 Be – 1 Li  4 – B & W RMs Fe Co  5 – HAFM 3 Be – 1 Li Nb (MOL) 2 Nb (ToyoSoda)
R [ ]	1 – Bechtel RMs Fe Co  2 – Bechtel SSTR (B & W-1) B & W SSTR (1B)	3 – LiF  4 – Bechtel RMs Fe Ni 3 Cu Co B & W SSTR (1C)  5 – Bechtel SSTR (B & W-3) Bechtel SSTR (B & W-2)

Holder and Location	Unshielded Positions 1, 2 (Aluminum Cases)	Shielded Positions 3, 4, 5 (Gadolinium Cases)
S [ ]	1 – B & W RMs Fe Co  2 – B & W SSTRs (5B, 6B)	3 – B & W RMs Fe Ni Cu Co  4 – Nb (ToyoSoda) B & W SSTRs (6C, 5C, B & W-15, B & W-16)  5 – MOL RM
T [ ]	1 – HEDL RM  2 – B & W RMs Fe Co	3 – LiF  4 – HEDL RM Bechtel SSTR (B & W-6)  5 – HAFM 3 Be – 1 Li HAFM 3 Be – 1 Li 2 Be – 1 Li 2 Nb (MOL) 2 ToyoSoda Nb B & W RMs Fe Ni Cu Co
U [ ]		4 – B & W RMs Fe Ni Cu Co B & W SSTR (7 & 8C)

## Notes:

- 1) LiF detector chips are in shielded locations, but are in aluminum cases.
- 2) MOL RMs use aluminum cases with internal Cd shielding.



## Key:

B & W	=	BWNS supplied dosimetry
HEDL	=	Hanford Engineering Development Laboratory supplied dosimetry package
MOL	=	Center for the Study of Nuclear Energy, MOL Belgium supplied dosimetry package
PUD	=	Paired Uranium Detector
RM	=	Radiometric Monitor
SSTR	=	Solid State Track Recorder
HAFM	=	Helium Accumulative Fluence Monitor
U of A	=	University of Arkansas supplied dosimetry package (now property of Arkansas Tech University)
LiF	=	Lithium Fluoride detector

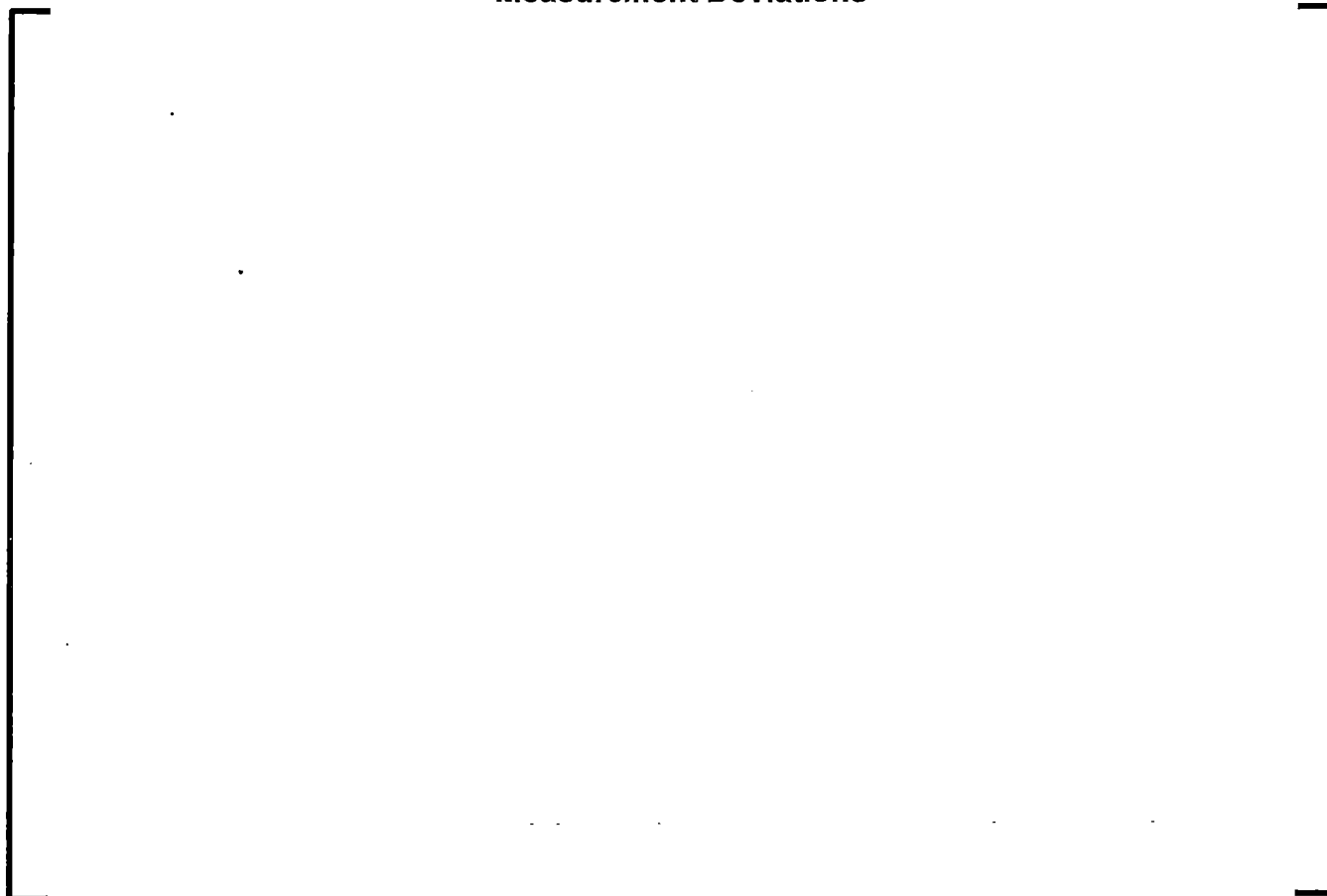
**Table 3-2**  
**Coordinate Location of Dosimetry**

\*Elevation dimensions for the Permanent dosimetry capsules are taken to the center line of the center capsule lid bolts for both the upper and lower capsules.

**Table 3-3**  
**Photopeak Analyzed for Each Reaction**

Reaction	Gamma Ray
$^{54}\text{Fe} (n,p) ^{54}\text{Mn}$	834 keV
$^{58}\text{Ni} (n,p) ^{58}\text{Co}$	811 keV
$^{63}\text{Cu} (n,\alpha) ^{60}\text{Co}$	1332 keV
$^{46}\text{Ti} (n,p) ^{46}\text{Sc}$	1121 keV
$^{109}\text{Ag} (n,\gamma) ^{110\text{m}}\text{Ag}$	658 keV

**Table 3-4**  
**Measurement Deviations**



The following explains the cause of the deviations in the parameters:

Dimensions – The dosimeter dimensions [

]

Weight – The weight of the target material establishes the [

]

Geometry – The geometrical configuration of the [

]

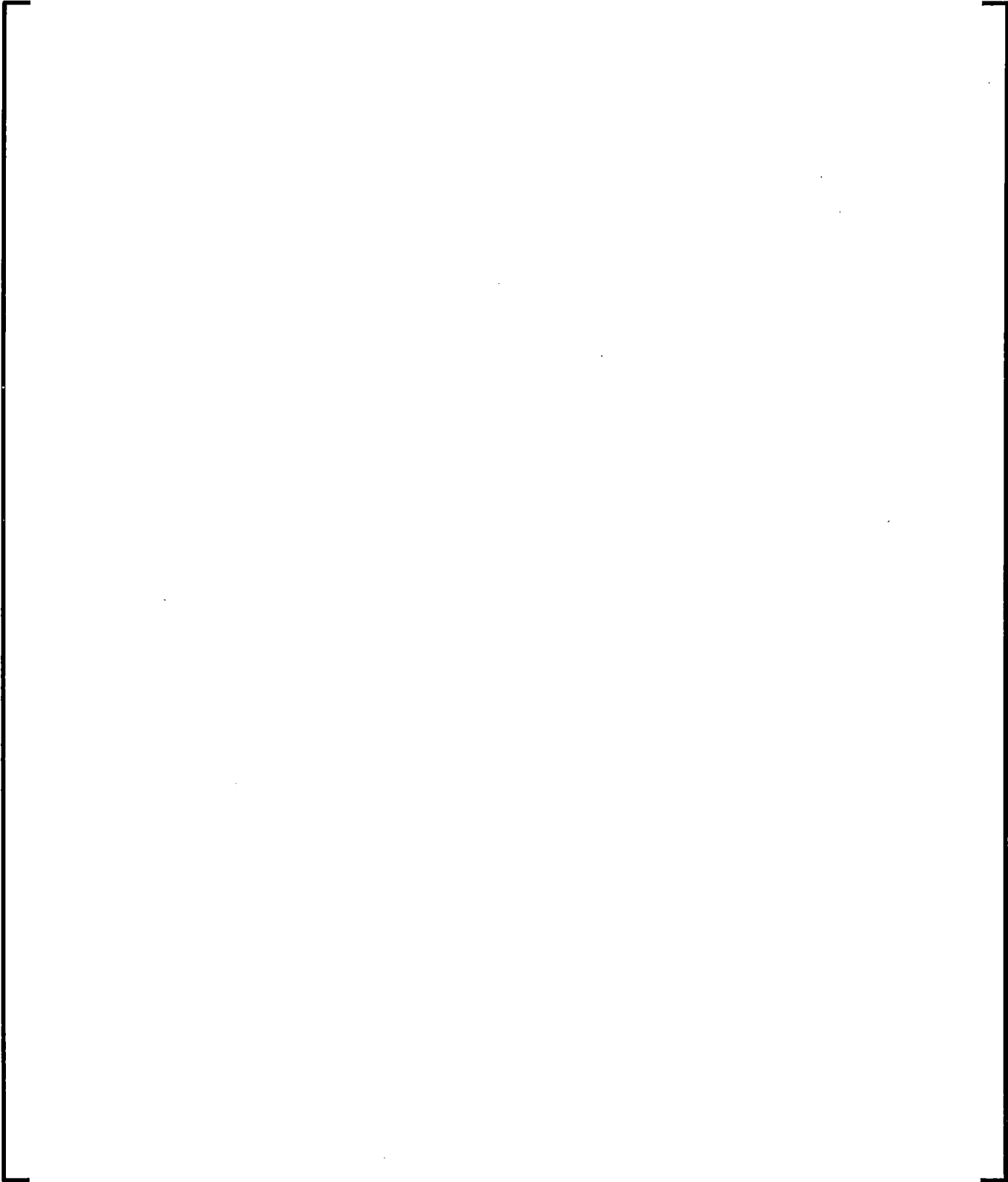
Activity – The [

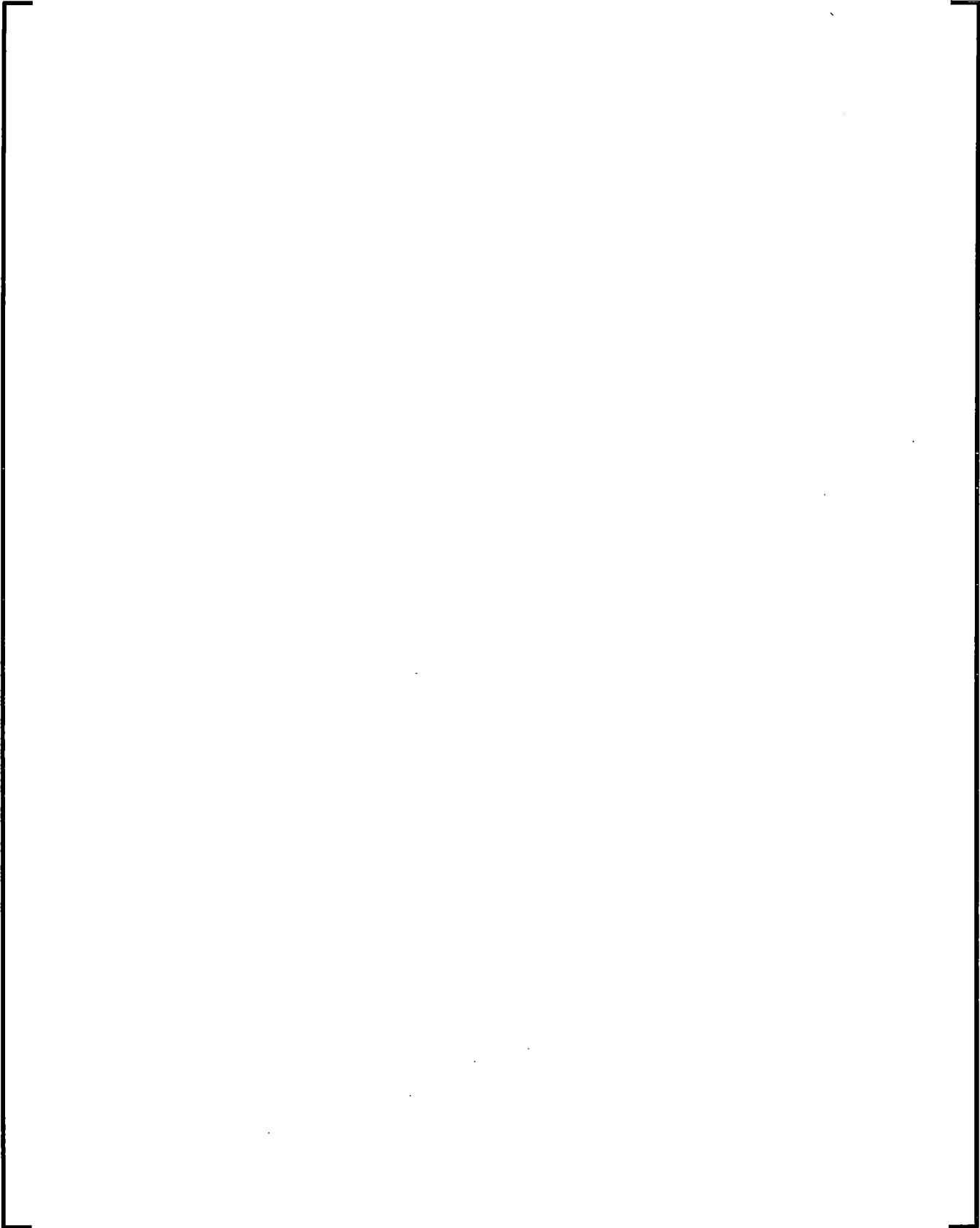
]

Procedures – The [

]

**Table 3-5**  
**Measurement Uncertainties**

A large, empty rectangular frame with a thin black border, centered on the page. It is intended to contain the data for Table 3-5, 'Measurement Uncertainties', but the content is currently blank.



There are several important points with respect to the information in Table 3-5:

- 1) The first point is evident from locations "18, 30 and 36" inches below the mating surface. There are locations (18 inches) [

]

- 2) The last row in the table provides the "Beltline Mean" values. The mean activation is [

] The laboratory's mean uncertainty estimate [

] which covers all fuel-beltline radiation reactions is 7.00 %.<sup>1</sup>

- 3) [

]





5) The last important point with respect to the information in Table 3-5 is [

]



6) As noted in Section 3.4, "Standard and Reference Field Validation", the laboratory's experimental techniques and uncertainties were validated by National Institute of Standards and Technology reference field evaluations. Thus, Framatome's Measurement and Benchmark (Section 5) databases have well-defined random uncertainties which may be appropriately applied to irradiation degradation safety analyses.

#### 4.0 SVAM METHODOLOGY

The SVAM methodology is an update of the Semi – Analytical DORT – Synthesis methodology (see Reference 1, Section 3.0) that Framatome uses for beltline analyses of PWRs and BWRs. The Semi – Analytical DORT – Synthesis methodology was developed in the 1990s for 60 year license renewal. It represented an update of the 1970s Least Squares Adjustment (Unfolding) methodology. (The unfolding methodology is described in Reference 12; this was Framatome’s fifth fluence topical report.) The reason for updating the previous topical reports was to improve the fluence – radiation methodology in concert with recommendations from the NRC.

The SVAM and DORT – Synthesis methodologies continue to be Semi – Analytical. That is, the benchmark database is used to assess biases in the analytical methods, procedures and modeling. As shown in Figure 1-1, in regions that are above the reactor beltline, the DORT – Synthesis methodology simply gives erroneous results that are biased, either too high or too low. The SVAM methodology provides accurate results in these regions.

The transition from the Least Squares Adjustment (Unfolding) methodologies began in 1988. Early in the year, Framatome submitted an update to its Least Squares Adjustment (Unfolding) topical report.<sup>13</sup> However, as explained above in Section 2.4, later that year the NRC expressed concern with the industry’s uncertainties in its “unfolded” fluence methodology. Unfolded fluence uncertainties do not provide sufficient fracture mechanics safety margins with respect to the Regulatory Guide 1.99, Revision 2 methods when the irradiation degradation results are applied to 60-year license renewal applications. As discussed in Reference 1, Section E.2.1, under the heading of “Measurement Biases”, the NRC’s issues included:

1. The FERRET-SAND least squares biasing of the industry’s fluence values,<sup>11</sup>
2. The comparison of PCA results from Hanford using FERRET-SAND and Oak Ridge using LSL-M2,<sup>14</sup> and
3. Scientists finding that unfolding methods did not provide a unique solution.<sup>15</sup>

In May of 1997, Framatome submitted its topical report<sup>1</sup> transitioning from a Least Squares Adjustment (Unfolding) methodology<sup>12</sup> to its updated Semi – Analytical DORT – Synthesis methodology. The updated topical followed the guidelines in Regulatory Guide 1.190 even though the Guide was still in draft form. The NRC approved Framatome’s topical in February of 1999.

As noted in Section 1 of this topical report, Framatome’s DORT – Synthesis methodology continues to be valid in the beltline region for any subsequent license renewal to 80 years and beyond. However, as shown in Figures 2-1 and 2-2, the discrete ordinate’s fluence methodology is not sufficient to geometrically represent nozzle regions and vessel support structures outside of the beltline.

In addition, the discrete ordinate’s methodology is not sufficient to represent the *dpa* degradation of the steel’s crystalline structure. This is due to the fact that the neutron spectrum, represented by the Regulatory Guide 1.99, Revision 2 specimen database, is not the same as the spectrum in the regions that are above and below the beltline. As shown in Figure 4-2 and explained in Subsection 4.4 below, the *dpa* reaction cross-section has numerous inelastic scattering resonances. Discrete ordinate’s DORT – Synthesis is based on the BUGLE-96 multigroup library.<sup>16</sup> There are not enough energy groups in the BUGLE libraries to represent the damage reactions due to the variable neutron spectra in the regions above and below the beltline. The SVAM methodology, with its continuous energy MCNP modeling is required to accurately compute the *dpa* reactions.

#### **4.1 Background**

In January of 2017, the NRC arranged a presentation to the industry with the title – “Computation of Neutron Fluence Information Exchange”.<sup>17</sup> The presentation outlined the concerns expressed in the Regulatory Requirements section (2.0) of this topical report. The presentation also outlined a technologically advanced methodology that the Oak Ridge National Laboratory had pioneered that would address the industry’s safety and licensing issues for subsequent license renewal (SLR).

The presentation reviewed the Regulatory Guide 1.190 discussion of deterministic (discrete ordinates) and stochastic (Monte Carlo) methods. The advantages and disadvantages of deterministic and stochastic methods were presented based on the analytical solution methods of each one. The conclusion was that the best methodology for analyzing internal structures, nozzle regions, and support structures was a hybrid combination of discrete ordinates and Monte Carlo methods. The specific computer codes described were ADVANTG and MCNP.

To support the conclusion, fluence calculations using the ADVANTG – MCNP hybrid method were presented. Parametric modeling of the source, geometry and materials indicated that the results in regions beyond the beltline would be better represented by the hybrid method than by discrete ordinates methods.

Framatome started an evaluation of the hybrid ADVANTG – MCNP method in 2015. The NRC's presentation solidified the development of SVAM. While the focus of this section (4) is the SVAM Methodology, like the Oak Ridge – NRC presentation, the key to any methodology is the results. Following the presentation, Framatome developed a plan of action [

] this plan of action validated the NRC's concerns. It demonstrated that the SVAM results outside the beltline were a marked improvement over the DORT – Synthesis methodology. Figures 1-1 and 5-1 provide graphical displays of the results and measurements.

#### **4.2 Validation of Concerns & Solutions**

Neutron transport methodologies are extremely complex. While the theoretical explanations of the methodologies may seem to be complete and comprehensive, many approximations are applied to develop a solution. Therefore, the most important part of the SVAM Methodology, or any methodology, is the benchmark comparison of its results to measured data. Consequently, this subsection (4.2) of the SVAM methodology (Section 4) briefly reviews the validity of the NRC's concerns and discusses a comparison of SVAM results to DORT – Synthesis results.

Figure 1-1 shows an excellent example of the NRC's concerns. The measured data presented in the figure is represented by a diamond (◆) with a blue color. [

]

Figure 1-1 provides a schematic of the three-dimensional, discrete ordinates calculations. [

]

The SLR issue that the NRC irradiation experts have questioned is the geometrically complex regions above the fuel, beyond the beltline. [

]

It is evident that three-dimensional, discrete ordinates models cannot accurately treat the geometrical complexity of the nozzle region. As shown in Figure 4-1, [

] too much complexity to be accurately described with discrete ordinates analyses. The cylindrical axis of the vessel requires one coordinate system. However, the cylindrical axis of the nozzles requires a completely different coordinate system. Interfacing the two systems must be very approximate.

---

[

]

As many experts in the industry have indicated, to model the complex regions beyond the beltline requires a significant technological improvement over the discrete ordinates – least squares adjustment (unfolding) methodologies.<sup>17</sup> This “Fluence Methodologies for SLR” topical report (ANP-10348P) describes a significantly more complex system of analysis and computer-code calculations that Framatome has incorporated into SVAM to improve the older methodologies.<sup>1, 12</sup>

### 4.3 *SVAM Methodology*

SVAM's complex system of computer codes used to analyze reactor regions beyond the beltline includes SOLIDWORKS<sup>3</sup>, VICTORIA<sup>4</sup> (a plugin for ANSYS<sup>5</sup>), ADVANTG<sup>6</sup> and MCNP.<sup>7</sup> The details of the SVAM methodology are presented in the following subsections: (4.3.1) MCNP Geometric Modeling, (4.3.2) Cross-Sections & Materials, (4.3.3) Source Modeling, (4.3.4) ADVANTG and (4.3.5) SOLIDWORKS – VICTORIA. Each subsection discusses the computer code's methodology as well as the models and procedures which are used to produce the results. [

]

The results of SVAM are the radiation rates. The important radiation with respect to material degradation is the neutron fluence rate. This fluence rate includes the entire range of neutron energies. There are: (1) thermal neutrons, which are in thermal equilibrium with the water molecules in the reactor system; (2) neutrons which are slowing down from the fission spectrum of the uranium and plutonium fissile; and (3) fission neutrons with a mean energy of approximately 2.0 MeV and a maximum value as high as 20.0 MeV.

Like the [

] model has tracked the core's measurements from the beginning of operation to the end. The reaction rate results [

]

[ ] provide accurate neutron leakage rates in conjunction with the pin-by-pin sources.

With the same [

] if the reactor and vessel are modeled as a symmetric – uniform cylinder, then the flux profile would be representative of the azimuthal integration of the sources for each nodal channel. The three-dimensional flux distribution would reflect the product of the source distribution and the leakage function.

[ ] would have exactly the same results.

Reviewing the beltline region of Figure 1-1 shows that [

] it is well known that the approximations used for discrete ordinates solutions are much more limiting than the Monte Carlo – MCNP solutions. [

]

The Reference 1 fuel-beltline code system (MERLIN) methodologies are presented in terms of DORT – Synthesis. [

]

This report explains that the methodologies used for SLR benchmark and calculational uncertainty analyses are an extension of the analyses performed for the “Fluence and Uncertainty Methodologies” topical report.<sup>1</sup> The additional benchmark and uncertainty



analyses have demonstrated that the [

]

The fuel-beltline benchmark results for SVAM [

] As shown by the dosimetry data in Figure 1-1, [

]

[

]

With SVAM and DORT – Synthesis having the same uncertainty characteristics compared to measured data in the fuel-beltline, SVAM and DORT – Synthesis results were benchmarked to one another. The benchmark comparison clearly indicated that the code systems are statistically the same. Therefore, in the beltline region SVAM is accurate [

]

The beltline in Figure 1-1 begins just above the top of the fuel and ends just below the bottom of the fuel. The nozzle region, with the vessel support beams, extends to the top of the core flood nozzle. It is clear that validation of SVAM in the nozzle region is required for SLR as suggested by the NRC.<sup>2</sup> The results that follow in Section 5 demonstrate that SVAM is accurate in the nozzle region with a well-defined random uncertainty. [

]

#### 4.3.1 MCNP Geometric Modeling

As discussed above (Section 4.3, SVAM Methodology), the MCNP methodology, which is described in Reference 18, provides an accurate solution to radiation transport phenomena. Theoretically, its accuracy and random uncertainty are better than finite difference – discrete ordinates ( $S_N$ ) solutions. However, the accuracy and random uncertainty can only be determined by benchmark comparisons to measured data. If the measurements are in geometrically simple regions, such as those that can be

modeled by symmetrically uniform cylinders, then the accuracy and random uncertainty for both Monte Carlo and discrete ordinates ( $S_N$ ) methods is equivalent. Moreover, the accuracy and random uncertainty for the Monte Carlo and discrete ordinates ( $S_N$ ) methods is limited by the accuracy and random uncertainty in the measurements. No analytical methodology can be more accurate, with a lower uncertainty, than the reference set of measurements used to benchmark the methodology.

Where SVAM's MCNP results are significantly better than those calculated with discrete ordinates – least squares adjustments (unfolding) is in regions that are geometrically complex, such as the nozzles for the inlet and outlet piping. Discrete ordinates modeling of geometrically complex nozzle regions require approximations that are not and cannot be precise. SVAM's MCNP geometric modeling is developed with Computer Aided Design technology that completely represents the complex curvatures of every region. Figure 2-2 shows a three dimensional computer design view of SVAM's modeling for a reactor's nozzles. The details clearly show the exceptional capability of SVAM.

The Framatome methodology begins with a three dimensional solid model of the reactor vessel, reactor internals, the cavity, and the concrete biological shield. The solid model is constructed from detailed plant drawings. An example of the solid model can be seen in Figure 4-1. This figure illustrates the complexity and detail that is included in SVAM's model. This solid model can be created with many different software packages and converted to a format that is able to be assimilated into MCNP.

MCNP uses a general combinatorial geometry that allows the entire reactor configuration to be exactly represented. Due to the complexity of the models, Framatome uses specialized software to convert the three dimensional solid model into the required MCNP format. Section 4.3.5 describes the SOLIDWORKS<sup>3</sup> – VICTORIA<sup>4</sup> processes used to generate the geometry files.

### 4.3.2 Cross-Sections & Materials

The benchmark calculations presented in Section 5 are based on the ENDF/B-VII.1 continuous energy cross-section library. The ENDF library includes cross-sections [

]

The SVAM methodology has the advantage of having exact models to represent the reactors' three dimensional geometry. [

] Framatome's cross-section and material modeling in SVAM – MCNP complies with the guidance provided in Regulatory Position 1.1.1.

### 4.3.3 Source Modeling

As discussed in Section 4.3, SVAM – MCNP uses the same source term as the DORT – Synthesis methodology. The radiation sources and isotopic compositions are obtained directly from three-dimensional core-follow computer code "measurements".

Framatome uses a variety of core-follow codes (such as ARTEMIS™, SIMULATE, NEMO, PRISM, etc.). The pin-wise, time averaged source terms are input to MCNP using SDEF "cards".

Each fuel pellet and pin, guide tube, and instrument tube is modeled independently. The methodology typically models the neutrons emitted by fission from U-235, U-238, Pu-239, and Pu-241. The spectral and spatial source variables are modeled using discrete intervals for the energy groups and spatial mesh. Within each of the intervals the neutron source does not vary. The three dimensional source terms are assimilated

into the sources used in MCNP for radiation transport throughout the model. This method and procedure complies with Regulatory Position 1.2 in Regulatory Guide 1.190.

#### **4.3.4 ADVANTG**

Regulatory Position 1.3.2 in Regulatory Guide 1.190 states that variance reduction methods should be qualified by comparison with calculations performed without variance reduction. Framatome's SVAM – MCNP methodology complies with this requirement by using a hybrid deterministic – Monte Carlo method. In this method, weight windows and source biasing parameters are generated from deterministic neutron transport calculations.

The importance weights ( -windows) used in SVAM benchmark calculations were generated with ADVANTG based on a Forward-Weighted CADIS (FW-CADIS) method. The method is a variation of the Consistent Adjoint Driven Importance Sampling (CADIS) method.

The FW-CADIS method ensures the accuracy of the MCNP results by removing "Engineering Judgment". With ADVANTG, the forward calculations are based on a DENOVO  $S_N$  transport model. The results generate a "global" flux map of the reactor configuration. ADVANTG uses the flux map to generate a WWINP file for MCNP.

Additionally, ADVANTG can generate source biasing parameters. The biasing produces more source particles in the most important locations, with suitably reduced weights. The importance biasing is based on DENOVO results.

SVAM benchmark calculations used variance reduction techniques. Employing these techniques provided the means of having global mesh tallies covering all reactor pressure vessel and internals components. The application of the variance reduction techniques is consistent with Regulatory Position 1.3.2. All statistical tests were evaluated and determined to be satisfactory for the SVAM results.

#### **4.3.5 SOLIDWORKS – VICTORIA**

As illustrated by Figures 2-2 and 4-1, nozzle configurations can be extremely complex. The key to having MCNP results that are accurate with reasonably small random uncertainties is to ensure that the geometric models are correct.

While MCNP allows a great deal of flexibility in defining the problem geometry, the input is relatively complex. It requires defining a large number of surfaces and cells. It is thereby a potential source of erroneous problems. Framatome's solution is to "automate" the generation of MCNP geometry models. This is accomplished by automatically converting three dimensional solid models, such as those from the Computer-Aided Design program SOLIDWorks, into MCNP's format.

Although there are multiple codes available, an ANSYS plug-in developed by Framatome called VICTORIA was used to generate the models used in this topical. VICTORIA automates the development of the MCNP combinatorial model. VICTORIA also simplifies the process of assigning materials in MCNP.

While SOLIDWORKS and VICTORIA were used to create SVAM's MCNP geometric model, the methodologies are not limited to the use of this software. Other software packages are available, such as Attila4MC and SuperMC. The MCNP geometry file produced by each code is essentially identical. Framatome will continue to use the best-available conversion software.

#### **4.4 ART Effective Fluence**

In Section 2.0, the "Regulatory Requirements" for this "Fluence Methodologies for SLR" topical report were presented. In Subsection 2.6, "Irradiation & Fracture Mechanics Safety Analysis", it was explained that the fluence-radiation *per se* is not the limiting safety parameter. The limiting parameters for operation are determined by fracture mechanics safety analysis. The safety analysis uses ART (Adjusted Reference Temperature) values to assess the structural material's ability to withstand high stress

intensity factors that may occur due to abnormal operating conditions. The safety limits for operation are directly related to the ART values.

The crystalline structure of the steel provides its toughness. Neutron irradiation damages the structure and degrades the toughness. The damage is caused by displacing the steel atoms forming the crystalline structure. The displacements per atom ( $dpa$ ) cause the shift ( $\Delta$ ) in the reference temperature ( $RT$ ) for the nil-ductility transition ( $NDT$ ) in the material's properties. Increasing  $\Delta RT_{NDT}$  values are characterized as embrittlement. It represents the material's loss of fracture toughness.

Over time, more and more irradiation occurs which causes more and more embrittlement. ART values thereby increase with reactor operation. As explained in Subsection 2.2, "Regulatory Guide 1.99, Revision 2" provides the functional relation between the increasing fluence-radiation and the  $\Delta RT_{NDT}$  (and thereby ART) values.

The Regulatory Guide 1.99, Revision 2<sup>8</sup> relationship comes from a correlation of material test specimen data to irradiation. Since the increasing embrittlement ( $\Delta RT_{NDT}$ ) is directly caused by  $dpa$  (displacements per atom) reactions, it would be logical to have  $dpa$  values as the primary independent variable in any correlation. If the correlation were to be graphed,  $dpa$  would be the independent variable on one coordinate axis and embrittlement would be the dependent variable on the other.

Material analysts developed a correlation of embrittlement ( $\Delta RT_{NDT}$ ) to  $dpa$ . Other independent variables were also evaluated. When correlating  $\Delta RT_{NDT}$  to the neutron fluence with energies above 1.0 MeV (million electron Volts), analysts found the "least squares" root mean deviation was a smaller value than correlations using  $dpa$  and the other independent variables.

In addition to a smaller root mean deviation, when the ratio of "test specimen  $dpa$ " to "the greater than 1.0 MeV fluence" was compared to the ratio at the vessel's fuel-beltline wetted surface, the ratio was essentially constant. As a consequence, the  $\Delta RT_{NDT}$  embrittlement was functionally correlated to the greater than 1.0 MeV fluence.

The advantage of the embrittlement – fluence relationship is the small standard deviation ( $\sigma_{\Delta}$ ) used for ART values. The disadvantage is that an “ART effective fluence” is required when the ratio of  $dpa$  to the greater than 1.0 MeV fluence changes due to changes in the neutron spectrum. Regulatory Guide 1.99, Revision 2 discusses using  $dpa$  ratios to determine the greater than 1.0 MeV ART effective fluence. Figure 4-2 provides graphs to visually understand the  $dpa$  modeling for the ART effective fluence.

The  $dpa$  (displacements of steel atoms with vacancies and interstitials) is the integral of the  $dpa$  reaction rate over the time of operation. The  $dpa$  increases to higher and higher values the longer the reactor operates. With longer operating times, the embrittlement of the reactor’s steel materials increases; this is due to the increasing  $dpa$  values.

With respect to locations on the reactor vessel’s wetted surface, the Regulatory Guide 1.99, Revision 2 (RG1.99,R2) embrittlement – fluence-factor<sup>8</sup> relationship is based on Equation 4-3.

$$\langle \sigma_{dpa}(E) \times \Phi(E, V_S) \rangle_E \triangleq \{ \Phi(E \geq 1 \text{ MeV}, V_S) \}_{\text{RG1.99,R2}} \quad (4-3)$$

The left side of the equation is the  $dpa$  reaction rate at some vessel wetted-surface location ( $V_S$ ) – integrated over all neutron energies ( $E$ ). The right side of the equation is the greater than 1.0 MeV flux at the same vessel location. The product of the right-side flux and the time of operation is applied to the Regulatory Guide 1.99, Revision 2 fluence-factor functional relation to determine  $\Delta RT_{NDT}$  and subsequently the ART values. The left and right sides of the equations are equivalent ( $\triangleq$ ) damage functions.

When the left and right sides of Equation 4-3 are multiplied by the time of operation, the results are the  $dpa$  and fluence values. If the left-side of the equation is divided by the right-side the result is a ratio that is consistent with the specimen database used in the Regulatory Guide 1.99, Revision 2 correlation. The generally accepted value for the



ratio of *dpa* reactions to flux values (that are greater than 1.0 MeV) is approximately 15 *dpa* per  $10^{22}$  neutrons per centimeter-squared. This ratio is displayed in Figure 4-2 (■) with the identification of  $14.8 \text{ dpa} / 10^{22}$  for neutron energies between 1.0 and 20.0 MeV.

As shown by Equation 4-4, Equation 4-3 is defined to be generically applicable at any location (*x*) within the reactor as long as the functional (*f*) relationship to embrittlement can be determined to be equivalent ( $\triangleq$ ).

$$\left\{ \sigma_{dpa}(E) \times \Phi(E, x) \right\}_E \triangleq f \{ \Phi(E \geq 1 \text{ MeV}, x) \} \quad (4-4)$$

The functional relationship of the flux  $\{ \Phi(E \geq 1 \text{ MeV}, x) \}$  to the Regulatory Guide 1.99, Revision 2 embrittlement – fluence-factor is based on the ratio of the *dpa* reaction rate on the left side of Equation 4-4 being equivalent to the flux on the right side. The ratio must be consistent with the specimen database for the ART values that are used in the fracture mechanics safety analysis. This ratio however is not generically consistent with the Regulatory Guide 1.99, Revision 2 specimen database.

Equation 4-5 defines ( $\triangleq$ ) the necessary conditions to have generic consistency between the *dpa* and the greater than 1.0 MeV fluence values used in Regulatory Guide 1.99, Revision 2 for fracture mechanics analysis at any location (*x*).

The ratios on the left side of Equation 4-5 are used to determine the ART effective flux  $\{ \Phi(E \geq 1 \text{ MeV}, x) \}$ . This flux is consistent with the Regulatory Guide 1.99, Revision 2 embrittlement – fluence relationship. Equation 4-6 provides the appropriate expression.

The ratio of *dpa*s in Equation 4-6 are discussed as part of the development of Equation 3<sup>8</sup> in Regulatory Guide 1.99, Revision 2. As explained in the Regulatory Guide, when the flux spectrum changes from that on the vessel wetted-surface an ART effective fluence is required.

The spectrum changes in the nozzle region compared to the fuel-beltline are due to the slowing down of the fission-spectrum neutrons. As neutrons, with energies greater than 1.0 MeV, travel to regions above and below the fuel-beltline, their overall population decreases. The high energy neutrons are not lost however; they simply become lower energy neutrons. As seen in Figure 4-2, *dpa* reactions are dependent on more than neutrons with energies greater than 1.0 MeV; the *dpa* is dependent on the entire neutron spectrum.

In nozzle regions, and in regions above the nozzles and below the fuel-beltline, the greater than 1.0 MeV flux becomes smaller and smaller. However, as shown by Framatome's updated benchmark database in Section 5, [

] the energy range below 1.0 MeV is calculated with the same accuracy and precision as the energy range above 1.0 MeV.

The *dpa* results, which are dependent on the entire neutron spectrum, are consistent with the Regulatory Guide 1.99, Revision 2 correlation of embrittlement ( $\Delta RT_{NDT}$ ) to the greater than 1.0 MeV fluence. The ART Effective Fluence values are calculated with Equation 4-6. When these values are used in the Regulatory Guide's formula for the ART, there is 95/95 confidence that the ART values are appropriate for fracture mechanics safety analyses of reactor vessels.

#### 4.5 *Best Estimate Fluence*

In the fuel-beltline region, Framatome's fluence methodologies for SLR [

] the best-estimate fluence is accurate; that is, completely unbiased.

[

] The fluence-radiation calculations are thereby best-estimates; they have no bias.

[

] The neutron source in SVAM and MERLIN comes from the fissions in the core. The fission rates in each nodal segment of the core come from core-follow calculations. The core-follow fission rates produce the distribution of relative power densities for each nodal segment. The core-follow power distributions are compared to measured data to confirm that deviations in the reactions are within the uncertainty criteria.

While the core-follow – “measurements” produce accurate – unbiased source distributions, these source distributions are [

] energy dependent flux values are needed to predict the energy distribution of the neutron leakage from the core. The energy dependent leakage is needed to predict reactions, such as those for dosimeters and the *dpa*. The energy dependent flux is also needed to determine the sum of flux values that are greater than 1.0 MeV.

[ Two eigenvalues provide the means of having energy dependent flux values that are consistent with the fission source. The first is an absorption value ( $\omega/v$ ) that is directly proportional to the inverse neutron velocity ( $1/v$ ). The second is a leakage value with a buckling ( $B$ ) that maintains a critical spectrum ( $B_{k_{eff}}$ ). [

]

[ In the fuel-beltline region, SVAM and MERLIN give the same results statistically. Both results have a standard deviation [

] the SVAM standard deviation is consistent with the 20.0% uncertainty assumed in the ART margin term. If there are biases in the results, such as those from the combination of measured and calculated FERRET results, then the biases would need to be combined with the random deviations. This is necessary to ensure 95/95 confidence that the ART values are appropriate for fracture mechanics safety analyses of reactor vessels.



The Table 5-2 measured data and calculated results reflect the values that were from the laboratory and the SVAM modeling respectively. These results are statistically combined in Table 5-3. [

]

**Figure 4-1**  
**Reactor Vessel Nozzles and Supports**

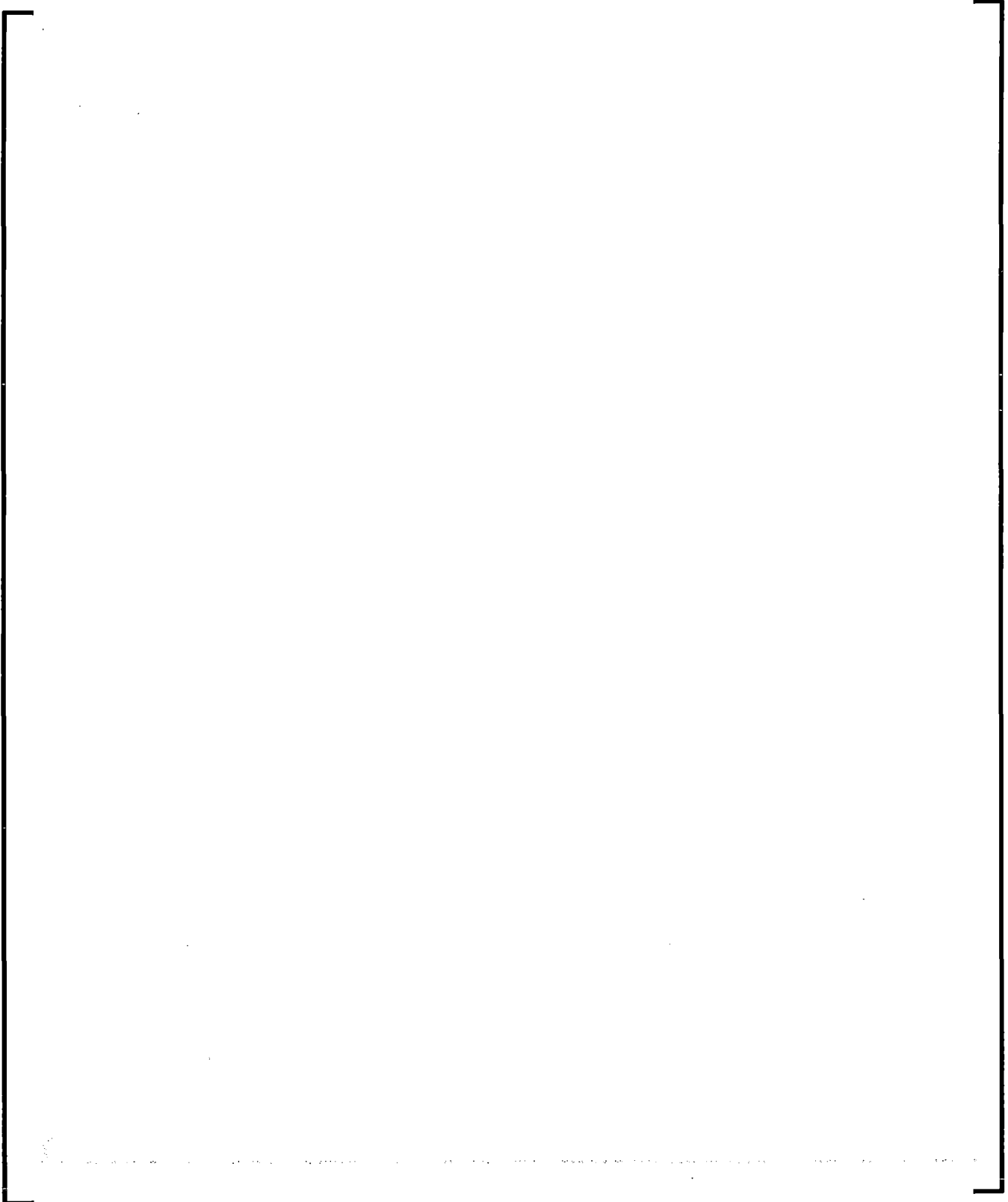
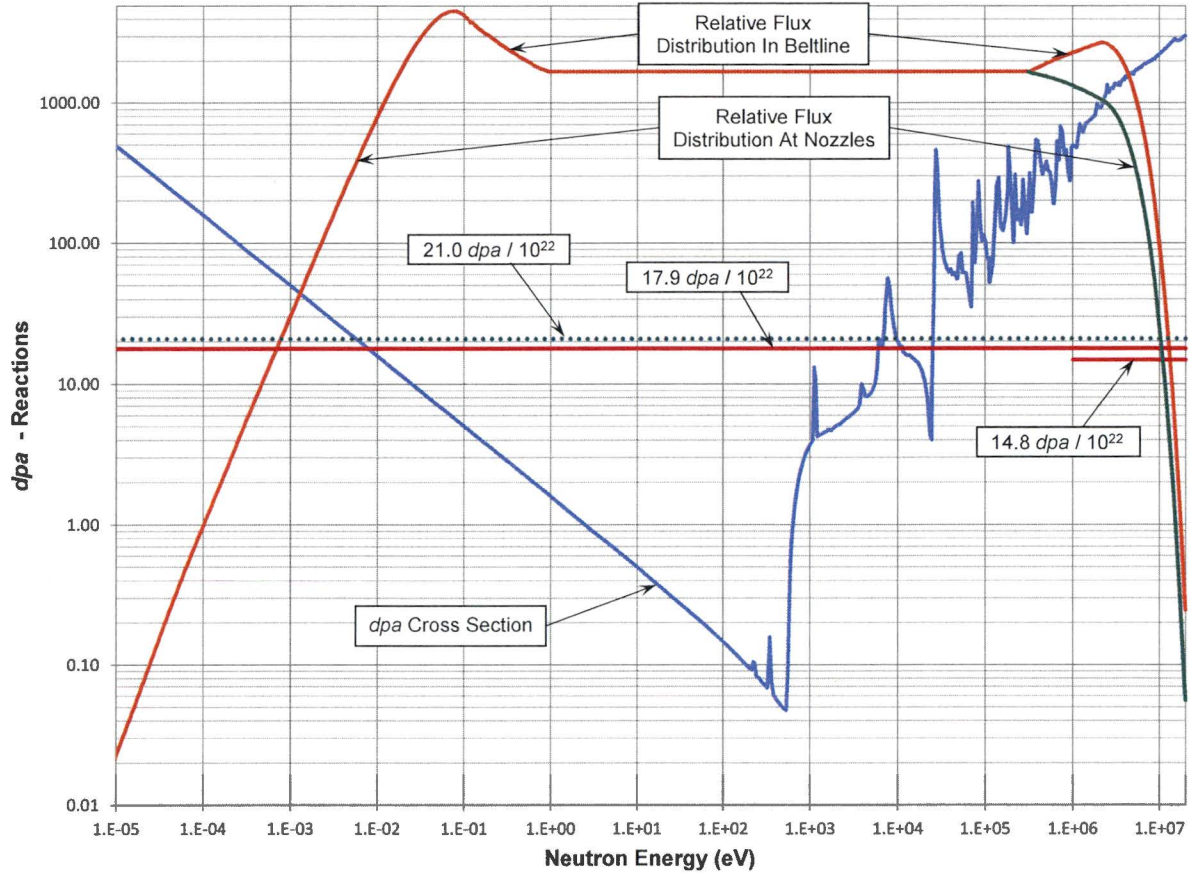


**Figure 4-2**  
***dpa* Reactions**



Three independent variables are shown in Figure 4-2: (1) the *dpa* cross-section (■) –  $\sigma_{dpa,E}$ ) of iron in the vessel material as a function of the neutron energy ( $E$ ), (2) the relative flux distribution (■) –  $\Phi_E$ ) associated with the fuel-beltline, and (3) the relative flux distribution (■) –  $\Phi_E$ ) associated with neutron leakage from the fuel-beltline to the nozzle region. The *dpa* reaction rate is the product of the *dpa* cross-section and the flux ( $\sigma_{dpa,E} \times \Phi_E$ , *dpa* reactions per second). The total *dpa* is the product of the *dpa* reaction rate and the irradiation time period.

The generally accepted value for the ratio of *dpa* to the greater than 1.0 MeV fluence values is approximately 15 *dpa* per  $10^{22}$  neutrons per centimeter-squared. This ratio is displayed in Figure 4-2 (■) with the identification of  $14.8 \text{ dpa} / 10^{22}$  for neutron energies between 1.0 and 20.0 MeV.

Two additional *dpa* to fluence (greater than 1.0 MeV) ratios are provided in Figure 4-2. The first (■) extends the energy range of the product of (a) the flux (■) –  $\Phi_E$ ) associated with the fuel-beltline, and (b) the *dpa* cross-section (■) –  $\sigma_{dpa,E}$ ). This dependent variable is identified as  $17.9 \text{ dpa} / 10^{22}$  and includes the entire energy spectrum between 0.0 and 20.0 MeV.

The second ratio (■) shows the product of (a) the flux (■) –  $\Phi_E$ ) associated with neutron leakage from the fuel-beltline to the nozzle region, and (b) the *dpa* cross-section (■) –  $\sigma_{dpa,E}$ ). This dependent variable is identified as  $21.0 \text{ dpa} / 10^{22}$  and includes the spectrum between 0.0 and 20.0 MeV.



## 5.0 BENCHMARKS

Section 4 explains the methodology that forms the basis for SVAM. There are four key parts: (1) The first is the geometric modeling; (2) The second is the discrete ordinates solution which approximates the three-dimensional geometry; (3) The third is the continuous energy modeling over the entire energy range, from 0.0 to 20.0 MeV; (4) Lastly, is the Monte Carlo solution process in MCNP.<sup>7</sup> This updated methodology can not only provide accurate and precise results of the fluence-radiation in fuel-beltline regions of PWRs and BWRs, but it can also provide accurate and precise results in the regions that are above and below the fuel-beltline. This section (5) provides the benchmark comparisons of SVAM's calculated results to the measured data. It is the benchmark database that confirms the accuracy and precision in the SVAM methodology.

The "Benchmarks" [

] Subsection 5.2

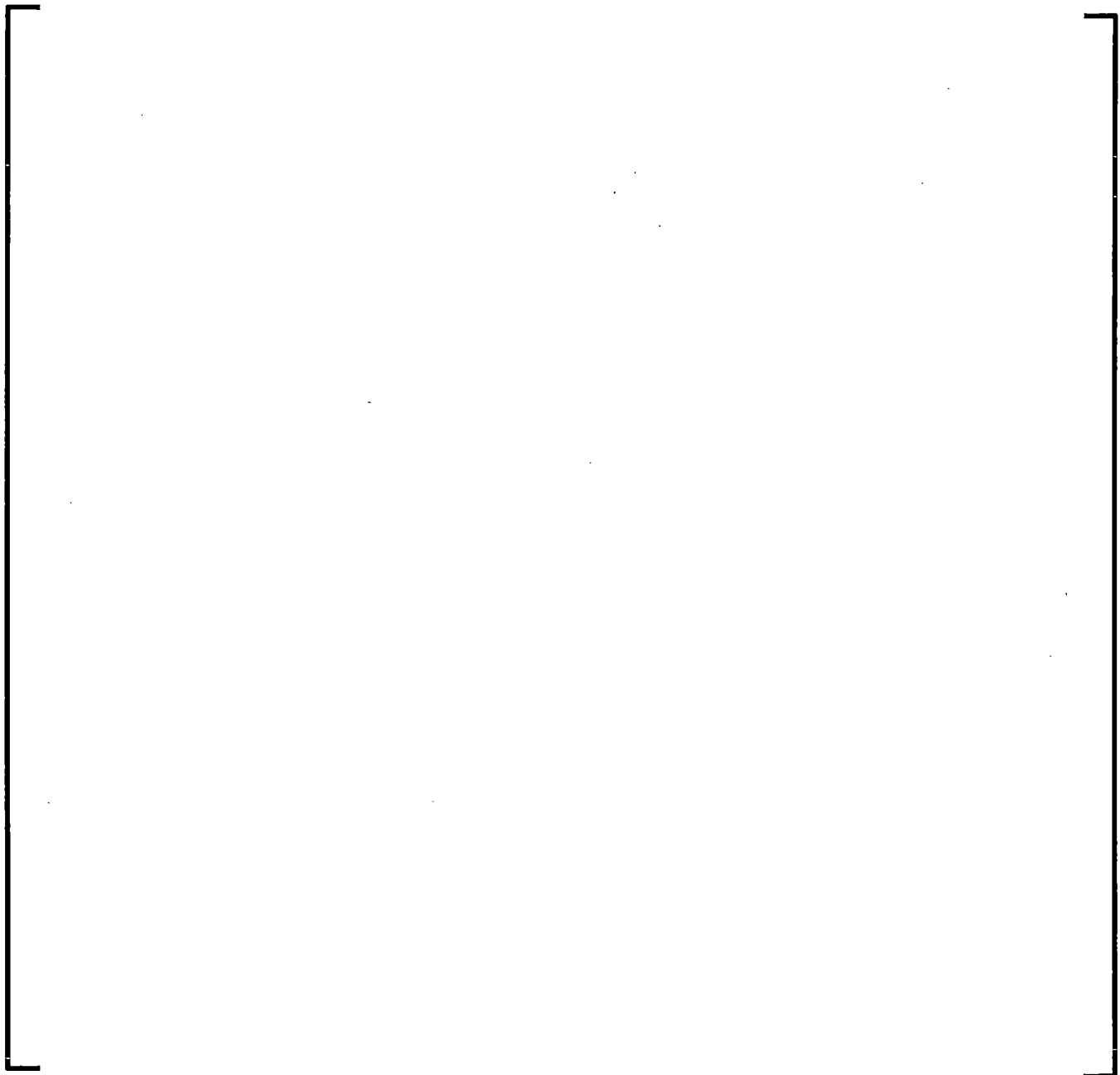
focuses on SVAM's results in the beltline region. Subsection 5.3 is the most significant; it provides the comparison of SVAM's results to the measurements that are above and below the fuel-beltline.

The benchmark database in the "Fluence and Uncertainty Methodologies"<sup>1</sup> topical report is valid for SLR analyses [

]

[

] The evaluation of the measurement methodology by the National Institute of Standards and Technology (NIST) found that the measurements (M) were unbiased ( $B_M = 0.0$ ) with an estimated mean relative standard deviation ( $\sigma_M$ ) that was no greater than 7.0% in the fuel-beltline.





Section 5.2 has the results of the SVAM benchmark for the fuel-beltline region. The benchmark comparison to the measurements [

]

Section 5.1 demonstrates that, within the fuel-beltline, [

]

5.1 [ ]

The benchmark database is used to assess biases in the analytical methods, procedures and modeling. As shown in Figure 1-1, discrete ordinates methodologies

(such as MERLIN) simply give biased results in regions that are above the fuel-beltline.

[

]

Based on the fact that SVAM and MERLIN methodologies can produce results with no bias, the statistical evaluation of the benchmark database can be used to estimate the relative standard deviation. For MERLIN, the standard deviation is evaluated in Reference 1. For SVAM, the standard deviation evaluation is in Section 5.2. [

]

[

As shown in Table 5-1, the comparison was as expected. [

] the uncertainty in

these results is consistent with the Regulatory Guide 1.99, Revision 2 ART margin term.

## 5.2 SVAM Beltline Benchmark

Table 5-2 lists the measurement database from Reference 1. The table also contains updated data for "ART Effective Fluence" modeling based on the energy range of *dpa* reactions; Figure 4-2 shows that *dpa* reactions in the energy range below 1.0 MeV are significant to the total *dpa*. In addition, the table contains updated data for the regions above and below the fuel-beltline.

In addition to measurements, Table 5-2 includes SVAM results. The comparison of the measured data to the calculated results generates the benchmark database. While the 887 data points in the table are the basis for the benchmark database, the comparisons of data to results need to be statistically evaluated to be meaningful. Table 5-3 summarizes the statistical evaluation of the benchmark database.

As explained in Section 3, the experimental methodology [

] in

the fuel-beltline (B) there is a single-constant relative standard deviation ( $\sigma_{MB} \leq 7.0\%$ ) for the measurements (M). The value was confirmed by the National Institute of Standards and Technology (NIST) with a Standard and Reference Field Validation (see Section 3.3).

Section 4.3 explains that the calculated results (C) cannot be more accurate, nor have a lower standard deviation than the measured data (M). This is expressed by Equation 4-1. Section 4.5 explains how the Best-Estimate Fluence and radiation reactions have no biases and are thereby completely accurate. Thus, when the relative standard deviation in the calculations is evaluated with the benchmark database, the

[

]



As explained in Section 3, [

] a statistically consistent

standard deviation. Moreover, the random deviations in the experimental methodology are representative of normal probability distributions.

[

] no deviations are greater than two relative standard deviations

(  $2 \times \sigma$  ).

The conclusion from this section [

]

### **5.3 SVAM Nozzle Region Benchmark**

Section 5.2 is important because it demonstrates that SVAM's methodology is accurate and has a completely generic unbiased standard deviation [

]

The importance of SVAM's development is in direct relation to the NRC's "Generic Aging Lessons Learned (GALL) Report".<sup>2</sup> In the report it is noted that SLR (Subsequent License Renewal) requires an expanded analysis of regions experiencing increased irradiation degradation. The primary components of concern are the vessel's inlet and outlet coolant nozzles.

The important SLR Regulatory Requirements discussed in Section 2.5 are the three components of Regulatory Guide's 1.190 uncertainty analysis: (1) the measurement database; (2) the benchmark database; and (3) the analytical sensitivity modeling.<sup>9</sup>

Section 3 explains that Framatome's measurement database has been updated to include the nozzle regions as well as regions above and below the fuel-beltline.

Section 5.2 reviews the updated benchmark database in the fuel-beltline which includes *dpa* reactions. This section (5.3) presents Framatome's updated benchmark database in the regions above and below the fuel-beltline to include the nozzles. Section 6 follows this one; it reviews the updated analytical sensitivity modeling.

The discussion in Section 4.1 explains that in January of 2017, the NRC arranged a presentation to the industry – “Computation of Neutron Fluence Information Exchange”.<sup>17</sup> The presentation not only outlined their concerns with fluence-radiation licensing issues, but also outlined an advanced methodology that the Oak Ridge National Laboratory had pioneered. The new methodology has been incorporated into SVAM. It resolves the industry’s safety and licensing issues concerning SLR.

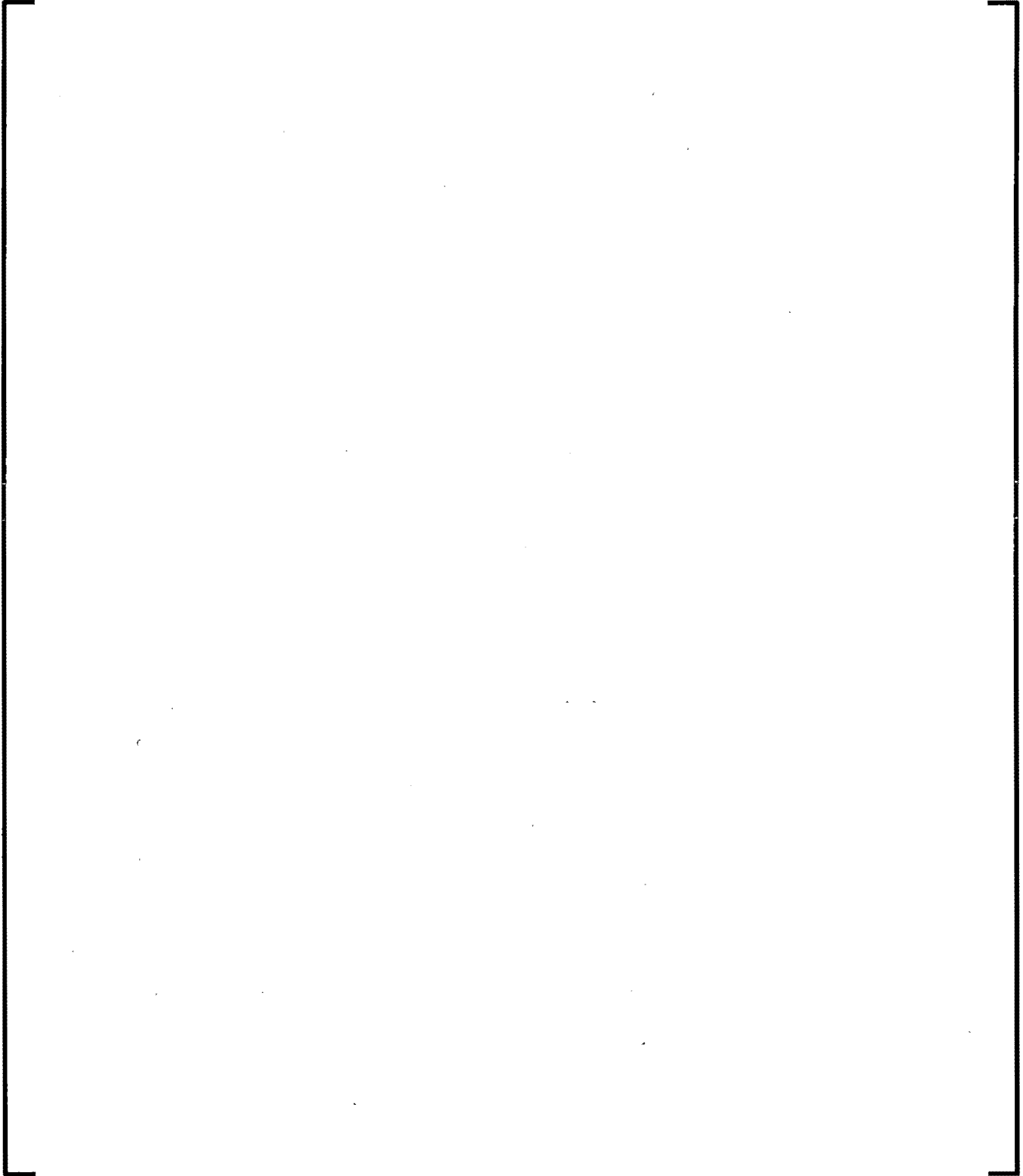


[

] In fact, the two deviations are statistically the same.







Figures 5-1, 5-2 and 5-3 provide illustrative graphs of SVAM's calculated results in comparison to the measured data. [

]

Figure 4-1 shows the "Reactor Vessel Nozzles and Supports" with the "I" beams. At the top of the figure, in the plane where the reactor vessel head is attached to the vessel shells, the instrumentation supports are shown. These instrumentation channels support the dosimetry chains that provide the data in Figures 5-1, 5-2 and 5-3. As seen in Figure 4-1, the chains' data begins above the nozzles, goes through the nozzle region, then through the support beams, the fuel-beltline region, and continues below the lower vessel head. The chains' data end just above the cavity floor.

Figure 2-2 shows the details of the nozzles from inside the vessel to the outside. Figure 4-1 continues with the details. The fuel assemblies are supported by the grid plate seen in Figure 2-2. The primary neutron sources degrading the structural toughness are coming from the top portion of the fuel located within the peripheral fuel assemblies.

Figure 5-1 is the same as Figure 1-1 – [

] It is clear that SVAM's results are exceptionally accurate in the nozzle region.

The accuracy shown in Figure 5-1 is confirmed by Figures 5-2 and 5-3. While all the data and results represent different locations around the vessel, they all confirm that the benchmark comparison has acceptable deviations above the fuel-beltline.

As noted in Section 5.2 and shown in Figures 5-1, 5-2 and 5-3, the benchmark database has acceptable random deviations through the fuel-beltline. The acceptable deviations continue to the bottom of the vessel. [

]

[ ] the margin term in Regulatory Guide 1.99, Revision 2 requires the chemistry and fluence factors have statistically valid standard deviations. [

]



**Figure 5-1**  
**X-Y Quadrant Benchmark**



**Figure 5-2**

**W-X Quadrant Benchmark**



**Figure 5-3**  
**Z-W Quadrant Benchmark**



**Figure 5-4**

[ ]

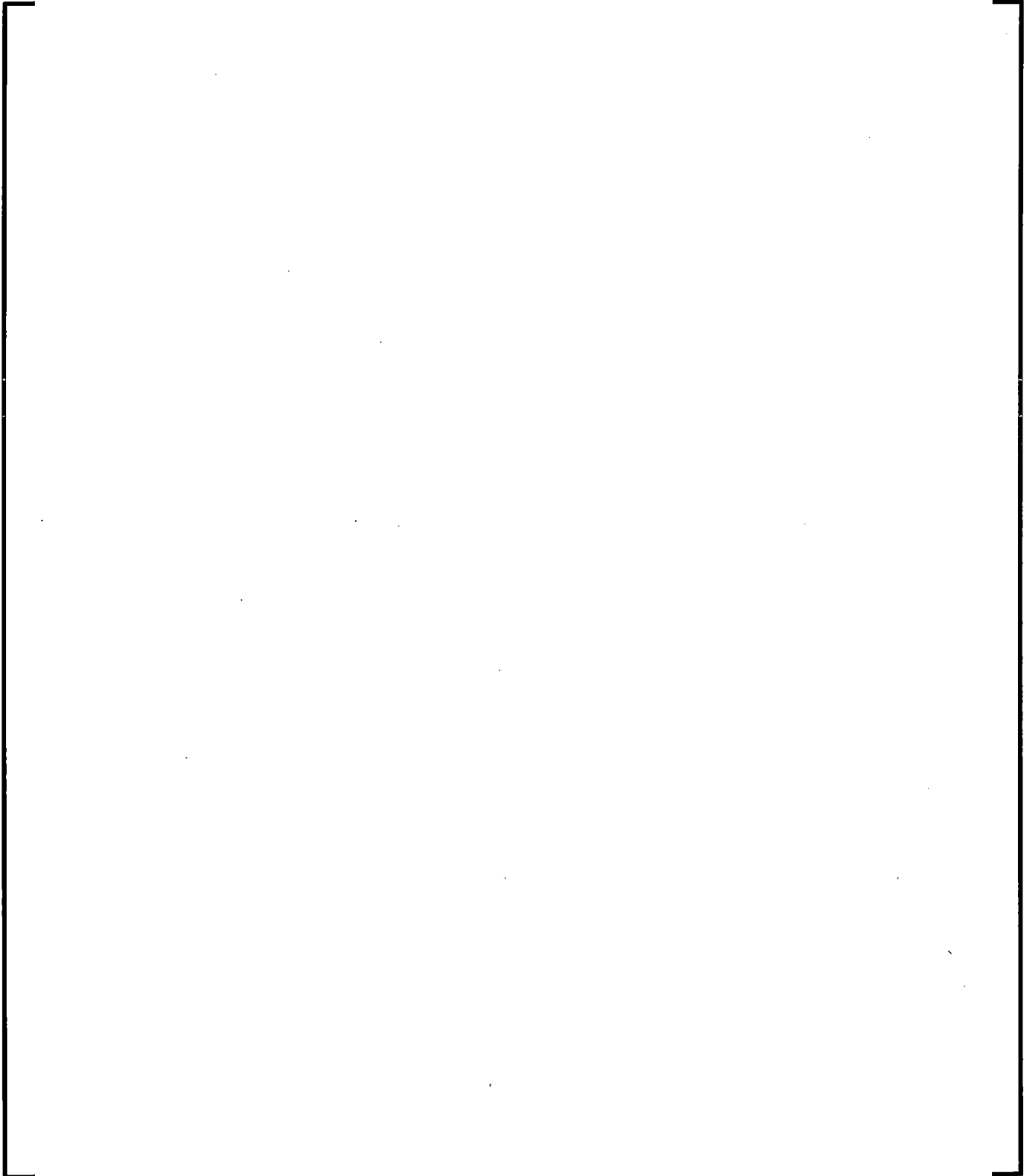


**Table 5-1**

[

]

A large, empty rectangular frame with a thin black border, intended to contain the data for Table 5-1. The frame is currently blank.



**Table 5-2**  
**Framatome Databases**

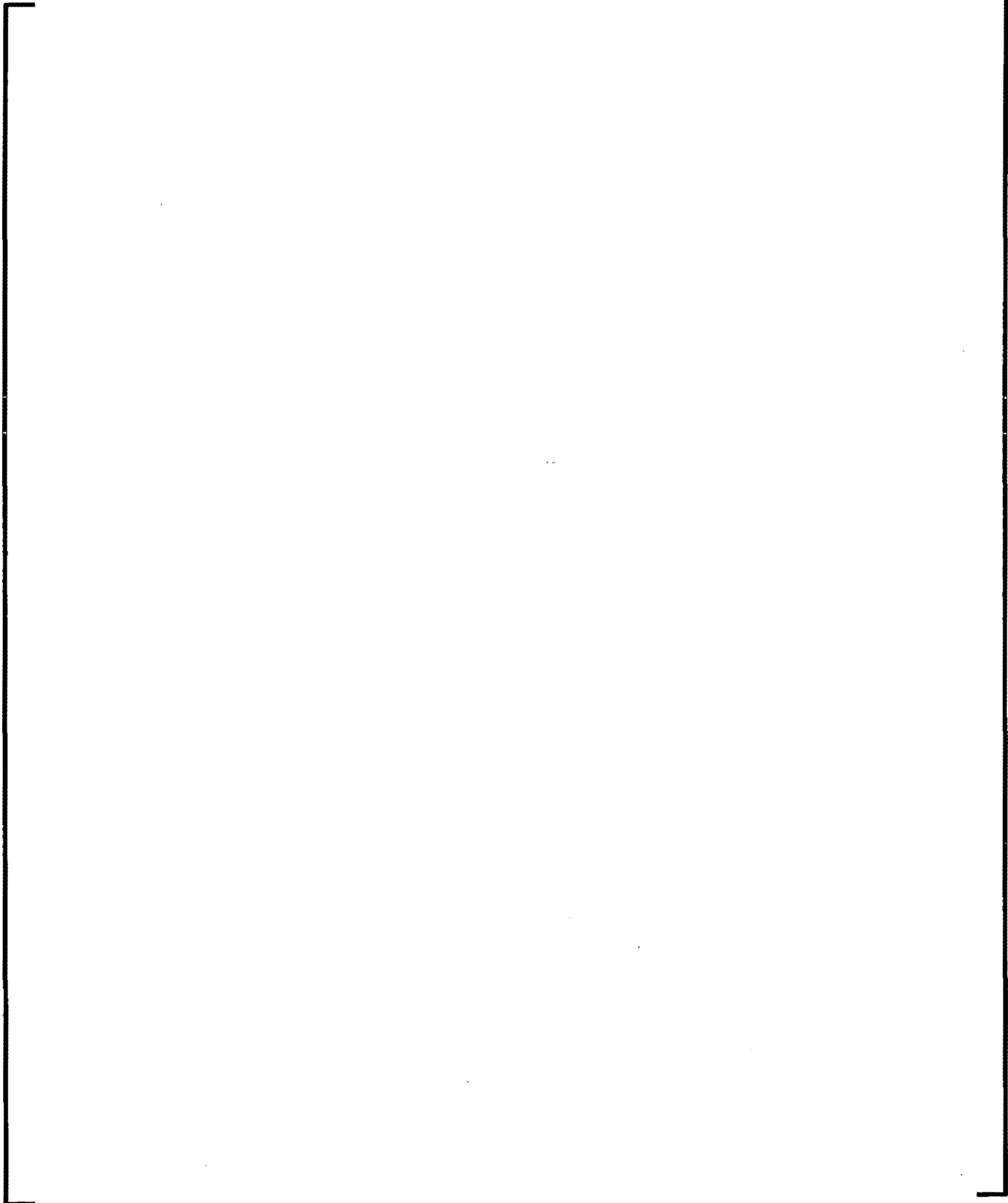
A large, empty rectangular frame with a thin black border, centered on the page. It is positioned below the section header and above the bottom margin, indicating that the content of Table 5-2 is missing or redacted.

Table 5-2 (Continued)

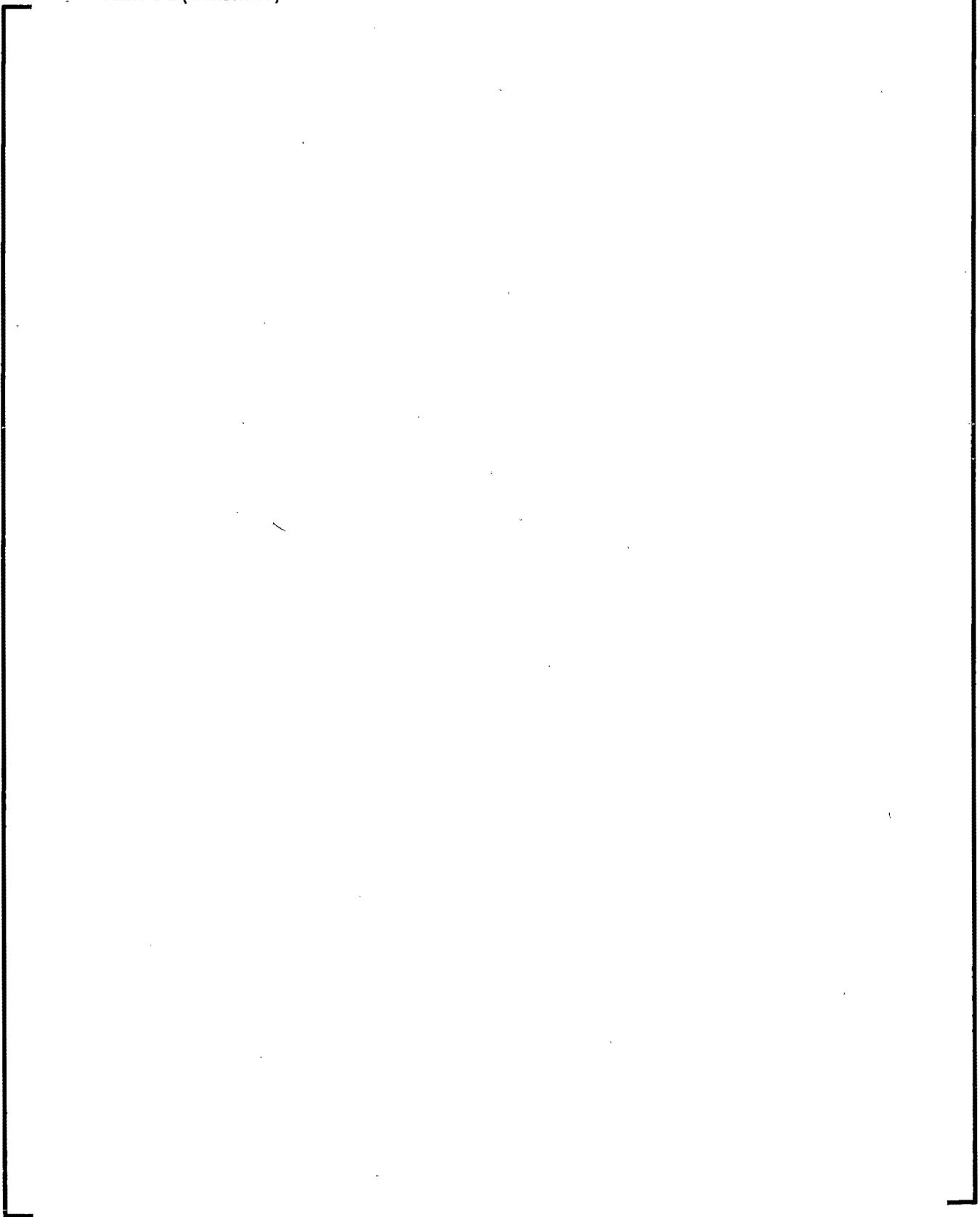
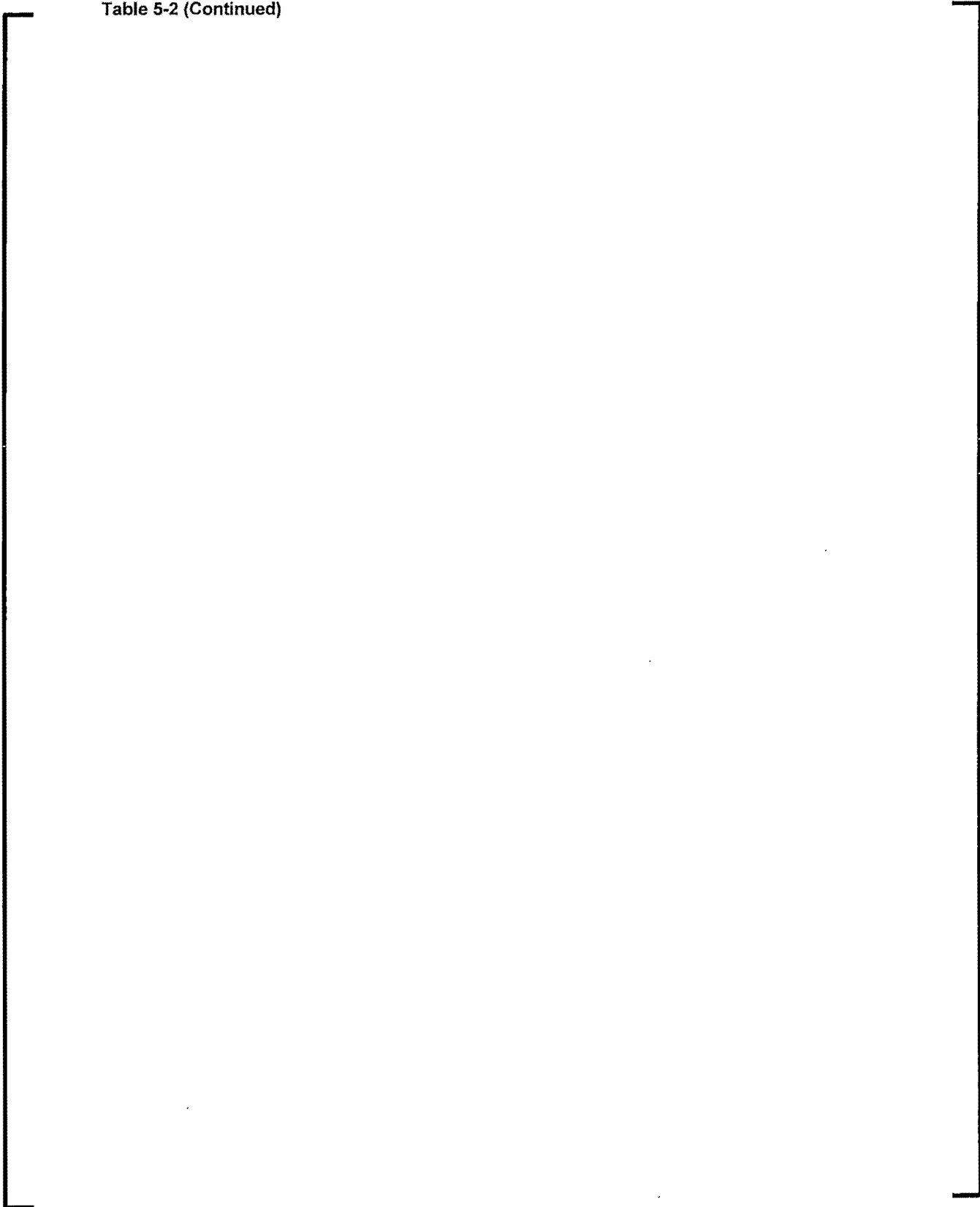


Table 5-2 (Continued)

A large, empty rectangular frame with a thin black border, occupying most of the page below the caption. It is intended for a table but contains no data.

Table 5-2 (Continued)

A large, empty rectangular frame with a thin black border, occupying most of the page. It is positioned below the caption 'Table 5-2 (Continued)'. The frame is currently empty, suggesting that the table content is either missing or has been redacted.

**Table 5-2 (Continued)**

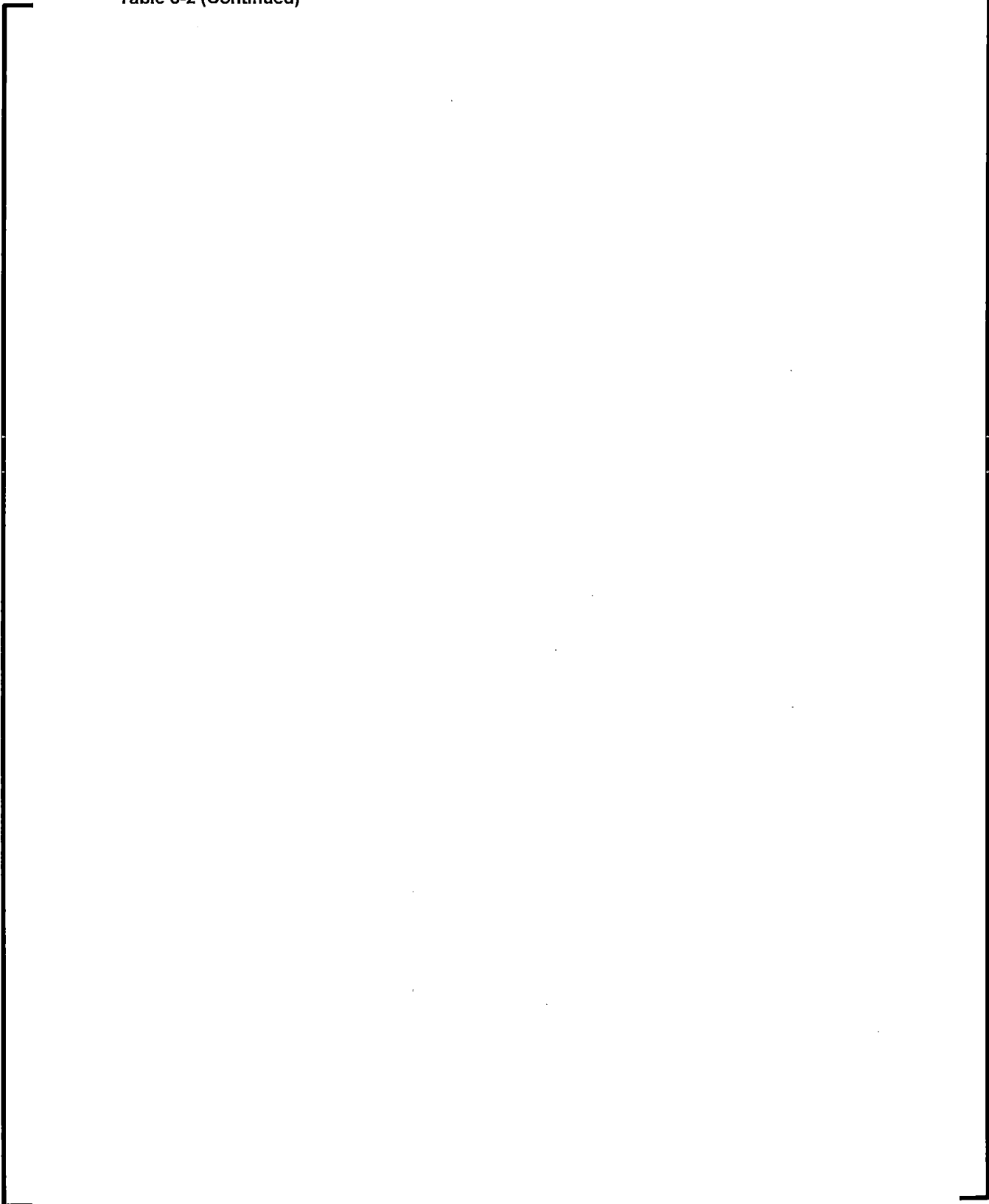
A large, empty rectangular frame with a thin black border, occupying most of the page. It is positioned below the caption 'Table 5-2 (Continued)'. The frame is currently empty, suggesting that the table content is either missing or has been redacted.

Table 5-2 (Continued)

A large, empty rectangular frame with a thin black border, occupying most of the page below the caption. It is intended for a table but contains no data.

**Table 5-2 (Continued)**

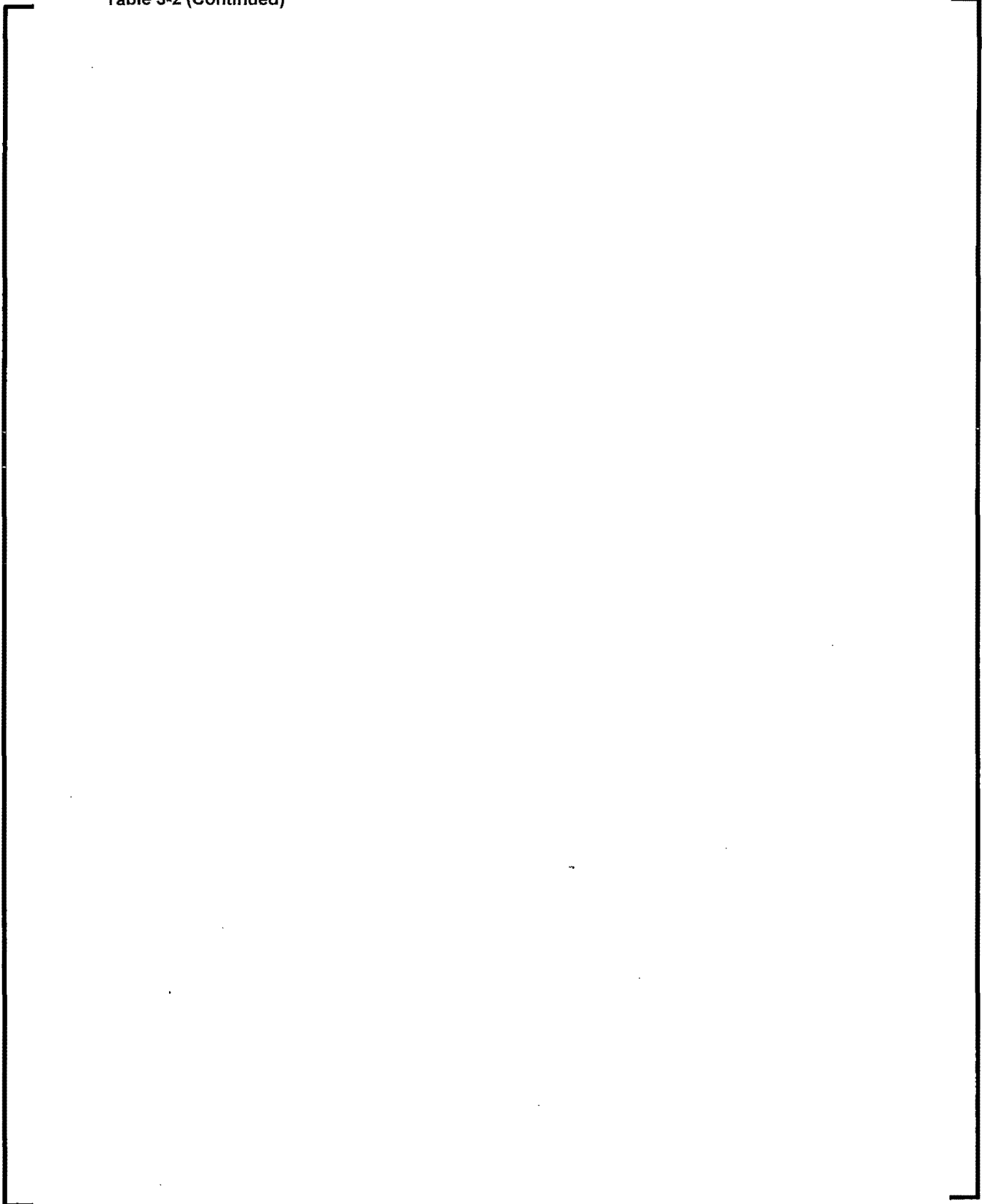
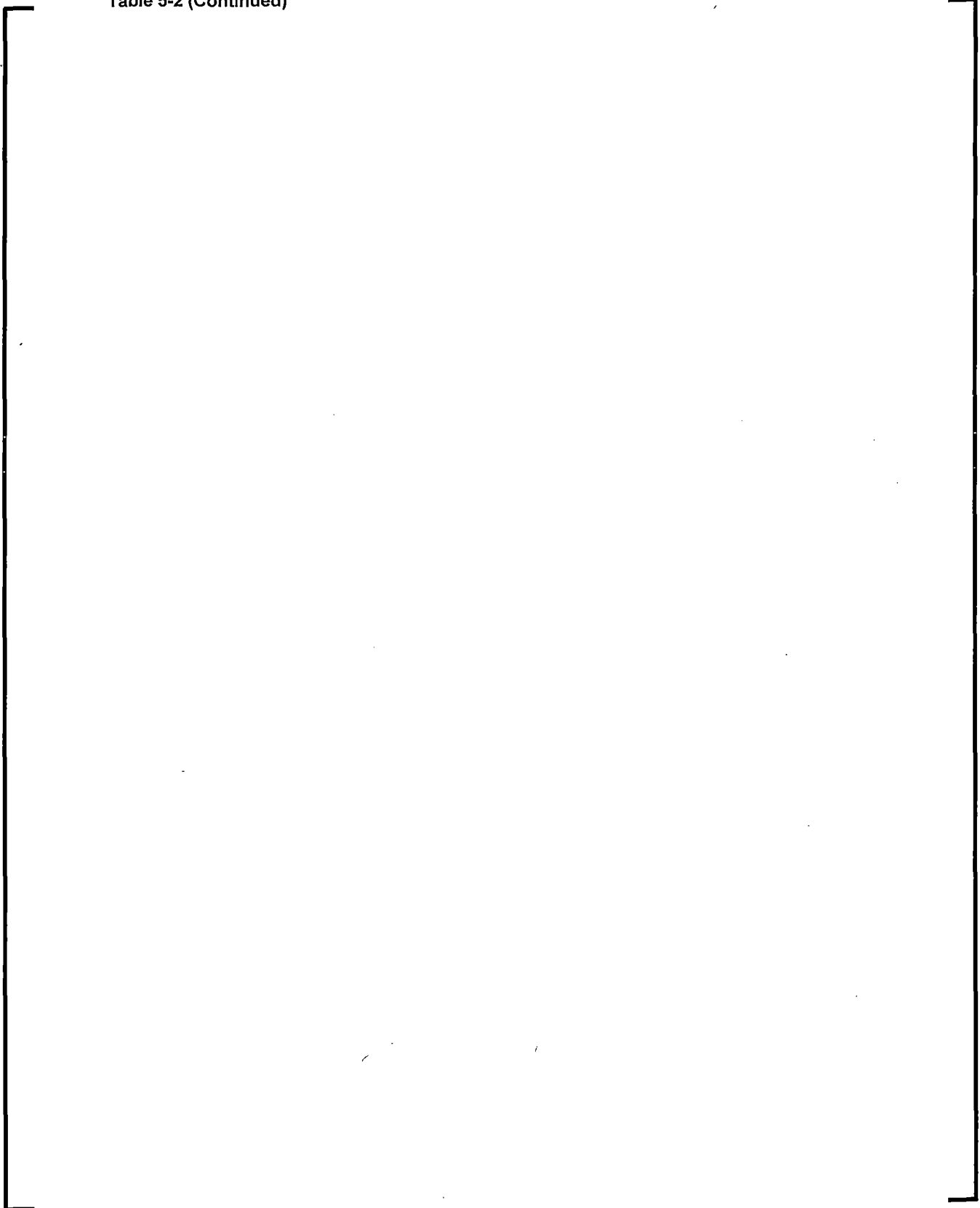


Table 5-2 (Continued)





**Table 5-2 (Continued)**

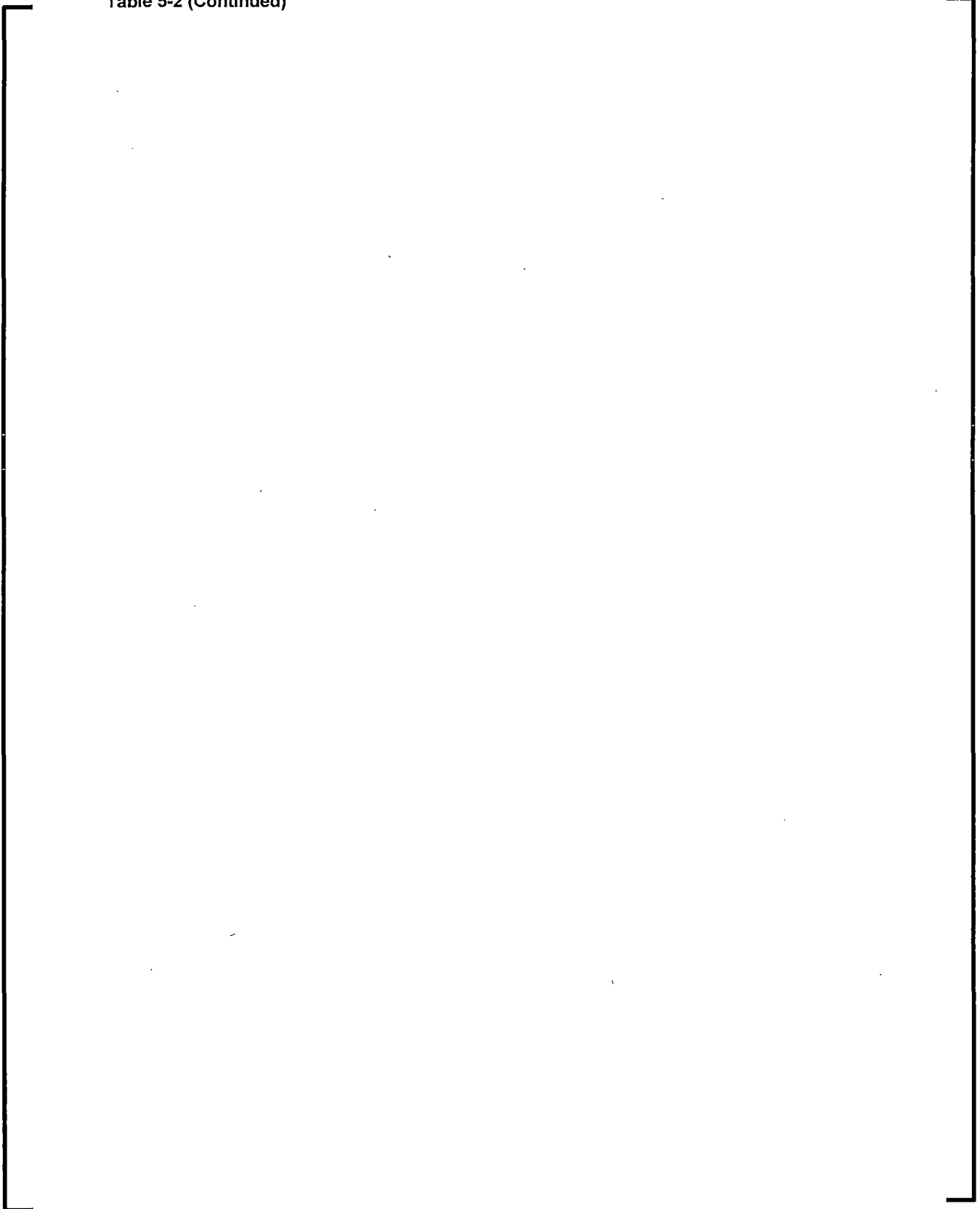
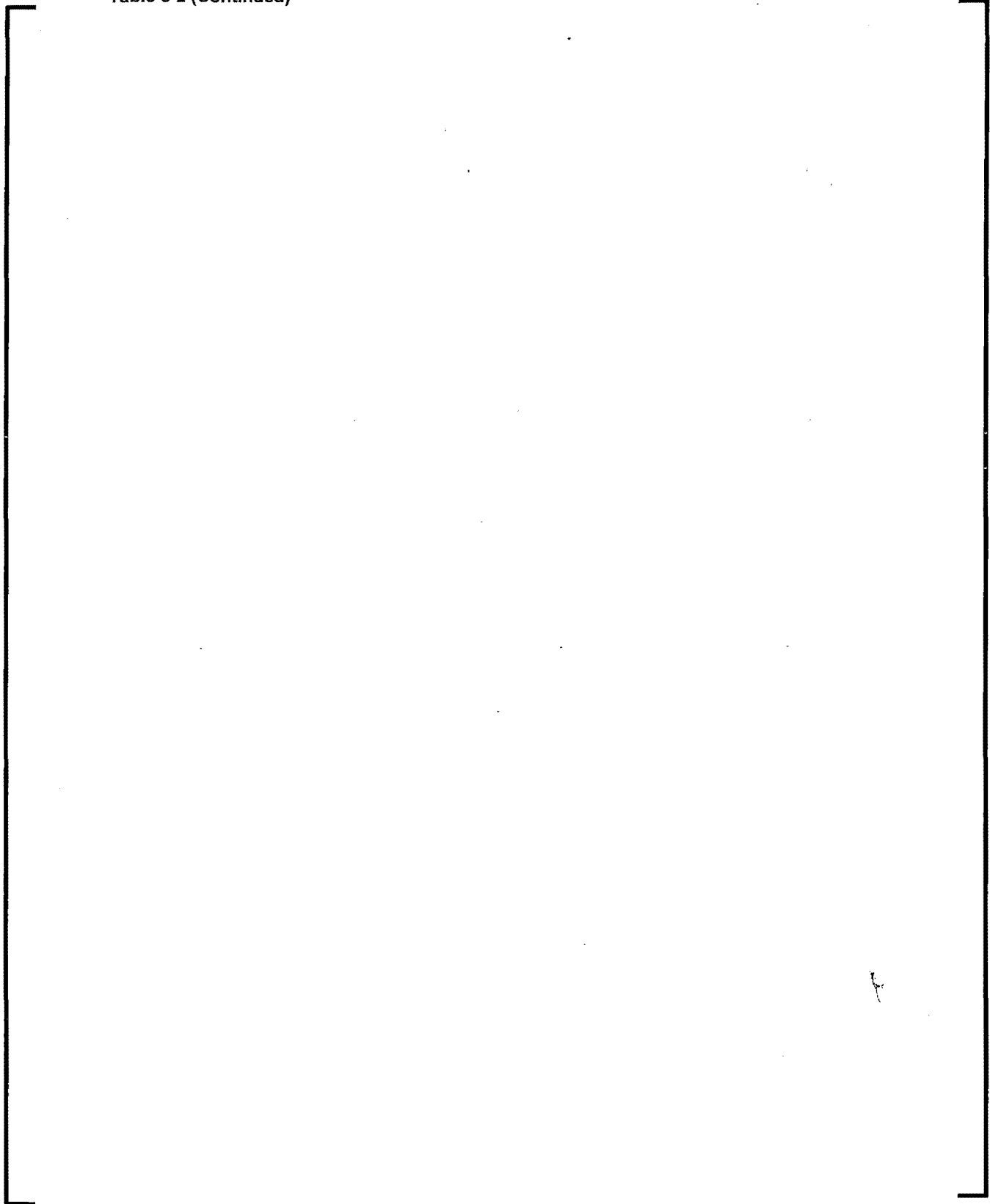


Table 5-2 (Continued)



**Table 5-2 (Continued)**

A large, empty rectangular frame with a thin black border, occupying most of the page below the caption. It is intended for a table but contains no data.

Table 5-2 (Continued)

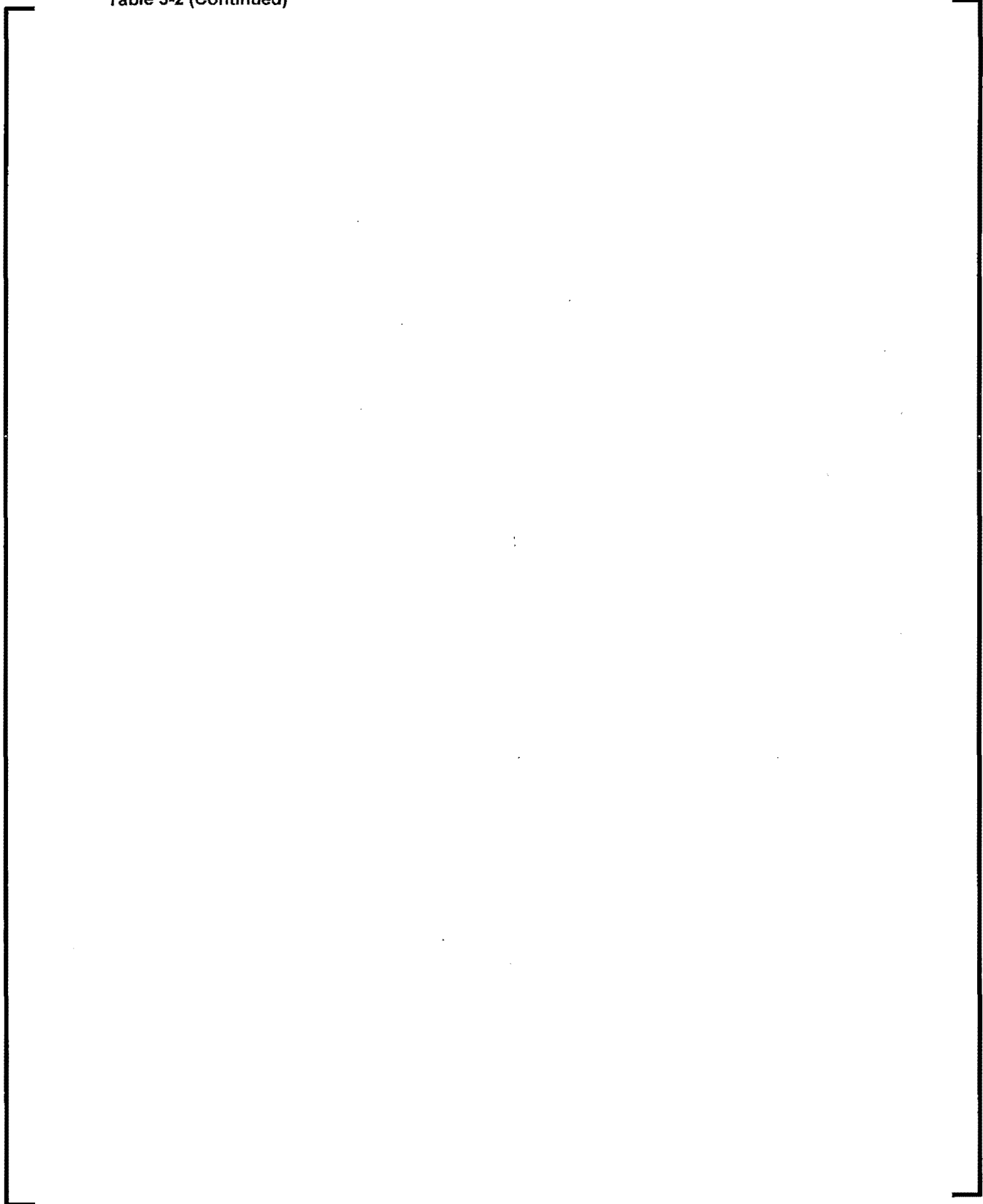


Table 5-2 (Continued)

A large, empty rectangular frame with a thin black border, occupying most of the page. It is positioned below the caption 'Table 5-2 (Continued)'. The frame is currently empty, suggesting that the table content is either redacted or not present on this page.

**Table 5-2 (Continued)**

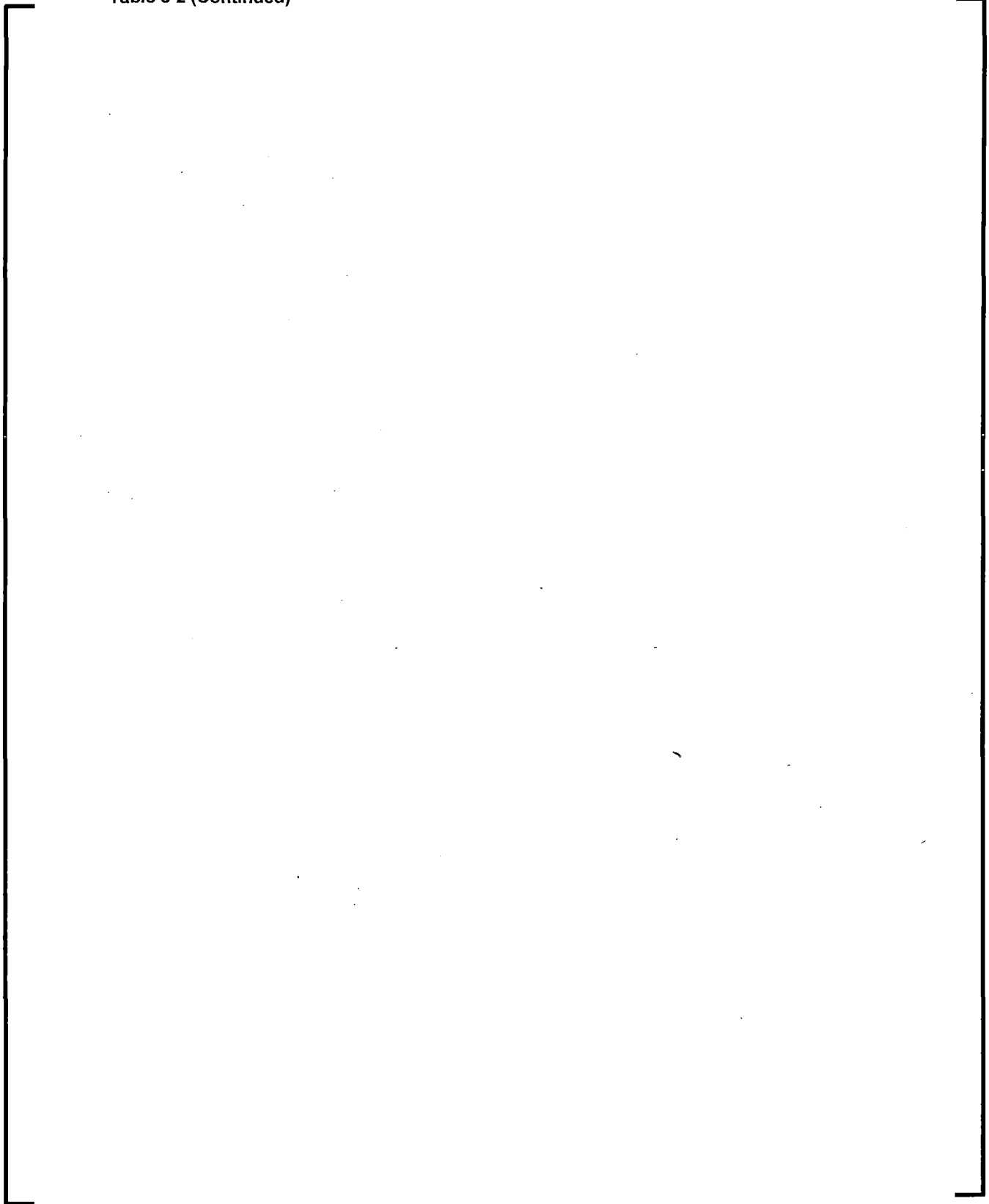


Table 5-2 (Continued)

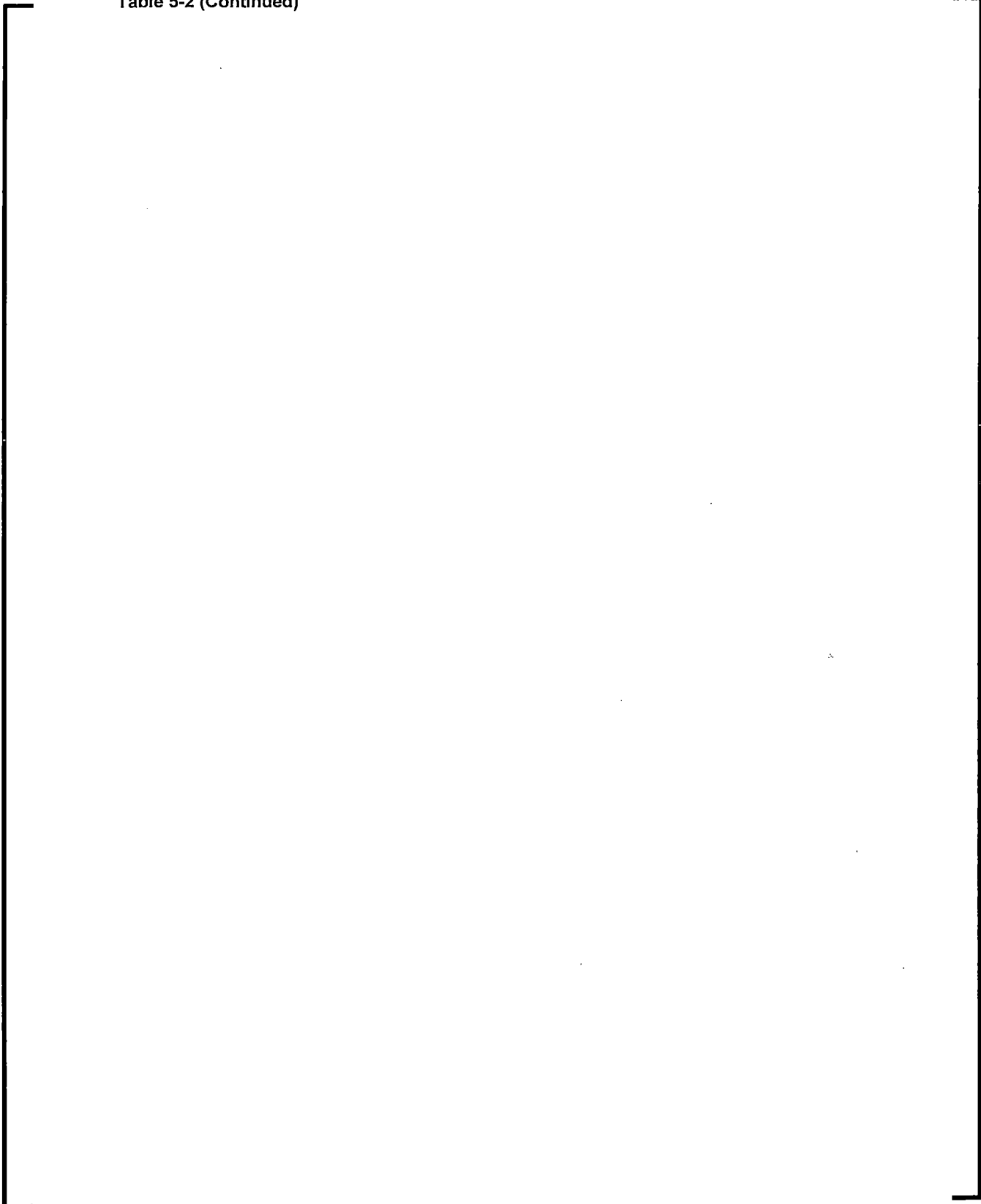
A large, empty rectangular frame with a thin black border, occupying most of the page. It is positioned below the caption 'Table 5-2 (Continued)'. The frame is currently empty, suggesting that the table content is either missing or has been redacted.

Table 5-2 (Continued)

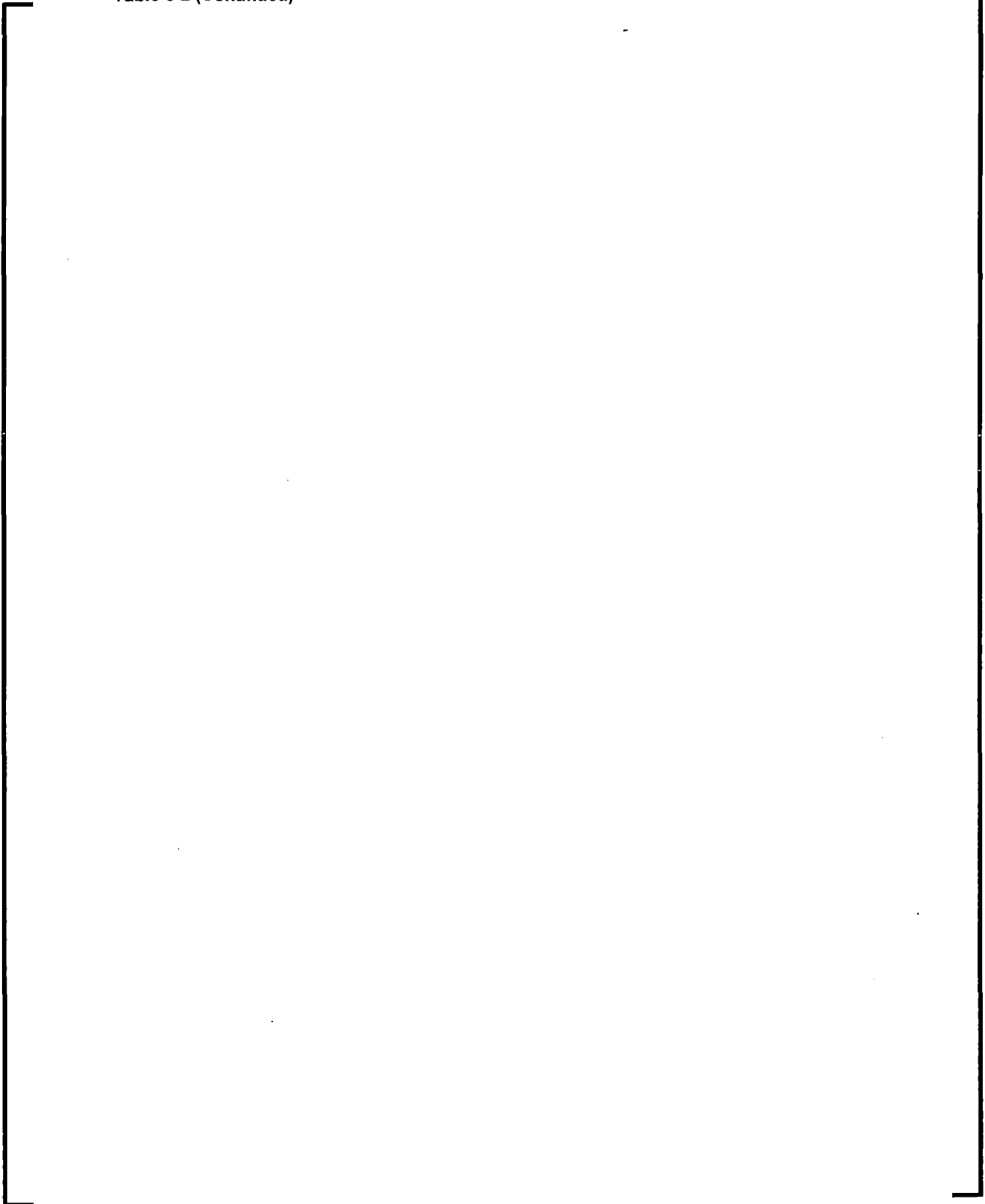




Table 5-2 (Continued)

A large, empty rectangular frame with a thin black border, occupying most of the page below the caption. It is intended for a table but contains no data.

Table 5-2 (Continued)

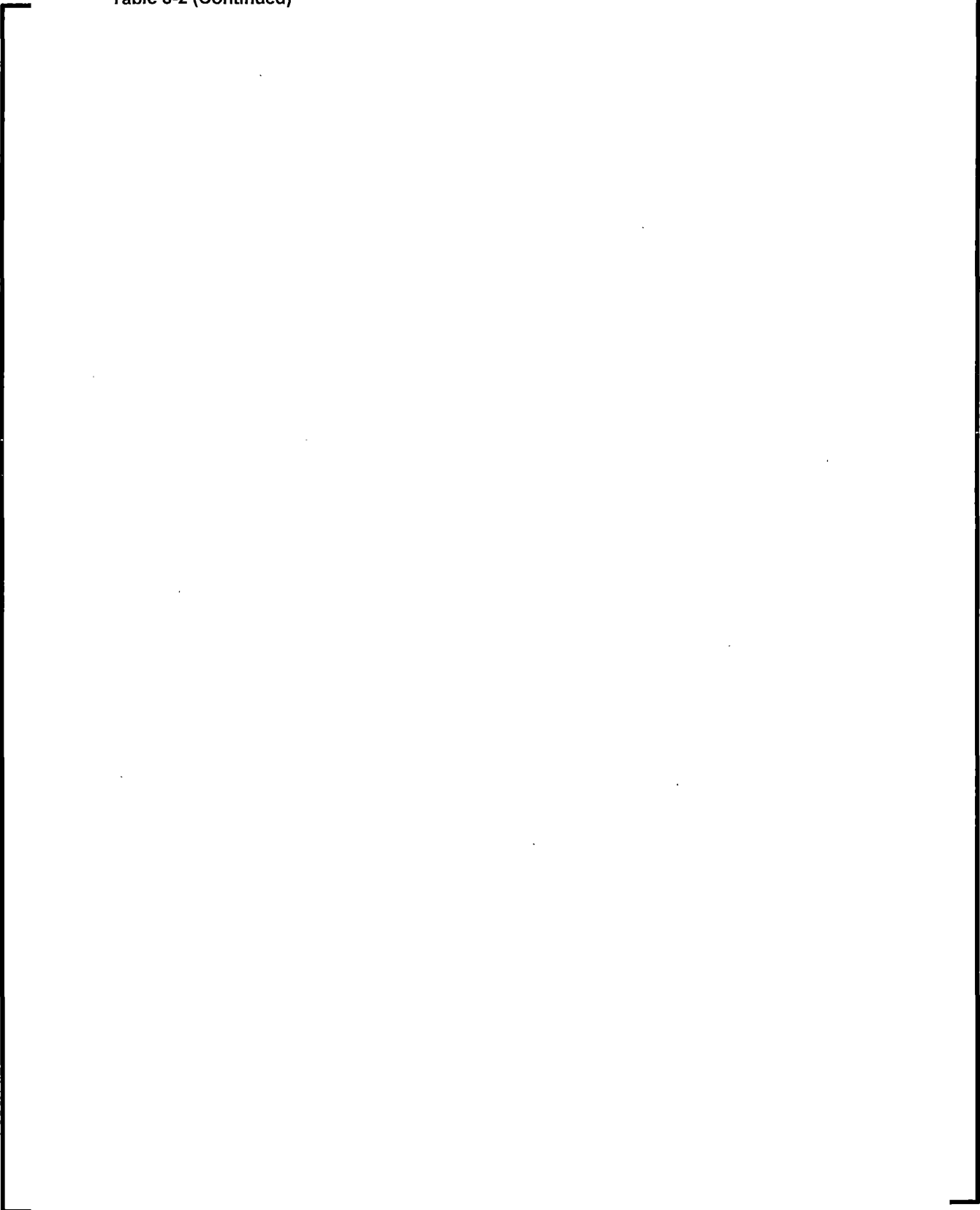
A large, empty rectangular frame with a thin black border, occupying most of the page. It is positioned below the caption 'Table 5-2 (Continued)'. The frame is currently empty, suggesting that the table content is either missing or has been redacted.

Table 5-2 (Continued)

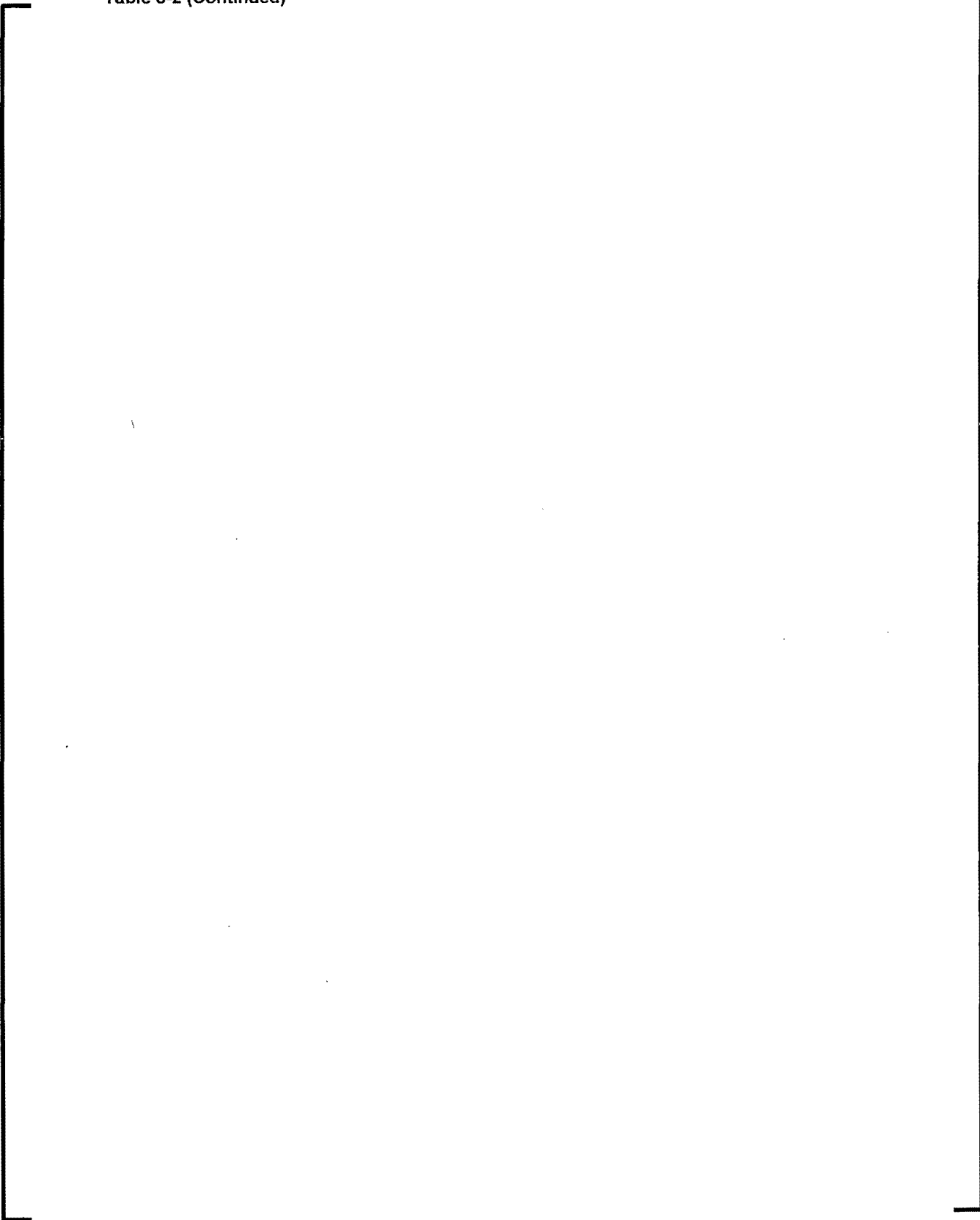
A large, empty rectangular frame with a thin black border, occupying most of the page. It is positioned below the caption 'Table 5-2 (Continued)'. The interior of the frame is completely blank, suggesting that the table content is either missing or has been redacted.

Table 5-2 (Continued)

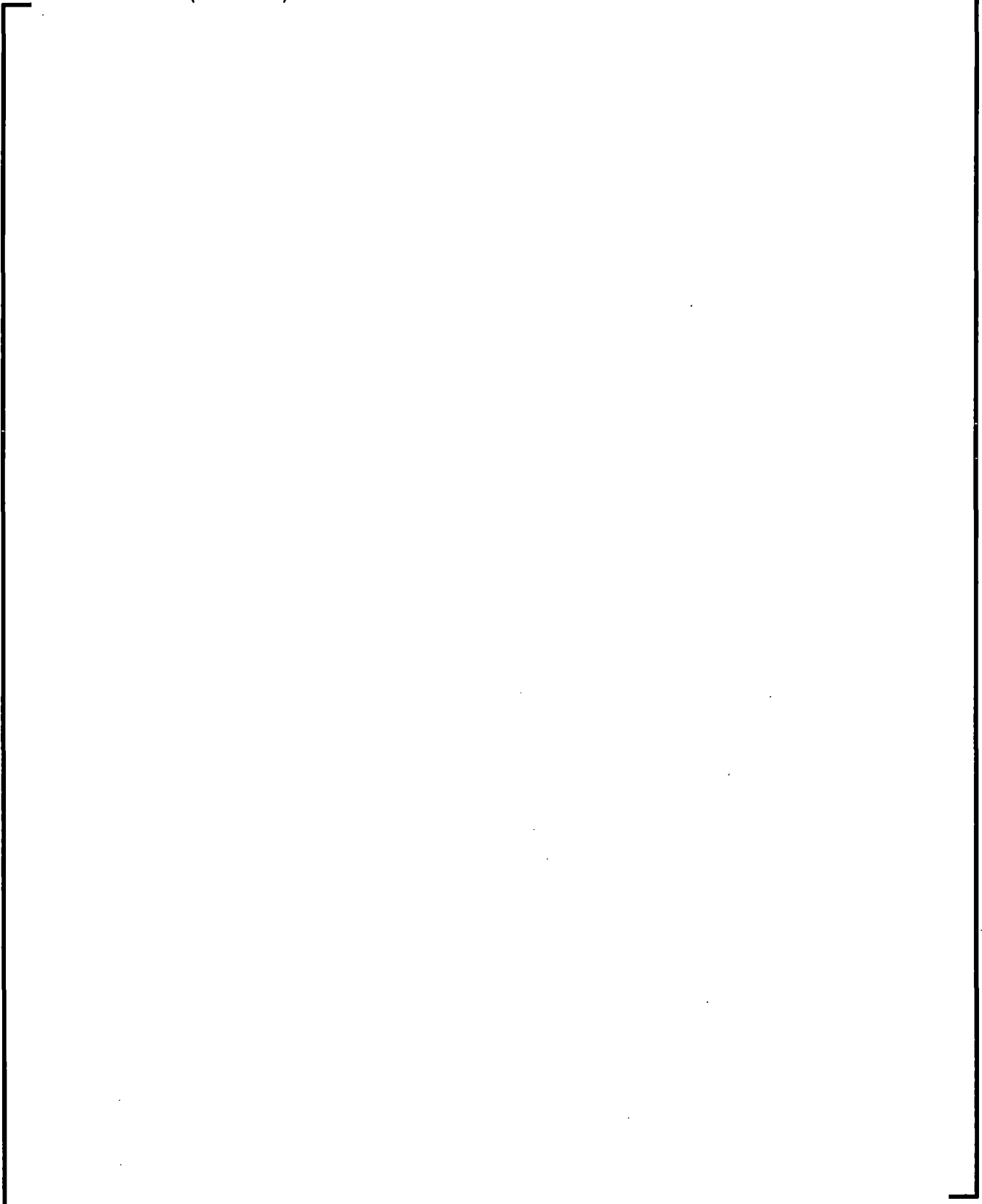


Table 5-2 (Continued)

A large, empty rectangular frame with a thin black border, occupying most of the page. It is positioned below the caption 'Table 5-2 (Continued)'. The frame is currently empty, suggesting that the table content is either missing or has been redacted.

Table 5-2 (Continued)

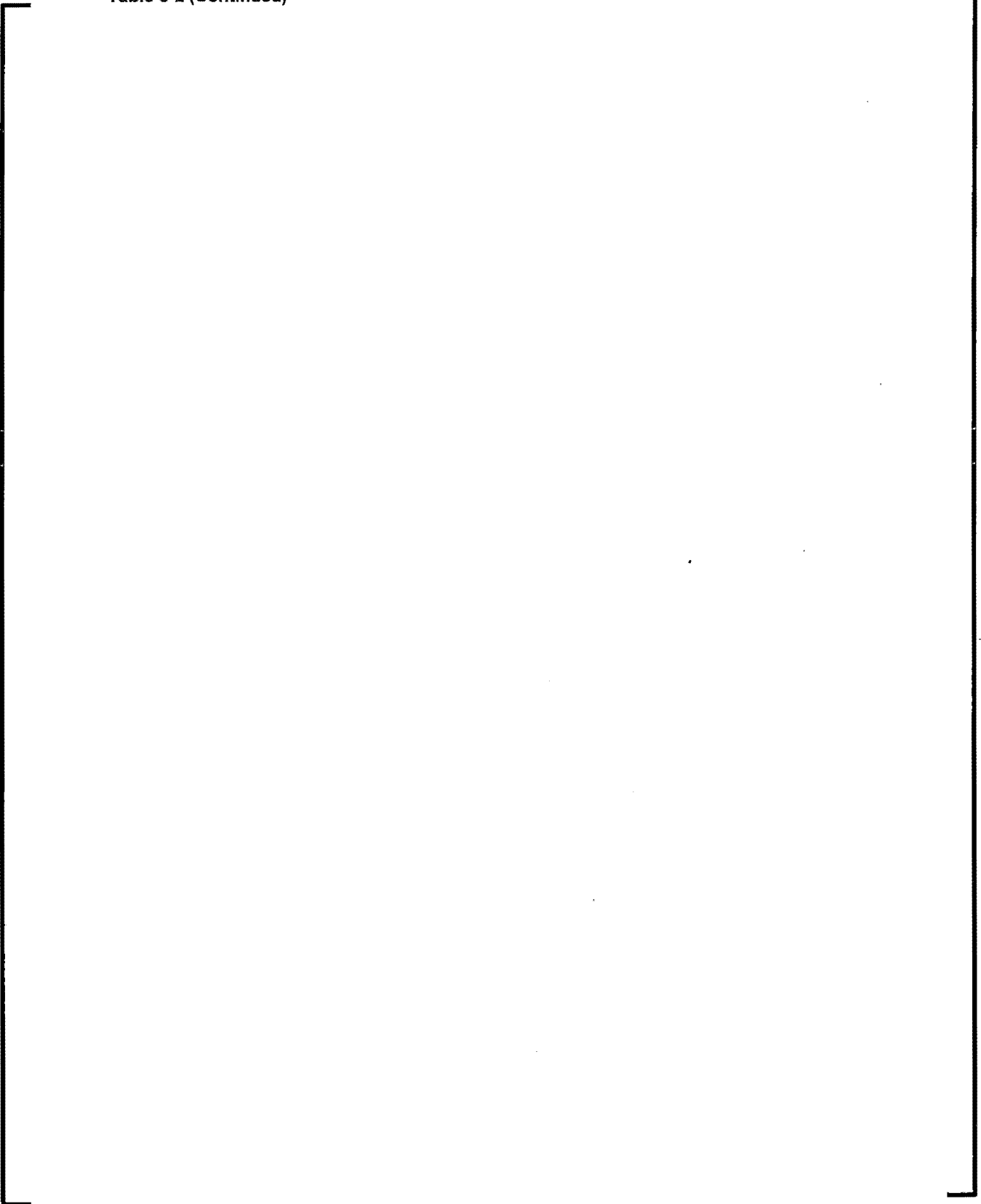


Table 5-2 (Continued)

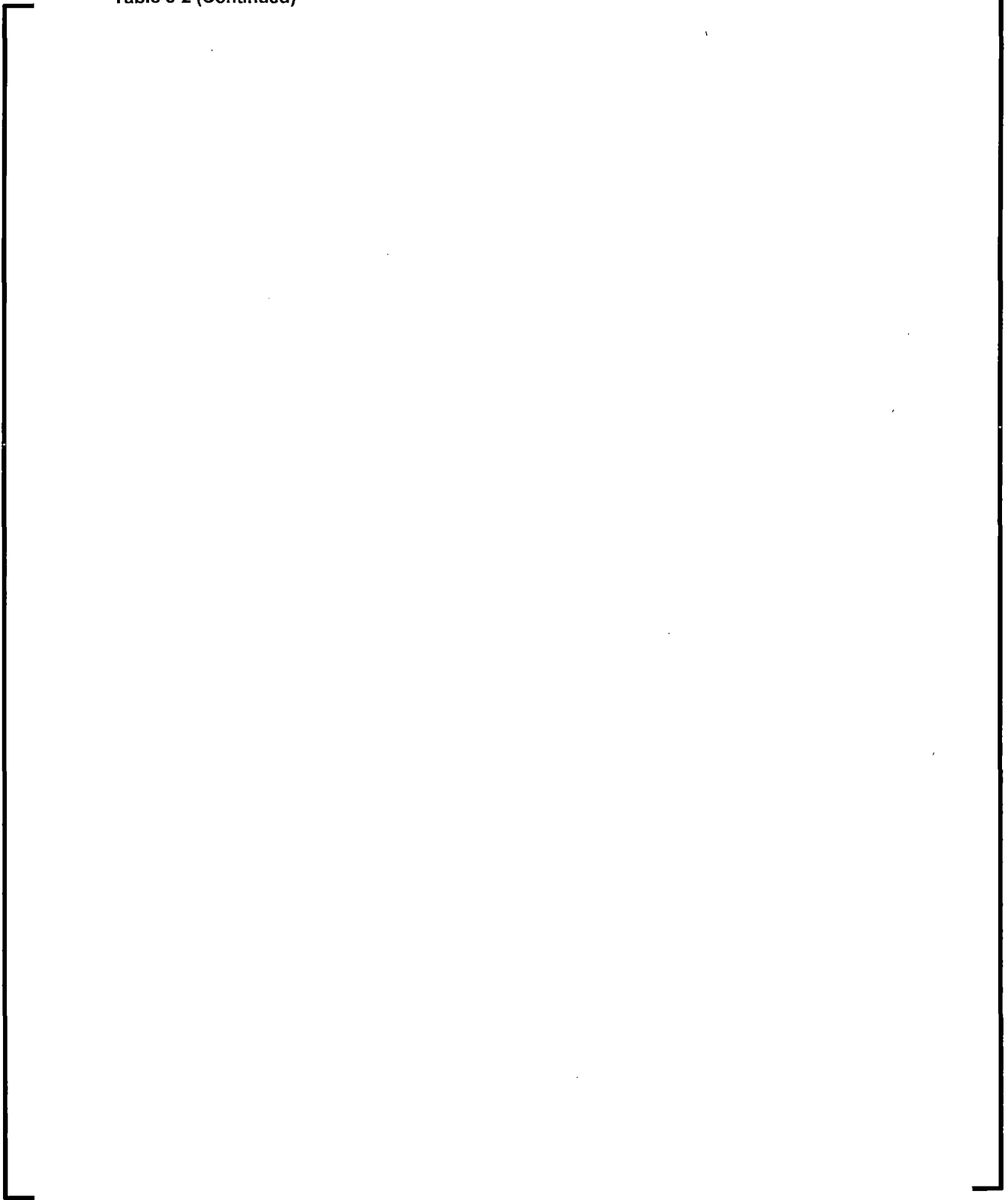
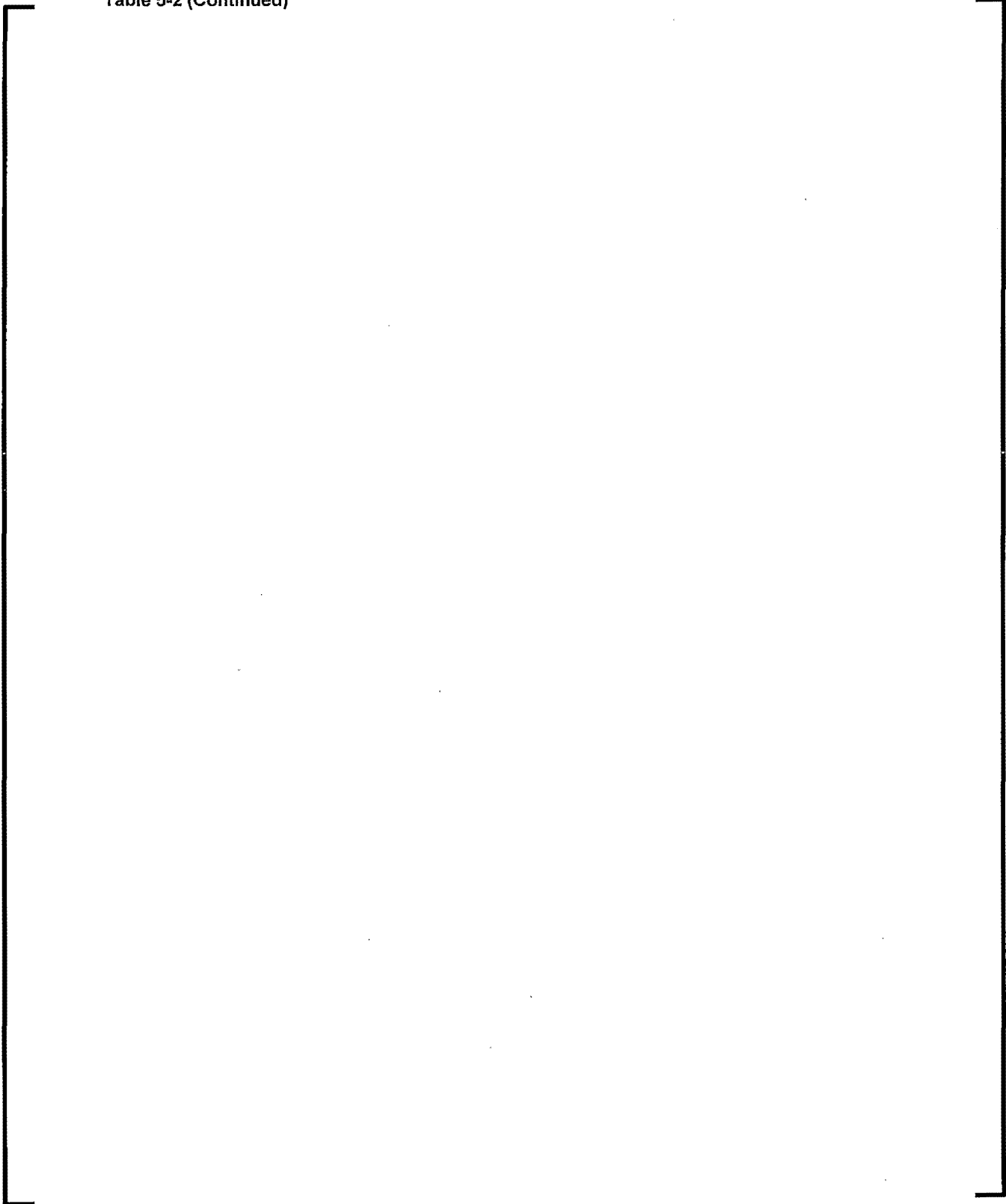
A large, empty rectangular frame with a thin black border, occupying most of the page. It is positioned below the caption 'Table 5-2 (Continued)'. The frame is currently empty, suggesting that the table content is either missing or has been redacted.

Table 5-2 (Continued)





**Table 5-2 (Continued)**

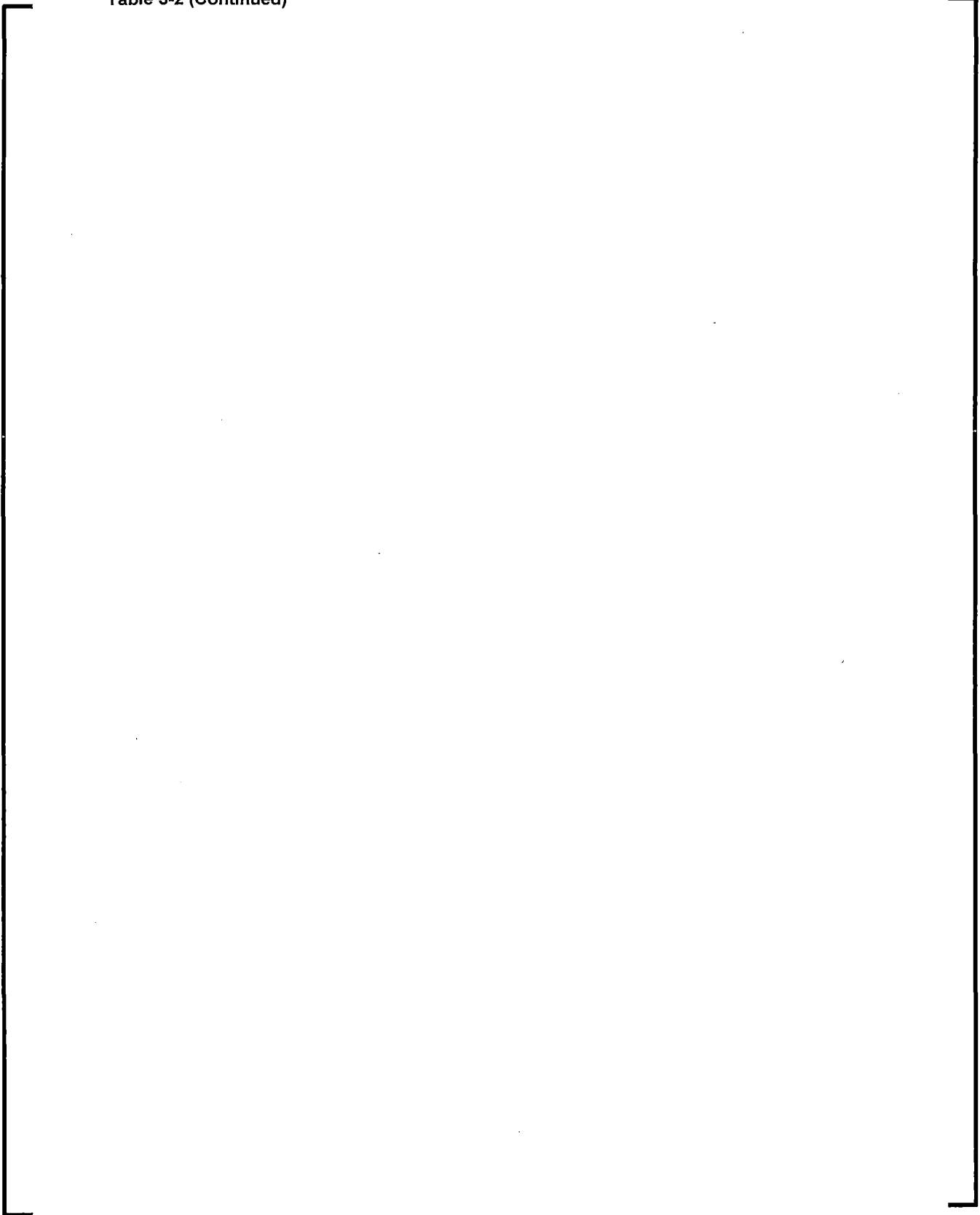
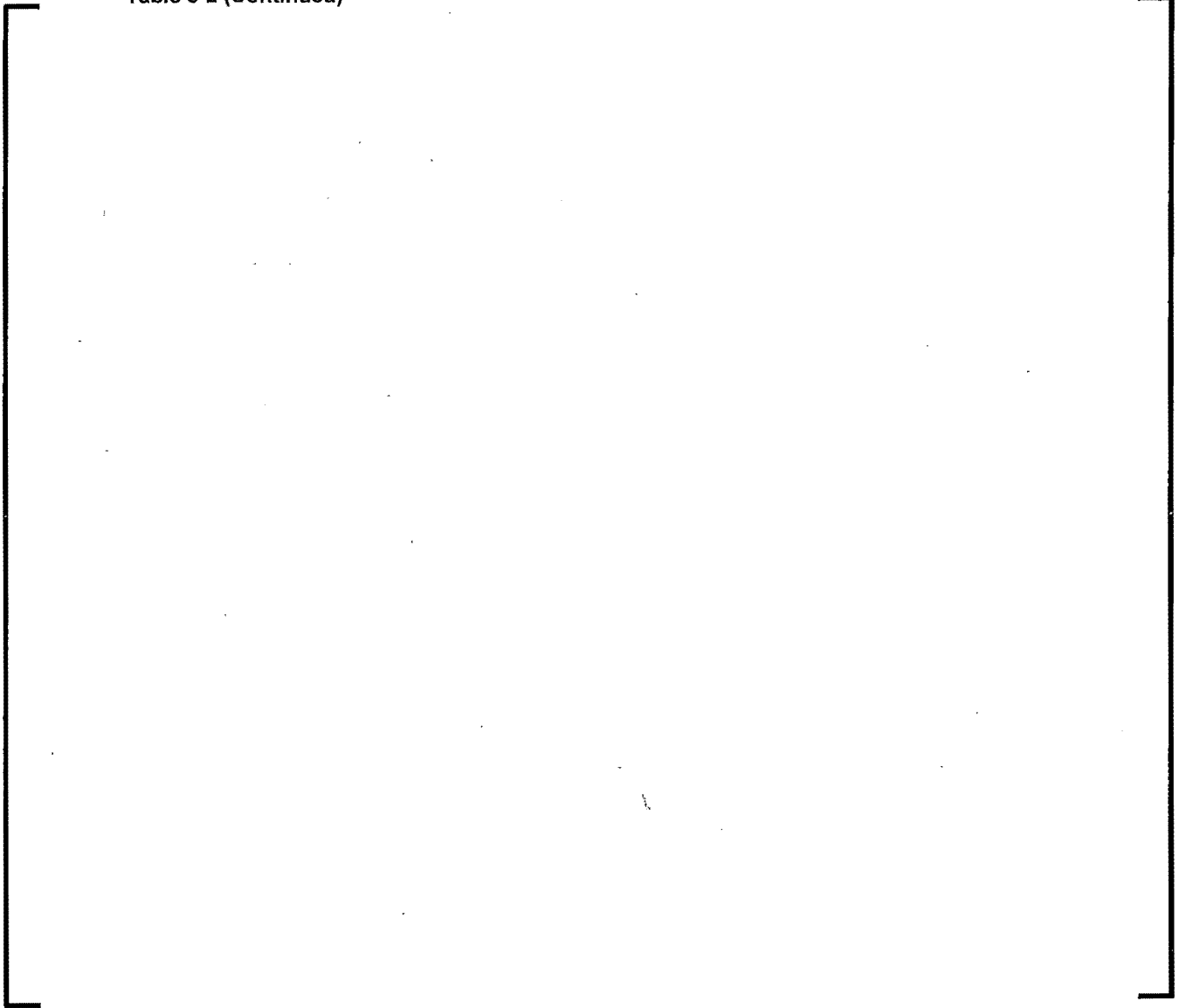
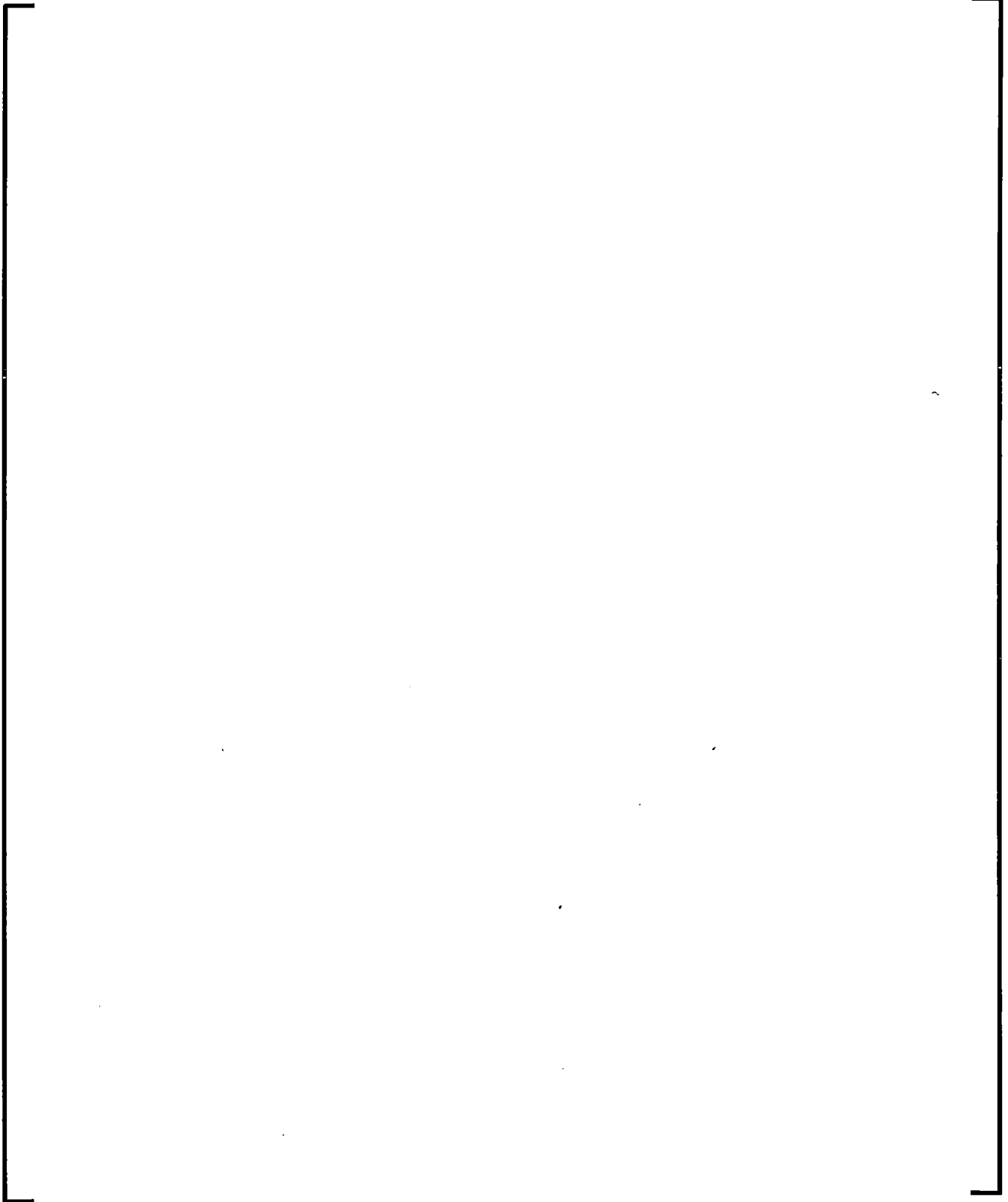


Table 5-2 (Continued)

A large, empty rectangular frame with a thin black border, occupying most of the page below the caption. It is intended for a table but contains no data.

---

**Table 5-3**  
**Benchmark Database Summary**

A large, empty rectangular frame with a thin black border, centered on the page. It is intended to contain the data for Table 5-3, 'Benchmark Database Summary', but the content is currently blank.

**Table 5-3 (Continued)**

A large, empty rectangular frame with a thin black border, occupying most of the page below the caption. It is intended for a table but contains no data.

## 6.0 SENSITIVITY

Section 1.4 of Regulatory Guide 1.190<sup>9</sup> discusses the "Methodology Qualification and Uncertainty Estimates". "The methods qualification consists of three parts: (1) the analytic uncertainty analysis (Regulatory Position 1.4.1), (2) the comparison with benchmarks and operating reactor measurements (Regulatory Position 1.4.2), and (3) the estimate of uncertainty in the calculated fluence (Regulatory Position 1.4.3)." This section (6) of the topical explains the modeling for the analytic uncertainty analysis.

[

] The estimate of uncertainty in the calculated fluence in the third part of the Methods Qualification was one of the more important points that Regulatory Guide 1.190 addressed.

The fracture mechanics safety analysis is based on stresses propagating hypothetical flaws within the vessel's steel material. The material's fracture toughness is determined from vessel test specimens that have been irradiated. The fluence-radiation uncertainties were determined by benchmark comparisons to dosimetry measurements. Unfortunately, the safety analysis within the actual vessel material is not supported by uncertainties from benchmark comparisons. There are no measurements within the vessel.

To ensure that the safety analysis is supported by well-known fluence-radiation uncertainties, the NRC's experts suggested [

] estimate of the uncertainty in the calculated fluence. Framatome developed a comprehensive uncertainty methodology in Reference 1 [

] This exact same methodology is incorporated in SVAM's methodologies.

The estimates of the uncertainties in SVAM's methodologies are statistically evaluated [

] There are no specific benchmarks for *dpa* reactions, or any

other reactions, that are deep within the vessel steel. Thus, the estimate of uncertainties in the calculated fluence-radiation (Regulatory Position 1.4.3) [

]

This section (6) addresses the fluence-radiation "Sensitivity" to uncertainties that could impact various high stress locations such as those noted in Figure 2-2.

Framatome examined the single and statistically combined effects of random fabrication and operational uncertainties on five independent variables that would increase the uncertainties in the fluence-radiation results. These uncertainties are:

- 1) ENDF cross-section covariance data
- 2) Geometric configurations
- 3) Isotopic composition of materials
- 4) Neutron sources
- 5) Computational methodology (analytical methods and procedures)

## 6.1 *Statistical Modeling*

The Statistical Modeling of the analytic uncertainties from the Sensitivity analyses [

]

Hypothetical sensitivities do not have independent degrees of freedom.

[

]

[

]

The results from the sensitivity calculations [

] The deviations in the fluence-radiation results include the statistical properties of the fabrication and operational uncertainties. [

] This thereby gives the 95 / 95 confidence that the estimated standard deviations are appropriate for the ART values used in the fracture mechanics safety analyses.

## 6.2 *Sensitivity Modeling*

The SVAM methodology is based on [

]

An important feature of the Sensitivity modeling is the requirement to be consistent with the ART margin term applied in the fracture mechanics safety analyses. The ART margin term in Regulatory Guide 1.99, Revision 2 reflects 95 / 95 confidence in the standard deviations by applying a tolerance factor of "2" ( $2 \times \sigma$ ) for the 177  $\Delta RT_{NDT}$  specimens. If the relation between the five variables and the fluence-radiation results was a (straight line) linear function, then the Sensitivity modeling could simply be based on applying the appropriate deviation in the fabrication and operational parameters.

The relation between the five variables and the fluence-radiation results is not linear. Neutron transport methods are based on exponential integral relationships between the variables and the fluence-radiation results. The Sensitivity model relates the tolerances associated with dimensional specifications and material properties to the exponential integral relationships. There is a problem however with the tolerances not having multiple measurements. The deviations affecting the five variables must have the tolerance factors appropriately increased to represent a 95 / 95 level of confidence.

For example, Babcock & Wilcox, one of the predecessors to the modern Framatome, manufactured many of the vessels and internal components that are currently operating in PWR and BWR plants. When performing the analytic uncertainty evaluation, the quality assurance specifications were checked. The tolerances met specifications, but the ASME quality assurance only specified "3" independent measurements. Thus, the 95 / 95 tolerance factor on the mean deviation of the components would need to be much larger than "2" to have 95 / 95 confidence in the safety analysis.



To conclude, the Sensitivity Modeling [

] The fluence-radiation results are consistent with the Regulatory Guide 1.99, Revision 2 ART margin term. The deviations in fabrication and operational uncertainties reflect 95 / 95 tolerance factors that are (a) greater than "2" for geometric configurations and material isotopic compositions, and (b) "2" for cross-section covariances, neutron sources and the calculational methods and procedures. [

] This gives 95 / 95 confidence in the fluence-radiation uncertainties that are part of the ART margin term used for fracture mechanics safety analyses.

### **6.3 Cross Section Covariance Data**

The ENDF/B-VII.1 cross section library is distributed with a comprehensive set of covariance files for the data. Table 6-1 shows the U-235 cross-section uncertainties as a function of energy.

The ENDF/B files contain cross-section uncertainty data, correlations, variances and covariances, along with the data. [

] the 95 / 95 random uncertainties in the macroscopic cross-sections represented a statistical combination of covariances that were modeled for the analytic uncertainty analyses.

## 6.4 *Geometric Configurations*

Even when the most robust computer model is developed, there will be differences between the computer model and the physical system. These differences can be divided into two broad categories (1) uncertainty in the "As-built" dimensions and (2) modeling simplifications.

Nuclear reactors built in the U.S. follow ASME code standards. The standards strictly define the manufacturing tolerances for the reactor vessels and internal components. The 95 / 95 random uncertainties in the dimensions include the accuracy of the measurement tools and the procedures followed by the manufacturer.

A source of uncertainty in the "As-built" dimensions is field-change variations. Field-change variations can occur for a variety of reasons. For the PWR and BWR vessels and internals that Babcock & Wilcox fabricated, excellent records were maintained on field-change variations. This allowed sensitivity calculations to combine 95 / 95 random uncertainties to appropriately determine the impact of the field-changes.

In the Framatome SVAM methodology, the key components, such as the reactor pressure vessel and the important reactor internal structures, are modeled heterogeneously – no approximation. However, it is common practice to apply modeling simplifications to components in less important locations. Simplifications, such as homogenization, are used in the SVAM methodology. For example, the upper end fittings of the fuel assembly, and the components in the reactor cavity, such as the insulation, have been homogenized. Sensitivity calculations were evaluated to determine the impact of approximate geometric configurations on the calculational uncertainty. [

]

## **6.5      *Isotopic Composition of Materials***

The ASME and ASTM provide material standards. These standards specify the isotopic-elemental composition of the materials used in the construction of PWRs and BWRs. The specifications further include material properties such as the density and coefficient of expansion. For water regions, the specifications include the variation in density as a function of pressure and temperature.

The isotopic compositions of the primary elements within each material are not specific. There is an allowable range of these elements. Other elements representing impurities are specified in terms of limits. This means that the material sensitivity modeling to evaluate the analytic uncertainties in the fluence-radiation is based on a mean – best-estimate reference composition.

Due to the lack of specific mean values, the uncertainties in the isotopic compositions are evaluated in terms of the allowable range of concentrations. The statistical properties are defined as normal probability distributions with tolerance factors represented by the concentration limits.

As noted above when discussing the microscopic cross-section covariances in Section 6.3, the uncertainties in the isotopic composition of materials are not separately analyzed. The independent variables in the neutron transport models are macroscopic cross-sections. The sensitivity calculations thereby statistically combine the isotopic composition deviations with microscopic cross-section covariances.

The statistical modeling of the sensitivity results considers the combination of [

] Covariance estimates coupling

the material and geometry uncertainties for the sensitivity calculations ensure that the determination of the fluence-radiation uncertainties is statistically valid.

For fluence-radiation calculations beyond the fuel region, the key materials are

[

] as explained in the Statistical Application of

Uncertainties section (6.8) below, the estimate of the fluence-radiation random uncertainties has a well-founded statistical basis.

From the discussions of (1) the cross-section covariance data, (2) the geometric configurations, and (3) the isotopic composition of materials, it is clear that various uncertainties are dependent on each [

] the statistical

distribution of the sensitivity results must be consistent with both the lower range of deviations as well as the higher range.

## 6.6 *Neutron Sources*

The neutron source [

]

[

The core-follow comparisons to the measurements show variations in the power and the spatial power distributions in every cycle [

] the statistical treatment of the sources

in the sensitivity calculations is to consider them as a completely independent random variable. This means that the effect of source uncertainties directly affects the fluence-radiation results. This is independent of the additional effects from other uncertainties.

Sensitivity results indicate that the relative fluence-radiation deviations at various locations are [

] with respect to the uncertainties in the energy distribution or burnup dependence of the sources.

The energy distribution uncertainties are defined by the uncertainties in the emission spectrum for each fissile isotope. The concentration of the fissile isotopes changes as the fuel produces power. The uncertainty in the concentration of each fissile isotope adds to the emission spectra uncertainties. The variation in the neutron source emission spectra is included in the sensitivity calculations for the analytic uncertainties in the fluence-radiation results.

### **6.7 *Calculational Methods and Procedures***

The analytic uncertainties in the fluence-radiation results due to variations in the calculational methods and procedures [

]

For example, using computer aided design models based on programs such as SOLIDWORKS<sup>3</sup> does not lead to uncertainties in the calculations. [

] SOLIDWORKS modeling

provides a means of specifying configurations with accurate geometric shapes and precise dimensions such that the fluence-radiation is accurate and precise.

The continuous energy model in MCNP's solution process also reduces the variation caused by deterministic discrete ordinates methods and collapsed energy groups.

[

]

[

]

### 6.8 *Statistical Application of Uncertainties*

Regulatory Guide 1.190<sup>9</sup> suggests a means of demonstrating that the calculational results have a valid standard deviation. The most important statistical property of the fluence-radiation standard deviation is that it provides consistency with the ART (Adjusted Reference Temperature) margin term in Regulatory Guide 1.99, Revision 2.<sup>8</sup>

[

]

The fundamental basis for the statistical properties of the fluence-radiation calculations is the [

]

Section 5 describes the benchmark database. It provides the comparison of SVAM results to the 887 data points in the measurement database. [

]

[ ] Furthermore, the uncertainties applied to SVAM's fluence-radiation results are consistent with the ART margin term which is used for safety analyses.

[ ] there are no measurements within the vessel structures. This is an important issue because it is the propagation of hypothetical flaws within the vessel material that are the basis for the fracture mechanics safety analyses. The discussions above in Sections 6.0 through 6.6 explain sensitivity evaluations to support an analytic uncertainty. Sensitivity results for the fluence-radiation, which is transported throughout the heads, shells, nozzles, supports, etc., provide an uncertainty that is applicable to every location within the vessel.

[ ] Framatome developed a comprehensive Sensitivity model [ ] Due to the exponential integral function that represents neutron transport throughout the internal and vessel components, the deviations modeled in the sensitivity calculations were based on 95 / 95 confidence levels. [ ]

]



Having a Sensitivity model that included (a) locations throughout the vessel where measurements were not feasible, [

]

The Statistical Application of Standard Deviations to vessel locations that had no measurements [

]

The problem with [ ] an unknown number of random variables. There is no question that a large number of [

It would be highly unlikely, but the probability is more than 0.00.

Framatome has taken the very conservative approach with estimating the relative standard deviation within locations where no measurements exist. [

]

**Table 6-1**  
**ENDF/B U-235 Uncertainties<sup>7</sup>**  
**MT= 1 total**

Energy range (eV)	xsec	% unc
1.000E-02 - 1.5200E-01	6.2410E+02	0.26
1.520E-01 - 4.1400E-01	2.2322E+02	0.26
4.140E-01 - 1.1300E+00	9.5370E+01	0.30
1.130E+00 - 3.0600E+00	4.2827E+01	0.40
3.060E+00 - 8.3200E+00	5.4989E+01	0.32
8.320E+00 - 2.2600E+01	1.1616E+02	0.20
2.260E+01 - 6.1400E+01	8.4605E+01	0.21
6.140E+01 - 1.6700E+02	4.5955E+01	0.34
1.670E+02 - 4.5400E+02	3.7251E+01	0.41
4.540E+02 - 1.2350E+03	2.7498E+01	0.55
1.235E+03 - 3.3500E+03	2.0458E+01	0.71
3.350E+03 - 9.1200E+03	1.7146E+01	1.51
9.120E+03 - 2.4800E+04	1.5167E+01	1.51
2.480E+04 - 6.7600E+04	1.3458E+01	1.51
6.760E+04 - 1.8400E+05	1.1744E+01	1.51
1.840E+05 - 3.0300E+05	1.0170E+01	1.51
3.030E+05 - 5.0000E+05	8.7974E+00	1.51
5.000E+05 - 8.2300E+05	7.5957E+00	0.93
8.230E+05 - 1.3530E+06	6.7881E+00	0.74
1.353E+06 - 1.7380E+06	6.7753E+00	0.67
1.738E+06 - 2.2320E+06	7.1208E+00	0.69
2.232E+06 - 2.8650E+06	7.5474E+00	0.69
2.865E+06 - 3.6800E+06	7.8700E+00	0.67
3.680E+06 - 6.0700E+06	7.7407E+00	0.68
6.070E+06 - 7.7900E+06	6.7253E+00	0.71
7.790E+06 - 1.0000E+07	6.0559E+00	0.77
1.000E+07 - 1.2000E+07	5.7468E+00	0.76
1.200E+07 - 1.3500E+07	5.7644E+00	0.75
1.350E+07 - 1.5000E+07	5.8347E+00	0.75
1.500E+07 - 1.7000E+07	5.9444E+00	0.76

## 7.0 FUTURE MONITORING

SVAM expands Framatome's fluence methodology to include both the traditional fuel-beltline region and the extended regions that are above and below the beltline. The uncertainties defined in this topical are valid for "monitored" cycles. That is, cycles that have been analyzed and are consistent with the benchmark database (see Tables 5-2 and 5-3).

In general, fracture mechanics safety analyses are for many cycles in the future. When considering SLR, the future would be 80 calendar years of operation. The licensing approval of the safety analyses generally sets the end of licensed-life (EOL) for the reactor. As a consequence, the maximum irradiation embrittlement of the reactor vessel occurs during the last cycle of operation when the end of cycle corresponds to EOL. Future cycles however not only have no "monitored" fluence-radiation results; they have not even been designed yet.

Acceptable EOL irradiation modeling is based on fluence-radiation rates that have been calculated from "monitored" cycles. These rates are projected to future time periods. This provides an estimate of the total fluence at locations of interest (LOI).

If (a) the projected fluence-radiation rates are used to support safety analyses that extend to future reload cycles, and (b) no future monitoring is planned, then – the assumption is – that the fluence rates for the projected time period represent equilibrium conditions. That is, the fluence rate, for a given location of interest from the last cycle analyzed, will be constant in all future cycles. As a consequence, the uncertainties in the fluence-radiation values will be consistent with the fracture mechanics ART margin term. This assumption is acceptable as long as future core designs have neutron characteristics that are identical to the core design of the last cycle analyzed.

Fluence-radiation values ( $\Phi$ ) at any time ( $t$ ) are determined from the cumulative fluence at the end of cycle (EOC) – "1" through "N" ( $EOC_N$ ). When the EOL time ( $t$ ) is beyond cycle  $N$ , the fluence rate ( $\Phi$ ) for cycle  $N$  is projected onto future cycles. Projected

fluence-radiation  $\Phi(t)$  values are determined by multiplying the fluence rate  $\{\Phi(N)\}$  by the difference between the cumulative time “ $T$ ” for EOL ( $t$ ) and the cumulative time “ $T$ ” to the end of cycle  $N$  ( $EOC_N$ ). This is expressed by Equation 7-1 for a *LOI*.

$$\Phi_{LOI}(t) = \Phi_{LOI}(EOC_N) + \Phi_{LOI}(N) \times (T(t) - T(EOC_N)) \quad (7-1)$$

where

$\Phi_{LOI}(t)$  = Fluence (n/cm<sup>2</sup>) at a location of interest with a variable time ( $t$  could be 40, 60, 80 years, etc.),

$\Phi_{LOI}(EOC_N)$  = Fluence (n/cm<sup>2</sup>) at end of cycle  $N$  for a location of interest,

$\Phi_{LOI}(N)$  = Fluence rate (n/cm<sup>2</sup>-sec) averaged over cycle  $N$ , at a location of interest,

$T(t)$  = Cumulative time (in seconds) when fluence-radiation values are desired ( $t$  could be for 40, 60, 80 years, etc.) normalized to the effective power-radiation level,

$T(EOC_N)$  = Cumulative time (in seconds) at end of cycle  $N$ , normalized to be consistent with the EOL power-radiation level.

The key point concerning the projections is that there are no operational or design limits which ensure that the fluence projections are accurate – with acceptable unbiased uncertainties. It is an assumption based on the fuel cycles having reached equilibrium neutronic conditions.

If a plant is truly in an equilibrium cycle, future fluence monitoring would not be required. Startup physics testing would show that the neutronic characteristics of each subsequent equilibrium cycle would be equivalent to the previous cycle.

The problem with equilibrium cycles is that reactors' operation staffs are always looking to improve performance. Current improvements being considered include Advanced

Fuel Management with increased burnups and enrichments, along with Accident Tolerant Fuel provided by changes to the pellet and cladding compositions.

When there are differences in a cycle's fuel design, and operating conditions, from those in previous cycles, not only could there be changes in the fluence-radiation level affecting the material embrittlement, but there are unknown statistical effects on the uncertainties. The uncertainties need to be evaluated in terms of the changes. For fluence projections to support fracture mechanics safety analysis; there needs to be 95 / 95 confidence in the fluence-radiation values.

The confidence required for safety analysis is directly related to the fluence methodologies described in Sections 3 through 6. [

]

The licensing basis for renewal to 60 or 80 years includes both projected EOL fluence values and the 10 CFR 50, Appendix H requirements for fluence monitoring. It is the fluence monitoring part of the Appendix H surveillance program that ensures that the fracture toughness – material embrittlement limits ( $RT_{PTS}$ , ART, USE, and J-integrals) for the vessel will not be exceeded. This section of the topical report describes the Framatome fluence monitoring methodology for future cycles in terms of calculated fluence-radiation values and the uncertainties in the values.

The "Fluence Methodologies for SLR" indicate that calculational based monitoring will accurately determine the vessel fluence-radiation values with uncertainties that are consistent with embrittlement evaluations. However, two issues that concern future monitoring need to be discussed: (1) How often will the vessel fluence values be monitored? (2) How are fluence-radiation values and their corresponding uncertainties estimated during periods when SVAM or MERLIN (or both) monitoring updates are not

being performed? These issues are addressed below as well as how surveillance will be accomplished to ensure that the safety limits remain valid.

### **7.1 60-Year Vessel Monitoring**

Prior to the 60-year licensing renewal period, the 10 CFR 50, Appendix H, monitoring requirements focused on capsules of material test specimens. Calculated, or functionally prescribed, neutron spectra were used to “unfold” the measured fluence values. An analytically calculated “lead factor” from the specimen location to the limiting embrittlement location on the wetted vessel surface provided “monitoring” of the safety limits.

When transitioning to the 60-year licensing renewal period, the NRC provided regulatory guidance<sup>9</sup> that updated the focus of the “monitoring” to directly include the vessel. Unbiased calculations of specimen degradation are required to be consistent with the *dpa* effective fluence calculations of vessel embrittlement safety limits. This means that the calculations for the vessel must be unbiased.

Once the specimens from surveillance programs have sufficiently characterized the properties of the reactor vessel materials – the specimen program would have completed its objective. Subsequently, surveillance requirements for the reactor vessel itself can be modified from capsule surveillance requirements.

#### **7.1.1 Monitoring Analytics**

During the first license renewal period, Framatome addressed reactor vessel aging management strategies with vessel monitoring programs. [

]

When the surveillance capsules are removed from the vessel internal components, the dosimetry is also removed. The NRC suggested that Regulatory Guide 1.190<sup>9</sup> requires some form of measurements. [ ]

[

]

Framatome installed the world's first cavity dosimetry beginning in 1985. [

]

Using the statistical methodology described in Reference 1, Framatome supported utilities going from 40 to 60 years with projected fluence rates. The methodology

[

]

### 7.1.2 Dosimetry Measurements

[

]

The overall effect of Framatome's methodology, [

] This factors into the "Licensee Cost" when implementing Regulatory Guide 1.190<sup>9</sup> for license renewal.

### 7.1.3 Cycle Monitoring

Section 7.1.1 discusses 60-year "Monitoring Analytics" for the vessel. The methodology complies with 10 CFR 50, Appendix H vessel monitoring requirements [

] is both cost-effective and satisfies licensing requirements.

[

] provides the means of incrementally tracking the vessel fluence on a cycle-by-cycle basis. This provides the appropriate monitoring to ensure that safety limits remain valid.





[

] the values are extrapolated to limiting locations previously determined by the fracture mechanics safety analyses. The previous "monitored" values are of course the licensing basis for the safety analyses. They are tracked relative to the current fluence-radiation values.

[

] results include the effective full power years of operation and any fluence-radiation values used in the safety analyses to set operational limits. The fluence-radiation values are related to those used for adjusted reference temperature (ART), pressure-temperature (P-T), pressurized thermal shock (PTS), etc. limiting values.



## 7.2 *SLR Vessel Monitoring*

The "Future Monitoring" methodology during the SLR time period will comply with 10 CFR 50, Appendix H requirements. The compliance will incorporate the same methodologies as those currently described in Section 7.1 for "60-Year Vessel Monitoring". The difference is that when the regions above and below the fuel-beltline set the safety limits, SVAM results will be used in place of MERLIN results.

It is anticipated that during the SLR time period, the fracture mechanics safety analysis will have limits ( $RT_{PTS}$ , ART, USE, and J-integrals) related to fluence-radiation degradation that occur well beyond the end of 60-years. It is likely that many of the limits will only occur at the 80-year end of licensed-life (EOL).

The "Fluence Methodologies for SLR" described in this topical report are accurate with well-defined standard deviations. [

] Future cycles leading to EOL rely on extrapolated fluence-radiation values. It is the extrapolated values that support the safety limits.

During the NRC's safety analysis review of licensing renewal topical reports for 60 years, three fundamental questions were proposed. The answers form Framatome's licensing basis for SLR vessel monitoring programs.

1. How does one know that the magnitude of the fluence-radiation in future unanalyzed reload cycles is not approaching a safety limit?
2. How does one know that the uncertainty in the fluence in future unanalyzed reload cycles is consistent with safety analyses?
3. How does one verify that the calculation-based fluence-radiation results continue to be accurate with well-defined uncertainties?

]

] evaluate

the fluence-radiation rates ( $\Phi$ ). These rates are used in Equation 7-1 to verify that the safety analysis remains valid.

### **7.2.1 Monitoring Safety Limits**

As the NRC has suggested, it is important to know whether the magnitude of the fluence-radiation in future unanalyzed reload cycles is approaching a safety limit. Fluence-radiation values *per se* are not safety limits. However, the values form the basis for the safety limits.

[

] This ensures that the reload cycles are not approaching a safety limit.



### 7.2.2 Deviations

The NRC has suggested that the ART values that are used for safety analyses are based on a normal distribution with 95 / 95 confidence in the (  $2 \times \sigma$  ) margin term. The ART margin term reflects a standard deviation of 20 % in the fluence-radiation values.

As discussed in Sections 7.1.1 and 7.1.3, the 20 % standard deviation applied to the fluence-radiation values in the development of Regulatory Guide 1.99, Revision 2 is maintained in the projection of fluence values to future cycles. [

]



### 7.2.3 Verifying Results

Verifying that the extrapolations of fluence-radiation values to future cycles are accurate with well-defined uncertainties [

]

The SVAM or MERLIN fluence-radiation results are currently compared to extrapolated fluence-radiation values and updated dosimetry data. [

] This same procedure will be applied to the SLR period.

### 7.3 Dosimetry

Cavity dosimetry is a [

] the cavity dosimetry provides no monitoring function. Moreover as indicated in Sections 5 and 6, dosimetry in PWRs and BWRs during the SLR period is only partially useful in confirming the accuracy and precision in each cycle's calculated results.

One benchmark comparison of calculated results to a single set of dosimetry measurements does not provide 95 / 95 confidence in the calculations. Independent of the number of dosimeters, the calculated results are not independent. They are dependent on a single transport model that is functionally coupled to every result's location.

The many previous cycles that have a set of dosimetry provide confidence in the  
[ ] one dosimetry set could  
indicate that a problem existed, but it could not significantly affect the 95 / 95 confidence  
in the results.



[

] This methodology is both cost-effective and provides assurance that  
safety limits are adequately monitored.

## 8.0 SUMMARY AND CONCLUSIONS

Framatome is the largest provider of services supporting the construction and operation of nuclear reactors in the world. In the United States (U.S.), the support includes the development of technologies for both PWRs and BWRs to continue operation beyond the original license of 40 years. As noted in the Introduction, Framatome's "Fluence and Uncertainty Methodologies" topical report<sup>1</sup> provided a new technological approach that is approved for licensing PWRs and BWRs to extend operation to 60 years.

The topical report presented in this document provides another new technological development. It addresses U.S. Nuclear Regulatory Commission (NRC) concerns for the subsequent license renewal (SLR) of PWRs and BWRs to operate for 80 years and beyond. The NRC's concerns are discussed in Reference 2 "Generic Aging Lessons Learned (GALL) Report". The "Computation of Neutron Fluence" in an information exchange public meeting<sup>17</sup> provides guidance with respect to alleviating the concerns.

Beginning in the late 1950's, scientists found that relatively low levels of neutron irradiation could degrade the toughness of steels used in the construction of reactor vessels. Framatome (formerly Babcock and Wilcox) was part of the team that led the way in determining the solution for the embrittlement – fluence-radiation problem.

When electric utilities with PWRs and BWRs wanted to extend their operating license for 20 years (60 total years), the NRC expressed concerns with modeling the fluence-radiation deep within the material structure of the vessels. An updated technology that only relied on calculational results was required. Framatome again led the way; the NRC approved its new methodology in February of 1999.<sup>1</sup>

When electric utilities with PWRs and BWRs wanted to pursue SLR for 80 years, the NRC agreed that Framatome's methodology was appropriate for analysis of the fuel-beltline; it satisfies the guidelines in Regulatory Guide 1.190<sup>9</sup>. However they questioned the ability of the model to produce accurate and precise results above the

beltline, in the nozzle region. As shown in Figure 1-1, Framatome agrees with the NRC's concern.

ART effective fluence-radiation values can grow to exceed  $1 \times 10^{17}$  neutrons per centimeter-squared ( $n/cm^2$ ) in the nozzle regions. Due to the geometrical complexity shown in Figure 2-2, nozzle region analyses are challenging. Nonetheless, they are necessary; fracture mechanics analysts have found that high stress intensity factors in the nozzles with small ARTs could be more limiting than larger ARTs in the beltline with smaller stress intensity factors.

The "Regulatory Requirements" discussed in Section 2 for SLR include those in Regulatory Guide 1.190.<sup>9</sup> Thus during the SLR time period, the computer code MERLIN, that Framatome developed for 60 year license renewal, can be used for fuel-beltline analyses. However, there are four significant developments required for fluence-radiation analyses above and below the beltline to comply with Regulatory Guide 1.190. These developments are (1) the geometric modeling, (2) importance weights from deterministic transport solutions, (3) continuous energy modeling over the entire energy range from 0.0 to 20.0 MeV, and (4) a precise Monte Carlo solution process such as MCNP. Framatome has incorporated these developments into the SVAM computer code system. [

]

As with Framatome's "Fluence and Uncertainty Methodologies" topical report<sup>1</sup> that supports PWR and BWR operation to 60 years, the results from SVAM are not useful without verification based on the benchmark database. However, before the uncertainties in the calculational methodologies can be validated, there must be a measurement database with uncertainties that have been validated.



In Section 3, Framatome provides an expanded measurement database that includes regions above and below the fuel-beltline. The accuracy and precision in the experimental methods and procedures was verified by the National Institute of Standards and Technology's "Standard and Reference Field Validation".<sup>19</sup>

The database includes measurements from Westinghouse, Combustion Engineering, Babcock & Wilcox, and General Electric reactors, as well as test reactors like the Pool Critical Assembly. [

]

[

] In the fuel-beltline region all measurements have a relative standard deviation of 7.0%.

[

Section 4 describes the "SVAM Methodology". This methodology uses a hybrid deterministic – Monte Carlo approach. A deterministic code like DENOVO is used to generate importance weights for a code like MCNP. The methodology is much like that described by Risner of the Oak Ridge National Laboratory in a public meeting arranged by Parks and Wallace, et al, of the NRC.<sup>17</sup>

The SVAM methodology has been validated with hundreds of dosimetry measurements in the regions above and below the fuel-beltline as well as measurements in the beltline.

[

] The modeling

extends throughout the reactor system, from the core regions, through the reactor internal components, to every part of the reactor vessels – and beyond the vessels, to the nozzles and vessel support structures in the cavity regions. Moreover, the methodologies are applicable to all time periods (the beginning of the first cycle to the end of the last cycle), and to various operating conditions (partial power, load following, etc.).

As important as SVAM's integrated methodologies are – the true assessment of SVAM comes from modeling the measurement database. The benchmark of SVAM results to the measurement data, along with the sensitivity modeling, provides a 95 / 95 level of confidence that SVAM results can be applied to safety analyses.

The benchmark database in Tables 5-2 and 5-3 [

]

In the regions above and below the fuel-beltline, the SVAM benchmark database

[

]

[

] the safety limits are generally at the end of the licensed-life (EOL). In order to support operation to EOL, some type of "Future Monitoring"

(Section 7) is necessary to ensure that the safety limits remain valid. [

]

[

]

## 9.0 REFERENCES

1. BAW-2241P-A, Revision 2, "Fluence and Uncertainty Methodologies," (now Framatome Inc.) J.R. Worsham, III, April, 2006.
2. NUREG-1801, "Generic Aging Lessons Learned (GALL) Report," Division of Regulatory Improvement Programs, Office of Nuclear Reactor Regulation, U.S. NRC, July, 2001.
3. [ ]
4. [ ]
5. ANSYS 2019, Release 2, ANSYS Inc., © 2019
6. ORNL/TM-2013/416 Revision 1, "ADVANTG – An Automated Variance Reduction Parameter Generator," Oak Ridge National Laboratory, August, 2015.
7. LA-UR-03-1987, "MCNP — A General Monte Carlo N-Particle Transport Code, Version 5, Volume I: Overview and Theory," Los Alamos National Laboratory, X-5 Monte Carlo Team, February 2008.  
  
LA-CP-03-0245, "MCNP — A General Monte Carlo N-Particle Transport Code, Version 5, Volume II: User's Guide," Los Alamos National Laboratory, X-5 Monte Carlo Team, February 2008.
8. Regulatory Guide 1.99, Revision 2, "Radiation Embrittlement of Reactor Vessel Materials," Office of Nuclear Regulatory Research, U.S. Nuclear Regulatory Commission, May, 1988.
9. Regulatory Guide 1.190, "Calculational and Dosimetry Methods for Determining Pressure Vessel Neutron Fluence," Office of Nuclear Regulatory Research, U.S. Nuclear Regulatory Commission, March, 2001.

10. NUREG/CR-3391, Volume 2, "LWR Pressure Vessel Surveillance Dosimetry Improvement Program", Office of Nuclear Regulatory Research, U.S. Nuclear Regulatory Commission, "Charpy Trend Curves Based on 177 PWR Data Points," G.L. Guthrie, April, 1984.
11. NUREG/CP-0029, Volume 2, "Re-Evaluation Of The Dosimetry For Reactor Pressure Vessel Surveillance Capsules," L. Simons, L.S. Kellogg, E.P. Lippincott, W.N. McElroy and D.L. Oberg, Proceedings of the Fourth ASTM – EURATOM Symposium on Reactor Dosimetry, March, 1982.
12. BAW-1485, "Pressure Vessel Fluence Analysis For 177-FA Reactors," C.L. Whitmarsh, June, 1978.
13. BAW-1485, Revision 1, "Pressure Vessel Fluence Analysis For 177-FA Reactors," S.Q. King et al., April, 1988.
14. NUREG/CR-1861, "LWR Pressure Vessel Surveillance Dosimetry Improvement Program: PCA Experiments And Blind Test," W.N. McElroy (HEDL-TME 80-87), July, 1981.
15. ASTM STP 1228, "Neutron Fluence Determination at Reactor Filters by <sup>3</sup>He Proportional Counters: Comparison of Unfolding Algorithms," M. Matzke, W.G. Alberts, and E. Dietz, American Society for Testing and Materials, Philadelphia, 1994.
16. DLC 185/BUGLE 96, "Coupled 47 Neutron, 20 Gamma-Ray Group Cross Section Library Derived from ENDF/B VI for LWR Shielding and Pressure Vessel Dosimetry Applications," Oak Ridge National Laboratory, March, 1996.
17. ML17038A125, "Computation of Neutron Fluence Information Exchange Public Meeting Summary," J.M. Risner, et al, Oak Ridge National Laboratory; B. Parks, J.S. Wallace, et al, U.S. Nuclear Regulatory Commission, February, 2017.
18. LA-CP-03-0245, "MCNP — A General Monte Carlo N-Particle Transport Code, Version 5, Volume II: User's Guide," Los Alamos National Laboratory, X-5 Monte Carlo Team, February 2008.
19. BAW-2241P-A, Revision 2, "Fluence and Uncertainty Methodologies," (now Framatome Inc.) J.R. Worsham, III, April, 2006.

20. BAW-1698, "Analysis of Capsule ANI-B, Arkansas Power & Light Company, Arkansas Nuclear One, Unit 1," A. L. Lowe, et. al., November 1981.
21. BAW-2075, Rev. 1, "Analysis of Capsule ANI-C, Arkansas Power & Light Company, Arkansas Nuclear One, Unit 1," A.L. Lowe, Jr., L. Petrusha, et. al., October, 1989.
22. BAW-1440, "Analysis of Capsule AN1-E from Arkansas Power and Light Company, Arkansas Nuclear One Unit 1," A. L. Lowe, et al., April, 1977.
23. BAW-2199, "Analysis of Capsule 97° Baltimore Gas & Calvert Cliffs Nuclear Power Plant Unit No. 2," A.L. Lowe, Jr., D.J. Skulina, et. al., February 1994.
24. BAW-2049, "Analysis of Capsule CR3-F Florida Power Corporation Crystal River Unit-3," A.L. Lowe, Jr., L.B Wimmer, et. al., September 1988.
25. BAW-1910P, "Analysis of CR3-LG1," A. L. Lowe, et al., August, 1986.
26. BAW-2254P, "Test Results of Capsule CR3-LG2, B&W Owners Group," M.J. Devan, et al., October, 1995.
27. BAW-2205-00, "B&WOG Cavity Dosimetry Benchmark Program Summary Report," J.R. Worsham, III, et. al., December 1994.
28. BAW-2208, "Fracture Toughness Test Results from Capsule TE1-D, The Toledo Edison Company, Davis-Besse Nuclear Power Station, Unit 1," A.L. Lowe Jr., et. al., October 1993.
29. BAW-1719, "Fracture Toughness Test Results from Capsule TE1-F, The Toledo Edison Company, Davis-Besse Nuclear Power Station, Unit 1," A.L. Lowe Jr., et. al., March 1982.
30. BAW-1920P, "Analysis of Capsule DB1-LG1," A. L. Lowe, et al., October, 1986.
31. BAW-2142, "Analysis of Capsule W-104, Northeast Nuclear Energy Company, Millstone Nuclear Power Station, Unit No. 2," A.L. Lowe Jr., et. al., November, 1991.
32. BAW-2277, "Test Results of Capsule W, Northern States Power Company, Monticello Nuclear Generating Plant, (Irradiated at Prairie Island Unit 1)," M.J. DeVan and D.J. Skulina, June, 1996.

33. BAW-1638, "Analysis of Capsule V, Virginia Electric & Power Company, North Anna Unit No.1," A.L. Lowe Jr., et. al., May, 1981.
34. BAW-1794, "Analysis of Capsule V, Virginia Electric & Power Company, North Anna Unit No.2," A.L. Lowe Jr., et. al., May, 1981.
35. BAW-2050, "Analysis of Capsule OC1-C, Duke Power Company, Oconee Nuclear Station Unit-1," A.L. Lowe Jr., S. Q. King, et. al., October, 1988.
36. BAW-1436, "Analysis of Capsule OC1-E, Duke Power Company, Oconee Nuclear Station 1," A.L. Lowe Jr., et. al., September, 1977.
37. BAW-1699, "Analysis of Capsule OCII-A, from Duke Power Company's Oconee Nuclear Station, Unit 2," A.L. Lowe Jr., J.W. Ewing, et. al., December, 1981.
38. BAW-1437, "Analysis of Capsule OCII-C, from Duke Power Company, Oconee Nuclear Station Unit 2," A.C. Cone Jr., E.T. Chulick, et. al., May 1977.
39. BAW-2051, "Analysis of Capsule OCII-E, Duke Power Company, Oconee Nuclear Station Unit-2," A.L. Lowe, Jr., L. Petrusha, et al., October, 1988.
40. BAW-1438, "Analysis of Capsule OCIII-A, from Duke Power Company, Oconee Nuclear Station Unit 3," A.L. Lowe Jr., E. T. Chulick, et. al., July, 1977.
41. BAW-1697, "Analysis of Capsule OCIII-B, from Duke Power Company, Oconee Nuclear Station, Unit3," A.L. Lowe Jr., J.W. Ewing, et. al., October 1981.
42. BAW-2128, Rev. 1, "Analysis of Capsule OCIII-D, Duke Power Company, Oconee Nuclear Station, Unit-3," A.L. Lowe Jr., M.A. Rutherford, et. al., May, 1992.
43. BAW-1702, "Analysis of Capsule RS1-B, Sacramento Municipal Utility District, Rancho Seco Unit 1," A.L. Lowe, W. A. Pavinich, et. al., February, 1982.
44. BAW-1792, "Analysis of RS1-D, Sacramento Municipal Utility District, Rancho Seco Unit 1," A.L. Lowe, L.L. Collins, et. al., October, 1983.

45. BAW-2074, "Analysis of Capsule RS1-F, Sacramento Municipal Utility District, Rancho Seco Unit 1," A. L. Lowe, J.D. Aadland, et. al., April 1989.
46. BAW-2083, "Analysis of Capsule U, Carolina Power & Light Company, Shearon Harris Unit No. 1," A.L. Lowe Jr., J.D. Aadland, et. al., August, 1989.
47. BAW-1880, "Analysis of Capsule W-83, Florida Power & Light Company, St. Lucie Plant Unit No. 2," A.L. Lowe Jr., L. L. Collins, et. al., September, 1985.
48. BAW-1439, "Analysis of Capsule TMI-1E, from Metropolitan Edison Company, Three Mile Island Nuclear Station-Unit 1," A.L. Lowe Jr., E.T. Chulick, et. al., January, 1977.
49. BAW-2253P, "Test Results of Capsule TMI2-LG1, B&W Owners Group," M.J. DeVan, et al., October, 1995.
50. BAW-2177, "Analysis of Capsule W-97, Waterford Generating Station, Unit 3," A.L. Lowe, et al., November, 1992.
51. BAW-2082, "Analysis of Capsule Y, Zion Nuclear Plant Unit 1," A.L. Lowe, et al., March, 1990.